DYNAMIC STRUCTURES OF MACROMOLECULES AND SUPRAMOLECULAR SYSTEMS STUDIED BY ^{1}H–^{31}P CROSS–POLARIZATION NMR

A Dissertation Submitted to Graduate School,
Faculty of Science, Osaka University
in Fulfillment of the Degree of
Doctor of Science

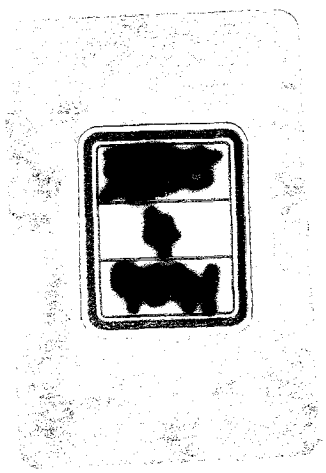

Takayuki Odahara

Division of Molecular Biophysics
Institute for Protein Research
Osaka University

DYNAMIC STRUCTURES OF MACROMOLECULES AND SUPRAMOLECULAR SYSTEMS STUDIED BY ^{1}H-^{31}P CROSS-POLARIZATION NMR

A Dissertation Submitted to Graduate School,
Faculty of Science, Osaka University
in Fulfillment of the Degree of
Doctor of Science

Takayuki Odahara

Division of Molecular Biophysics
Institute for Protein Research
Osaka University

CONTENTS

Summary

The main target of this thesis is to investigate the dynamic states of very large biological macromolecules and supramolecular systems such as nucleic acids and biomembranes in an intact system. For this purpose, the ^{1}H-^{31}P cross-polarization technique was applied to intact biological systems and substances.

In the first place, the conditions for separate observation of ^{31}P NMR spectra of lipid bilayers and nucleic acids in an intact biological system by the cross-polarization method were examined. A lipid-containing bacteriophage, PM2, and its host bacterium, *Alteromonas espejiana*, were used as intact systems, because the phage particle has simple structure and chemical composition, and the host cell is much more complicated in contrast. It was shown that ^{31}P NMR spectra of nucleic acids and lipid bilayers can be obtained separately with short and long thermal contacts, respectively.

In the second place, the dynamic states of the intact and extracted lipid bilayers of PM2 and *A. espejiana* were investigated. The temperature dependence of the chemical shift anisotropy ($\Delta\sigma=\sigma_{//}-\sigma_{\perp}$) was examined using the selectively observed cross-polarization spectra of the bilayers of intact PM2 and *A. espejiana*. The dynamic state of the biomembrane of intact bacteria was directly monitored in detail. The result for PM2 is in good agreement with the reported one [1]. Furthermore, the temperature dependence of the spin-lattice relaxation time of protons in the rotating frame ($T_{1\rho}(H)$) was examined for the lipid bilayer of the intact systems and the extracted lipid bilayers of *A. espejiana*. It was shown that the all lipid bilayers were in the fast-motional regime and that the mobility of the intact biomembranes were more suppressed than that of the extracted phospholipids bilayers. Thus, it turned out that the phase behavior of the intact biomembrane was different from that of the bilayer of the extracted lipids for both PM2 and the host cell. The direction of the change of the phase transition temperature in the two biological systems were found to be opposite. However, the measurement of $T_{1\rho}(H)$ showed that the motion of the

phospholipid molecules in the intact biomembranes is more suppressed than that in the extracted phospholipid bilayers in the temperature range examined, suggesting that the dynamic state of the intact biomembranes is different from that of pure extracted phospholipid bilayers because of the presence of membrane proteins.

In the third place, the relationship between dynamic state and structure of nucleic acids in protein-nucleic acid supramolecular complex was investigated. Used samples for this purpose were calf thymus DNA, ribosome of *A. espejiana*, chicken erythrocyte chromatin, *E. coli* phage λ, $\lambda\Delta$ mutant phage and PM2 phage, whose nucleic acid molecules take on different higher order structures. The addition of water to calf thymus DNA showed that the second hydration induced the transition from A to B form DNA [2], and increased drastically the mobility of the backbones. The heat treatment of the nucleic acid complexes mentioned above showed that the coat proteins of λ phage do not directly interact with the DNA in the core, and that there are direct interactions between the nucleic acids and protein molecules in the ribosome, chicken erythrocyte chromatin and PM2 phage. The temperature dependence of ^{31}P chemical shift anisotropy showed that the change in the mobility of the nucleic acids with temperature increased in order of intact chicken erythrocyte chromatin (smallest), ribosome of *A. espejiana*, *E. coli* phage λ, $\lambda\Delta$ mutant, PM2 phage and calf thymus DNA (largest). The measurements of $T_{1\rho}(H)$ also revealed that the nucleic acids of chromatin and ribosome were in more suppressed dynamic state than DNAs in the phage cores, however, the motions of which are more suppressed than the pure DNA.

Finally, the relationship between the dynamic state of nucleic acid macromolecules in intact *A. espejiana* cell and the physiological condition was investigated. It was shown that the growth phase of *A. espejiana* affected the ^{31}P cross-polarization spectrum. Namely, it was elucidated that nucleic acid molecules in an intact cell at logarithmic phase were quite rigid, because of either the viscosity of the cytoplasm in the active condition or the formation of the transcriptional complex.

It can be concluded that the cross-polarization technique can be used for the investigation of the dynamic state of the huge macromolecules and supramolecular structures in an intact biological system.

References

[1] Saenger, W. "*Principles of Nucleic Acid Structure*" (1983) Springer Verlag, New York.

[2] Akustu, H., Satake, H. and Franklin, M.(1980) *Biochemistry*, 19, 5265.

Chapter I

Introduction

The discovery of the phenomena of chemical shifts [1] in nuclear magnetic resonance (NMR) made NMR spectroscopy a powerful technique for investigation of structures and dynamics of small and large molecules in various phases of matter. NMR spectra reflect the electronic environments of nuclei and the conformation of a molecule. In particular, pulse-Fourier transform method introduced by Ernst *et al.* [2] has brought about revolution in NMR spectroscopy, and has enabled us to obtain new information on structure and dynamics of molecules. For examples, multi-dimensional NMR [3, 4] gives information on relation among sites of molecules depending on pulse-sequences selected for aims, and cross-polarization magic angle spinning method [5] and zero field NMR [6] give a number of pieces of high-resolutional information even on solid state samples. Moreover, in combination with computer analyses and biochemical techniques, NMR method has been used for precise structure determination of relatively small biological macromolecules such as proteins and nucleic acids with molecular weight below 10,000 [7, 8].

However, there are very large molecular complexes, supramolecular system, such as chromosomes and biomembranes, which play important roles in biological functions in intact cells. Chromosome is composed of a double-stranded DNA and proteins, and has very large apparent molecular weight over 2×10^9 [9] (Figure I-1). Biomembranes are generally composed of lipids and proteins, and their fundamental structures are explained by Singer-Nicolson fluid mosaic model [10] (Figure I-2). In case of the study of such macromolecules or supramolecular systems, it is difficult to determine detailed structures. But NMR method still has following merits. (i) It does not damage samples, (ii) non-perturbing probes are used, and (iii) only the sites of interest can be observed by choosing a suitable kind of nuclei. It is also desirable to get information on them in intact systems. In fact, small soluble metabolites in intact systems have been studied by

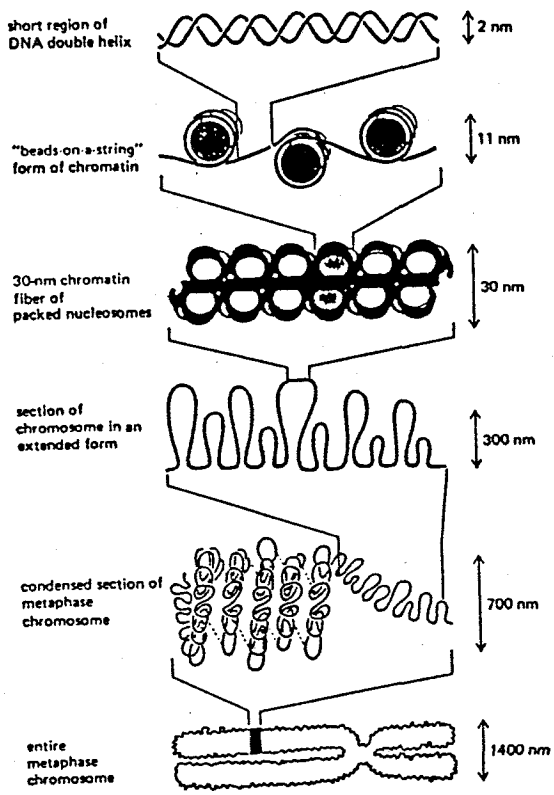

Figure I-1. Schematic illustration of some of the many orders of chromatin packing postulated to give rise to the highly condensed metaphase chromosome. (Alberts, B., Bray, D., Lewis, J., Raff, M., Roberts, K. & Watson, J. D. (1989) "*MOLECULAR BIOLOGY OF THE CELL*" 2nd ed., Garland Publishing Inc, New York.)

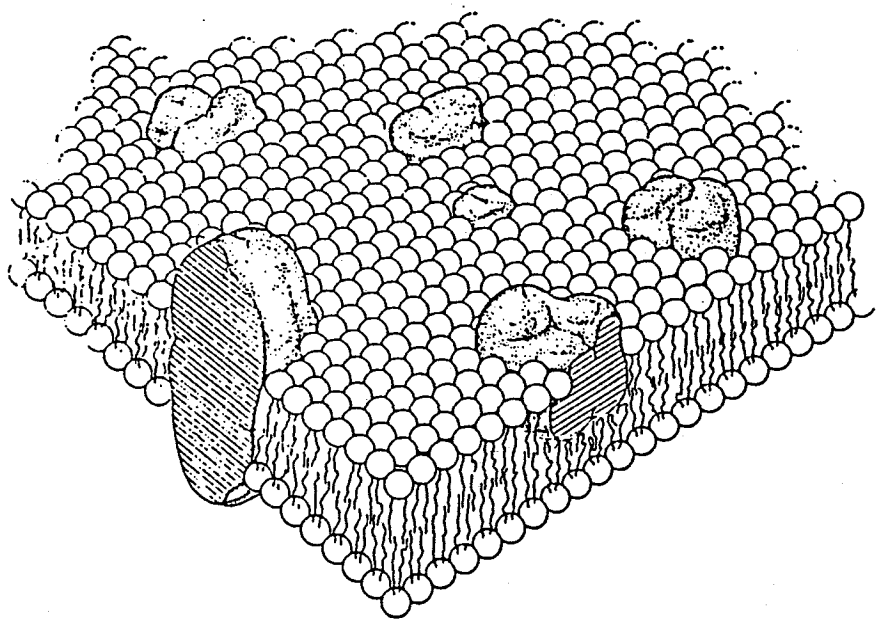

Figure I-2. Picture of Singer-Nicolson's fluid mosaic model. Biomembranes are dynamic, fluid structures, and most of their lipid and protein molecules are able to move about in the plane of the membrane. (Singer, S. J. and Nicolson, G. L. (1972) *Science* 17, 720.)

the use of ^{31}P and ^{13}C NMR in this decade [11, 12]. However, there are few studies of macromolecules or supramolecular complexes in intact biological systems.

It is indicated that functions of biological substances are closely connected with not only their structures but also their dynamic states. In the case of the study of huge biological substances, it is difficult to determine their fine structures. Nevertheless, it is important to study their dynamic states, and to investigate the relationship between the dynamic state and the function. Therefore, in order to get information on dynamic states of the macro- and supramolecular structures in intact biological systems, we have developed a new method based on one of the solid-state NMR techniques, ^{1}H-^{31}P cross-polarization method. Phosphorus nuclei were chosen from the following reasons. (i) In contrast to ^{1}H or ^{13}C, ^{31}P nuclei do not exist universally in biological systems but do only in particular substances such as phospholipids, nucleic acids and their metabolites, which are essential for biological activities, and (ii) its natural abundance is 100%. ^{31}P NMR signals occurring from the phosphorus-containing molecules in different dynamic states were separately observed by the cross-polarization method [13], since the efficiency of the polarization transfer from proton to phosphorus spin systems depends on the spin lattice relaxation time of proton in the rotating frame, $T_{1\rho}(H)$, of molecules as shown in Chapter IV.

In this investigation, a lipid-containing bacteriophage, PM2, and its host cell, *Alteromonas espejiana*, were used as major intact systems. As mentioned in Chapter II, PM2 phage has a simple chemical composition, while *A. espejiana* has a much more complicated composition. PM2 phage is also a good system for the study of intact biomembranes for the reason of its simplicity. Thus, they are suitable systems for the selective observation of each different dynamic components such as phospholipids and nucleic acids. The selective observation of ^{31}P NMR spectra of mobile phospholipid and rigid nucleic acid molecules in intact PM2 phage and its host cells, and the assignments of the signals are described in Chapter IV. We investigated the dynamic states

of the intact biomembranes and the extracted phospholipid bilayers by examining the temperature dependence of chemical shift anisotropy ($\Delta\sigma$) and $T_{1\rho}$(H). In Chapters V and VI, new insight into the differences of their dynamic states is described. In biological systems, nucleic acid molecules take on a variety of dynamic structures by interacting with proteins. We observed the cross-polarization spectra of nucleic acid-protein complexes in different systems. The relationships between their structures and dynamics are described in Chapter VII. Finally, we applied the cross-polarization method to intact *A. espejiana* cells in order to get the relationship between the physiological condition and the dynamic state of ribosomes in intact cells. The result is described in Chapter VIII.

References

[1] Arnold, J. T., Dharmatti, S. S. and Packard, M. E. (1951) *J. Chem. Phys.*, **19**, 507.

[2] Ernst, R. R. and Anderson, W. A. (1966) *Rev. Sci. Instrum.*, **37**, 93.

[3] Sörensen, O. W., Eich, G. W., Levitt, M. H., Bodenhausen, G. and Ernst, R. R. (1983) *Prog. NMR. Spectro.*, **16**, 163.

[4] Griesinger, C., Sörensen, O. W. and Ernst, R. R. (1989) *J. Magn. Reson.*, **84**, 14.

[5] Terao, T., Fujii, T. Onodera, T. and Saika, A. (1984) *Chem. Phys. Lett.*, **107**, 145.

[6] Waitekamp, D. P., Bielecki, A., Zax, D., Zilm, K. and Pines, A. (1983) *Phys. Rev. Lett.*, **50**, 1807.

[7] Kline, A. D., Braun, W. and Wuthrich, K. (1986) *J. Mol. Biol.*, **189**, 377.

[8] Opella, S. J. Stewart, P. L. and Valentine, K. G. (1987) *Quart. Rev. Biophys.*, **19**, 7.

[9] Watson, J. D. and Crick, F. H. C. (1953) *Nature*, **171**, 737

[10] Singer, S. J. and Nicolson, G. L. (1972) *Science*, **175**, 720

[11] Brindle, K. M., Rajagopalan, B., Bolas, N. M. and Radda, G. K. (1987) *J. Magn. Reson.*, **74**, 356.

[12] Muller, S., Aue, W. P. and Seelig, J. (1985) *J. Magn. Reson.*, **63**, 530.

[13] Odahara, T., Akutsu, H. and Kyogoku, Y., submitted.

CHapter II

Materials and Methods

II-1 Introductory remarks for materials

A Lipid-Containing Bacteriophage, PM2, and Its Host Bacterium, Alteromonas espejiana[1, 2, 3, 4]

Bacteriophage PM2 and its host bacterium, *A. espejiana*, were isolated from samples of seawater taken about one mile off Vina der Mar, Chile, in a terrestrially polluted bay by Spencer *et al.* in 1960. And then in 1968, Espejio and Canelo found that PM2 was a lipid-containing bacteriophage. The host cell is a psychrophilic and halophilic bacterium characteristic of a marine origin, i.e. growing only in media of an ionic strength similar to that of seawater and at temperatures below 30°C.

PM2 phage consists of four kinds of proteins (73.1 % by dry weight), lipids (12.6 %) and a circular double-stranded superherical DNA (14.3 %). The chemical composition of PM2 phage is summarized in Table II-1. PM2 phage is an icosahedral particle with a diameter of 60 nm and with spikes at the vertices of the icosahedral structure as schematically shown in Figure II-1. Two layers were seen in electron micrographs of negatively stained preparations and sectioned specimens reveal a membrane-like structure at the periphery of the virion [5, 6] The particle weight of the phage is 5.1×10^7 and the buoyant density of the phage is 1.28 g/cm^3. The DNA of PM2 phage exists in the virion as a double-stranded circular molecule with supercoils and its molecular weight is about 6×10^6. The G+C content of PM2 DNA is 42 to 43 %, which is the same as that of the host cell [7]. The phage particle contains four kinds of proteins, which are designated as I, II, III and IV in order of molecular weights. The molecular weight and characteristics of four proteins are summarized in Table II-2. The spikes are formed from protein I. Treatment of the virion with proteolytic enzymes and particularly with bromelin at 1 mg/cm^3, produces a particle lacking only

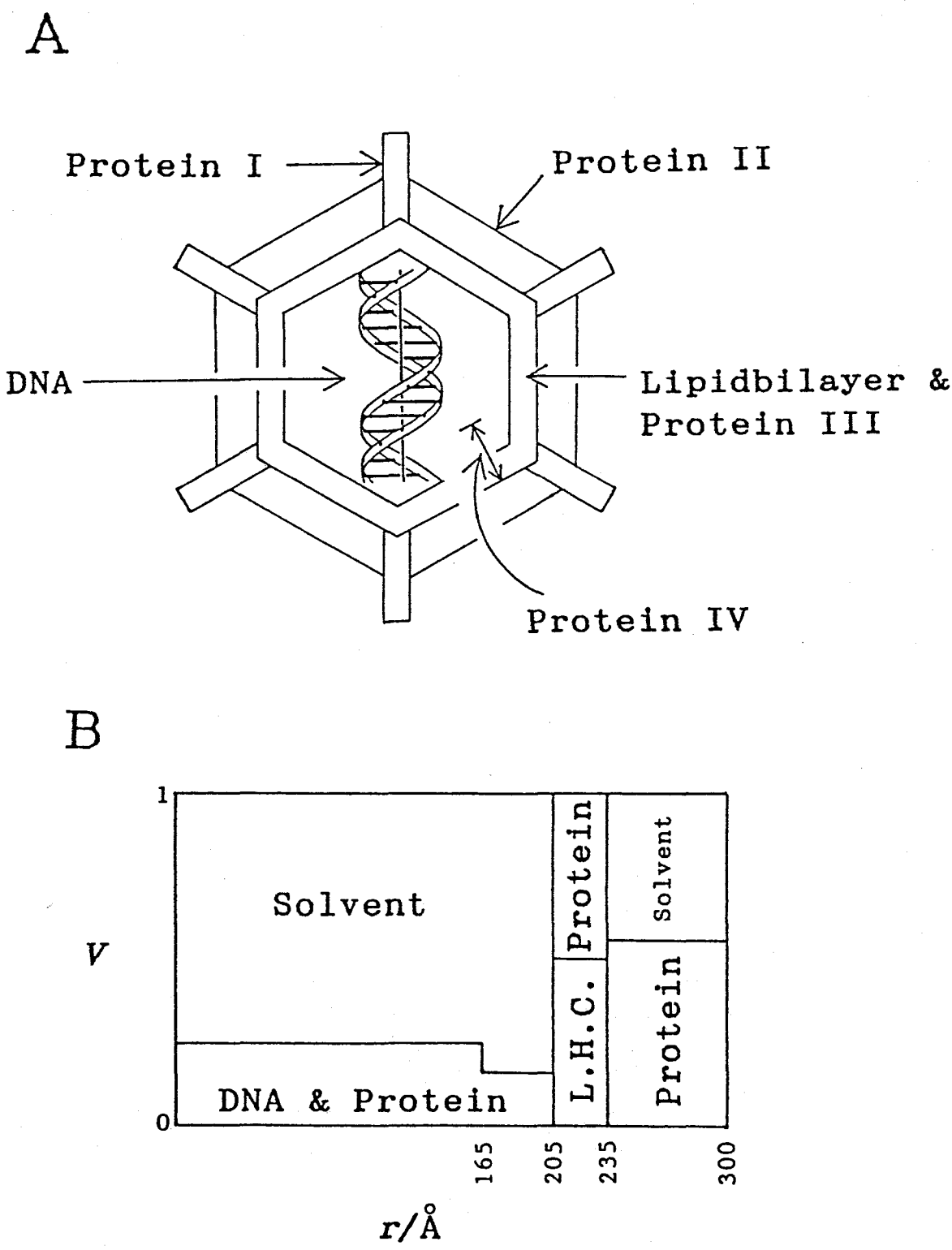

Figure II-1. (A) Model of the structure of bacteriophage PM2, and (B) volume fraction (V) of protein, lipid hydrocarbon (LHC), DNA, and solvent as a function of radius (r) in a model for bacteriophage PM2 consisting of 4 spherical shell. (Franhlin, R. M. (1974) *Current Topics in Microbiology and Immunology* 68, 107-159.; Schneider, D. *et al.* (1978) *J. Mol. Biol.* 124, 97.; Akutsu, H. *et al.* (1980) *Biochemistry* 19, 5264.)

Table II-1. Chemical composition of bacteriophage PM2. (Franklin, R. M. (1974) *Current Topics in Microbiology and Immunology* 68, 107)

DNA	14.3% by weight MW ~ 6.4×10^6 (sodium salt) 42–43% GC content
Lipid	12.6–14.0% by weight
phospholipid	64% phosphatidylglycerol, 27% phosphatidylethanolamine, 1% cardiolipin
neutral lipid	7 to 8%
Fatty acids	3.0% $C_{14:0}$, 12.0% $C_{16:0}$, 56.6% $C_{16:1}$, 7.3% $C_{17:cy}$, 13.9% $C_{18:1}$, 7.2% other

Table II-2. Characteristics of PM2 proteins. (Conrat, H. F. and Wagner, R. R. (1978) *Comprehensive Virology* 12, 271.)

Protein	Electrophoretic mol. wt.	Compositional mol. wt.	PI	Polarity	Mol/virion
I	43,000	43,580	6.2	49.4	~80
II	26,000–27,000	27,660	9–12.3	44.9	~820
III	12,500	13,040	5.8	40.1	~500
IV	4,700	6,640	5.5	36.2	~300

Table II-3. Lipid composition of *A. espejiana* and PM2 phage. (Conrat, H. F. and Wagner, R. R. (1978) *Comprehensive Virology* 12, 271.)

BAL-31			
PG	23%		
PE	75%		
		PG	PE
inner membrane		23.5%	71.5%
outer membrane		16%	79%
PM2			
PG	64%		
PE	27%		
neutral lipid	7%		
cardiolipin	1%		

Table II-4. Fatty acid composition of *A. espejiana* and PM2 phage. (Camerini-Otero, R. D. and Franklin, R. M. (1972) *Virology* 49, 385.)

	Fatty acids						
Source	$C_{14:0}$	$C_{16:0}$	$C_{16:1}$	$C_{17:cy}$	$C_{18:0}$	$C_{18:1}$	Others
BAL-31	1.1	19.8	51.7	5.3	1.5	13.2	7.4
Virus PM2	3.0	12.0	56.6	7.3	—[b]	13.9	7.2

protein I, unable to adsorb to the host cell, and lacking the spikes in the electron micrographs. Protein II is the most abundant viral protein and constitutes the layer exterior of the lipid bilayer. This protein is basic. Protein III is hydrophobic and interacts with the phospholipids in the lipid bilayer. Although the N- and C-terminal regions of protein IV are polar, the center of the molecule is hydrophobic [8, 9]. Protein IV is supposed to anchor itself partly to the inner leaflet of the PM2 bilayer membrane and interacts with the DNA inside the virion. The lipid content of PM2 is in the region between 12.6 and 14.0 % by dry weight. The phospholipid composition in the phage is in an inverse ratio of the host cell. Thus, the phage has the composition of 64 % phosphatidylglycerol (PG) and 27 % phosphatidylethanolamine (PE), whereas the host cell has that of 23 % PG and 75 % PE [10, 11]. Besides the above phospholipids, there is small amount (7.4 %) of neutral lipids in the phage, and traces of other phospholipids, in which the main component is probably cardiolipin (Table II-3). The fatty acid composition of PM2 and host cell are very similar to each other with predominance of $C_{16:1}$ fatty acid (Table II-4) [12].

*E. coli Phage*λ *and E. coli*

λ Phage is a temperate phage of *E. coli* K-12 and infects *E. coli* by attaching itself to the bacterial cell wall in the presence of 10^{-2} to 10^{-3} M of Mg^{2+}. A mature particle of λ phage consists of twenty kinds of proteins (50 %) and one double-stranded DNA molecule (50 %). The phage is made of an icosahedral head particle with a diameter of 54 nm and a tubular tail with a length of 180 nm (Figure II-2) [13]. The DNA molecule with molecular weight 3.1×10^7 is encapsulated in the icosahedral head and consists of 46,500 base pairs. The G+C content of the DNA is about 50 % and the buoyant density of the phage is 1.508 g/cm^3.

Ribosome[14, 15]

Ribosomes play important roles for biosynthesis of proteins i.e. the events in the assembly of new proteins take place on the

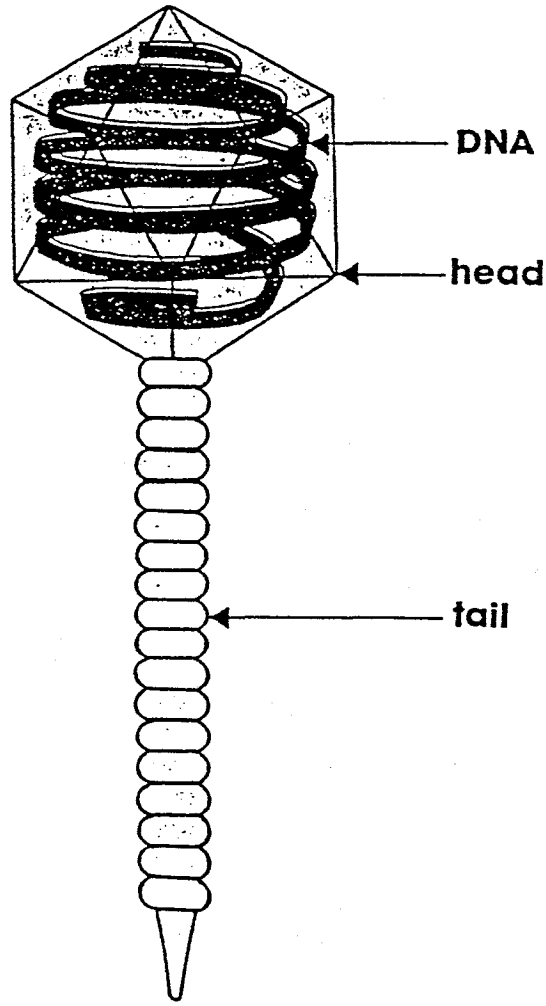

Figure II-2. Schematic drawings of the λ phage particle. The length of tail fiber is 135nm, and the diameter of the head is 50nm. (Ptashne, M. (1986) *A Genetic Switch*, Cell Press.)

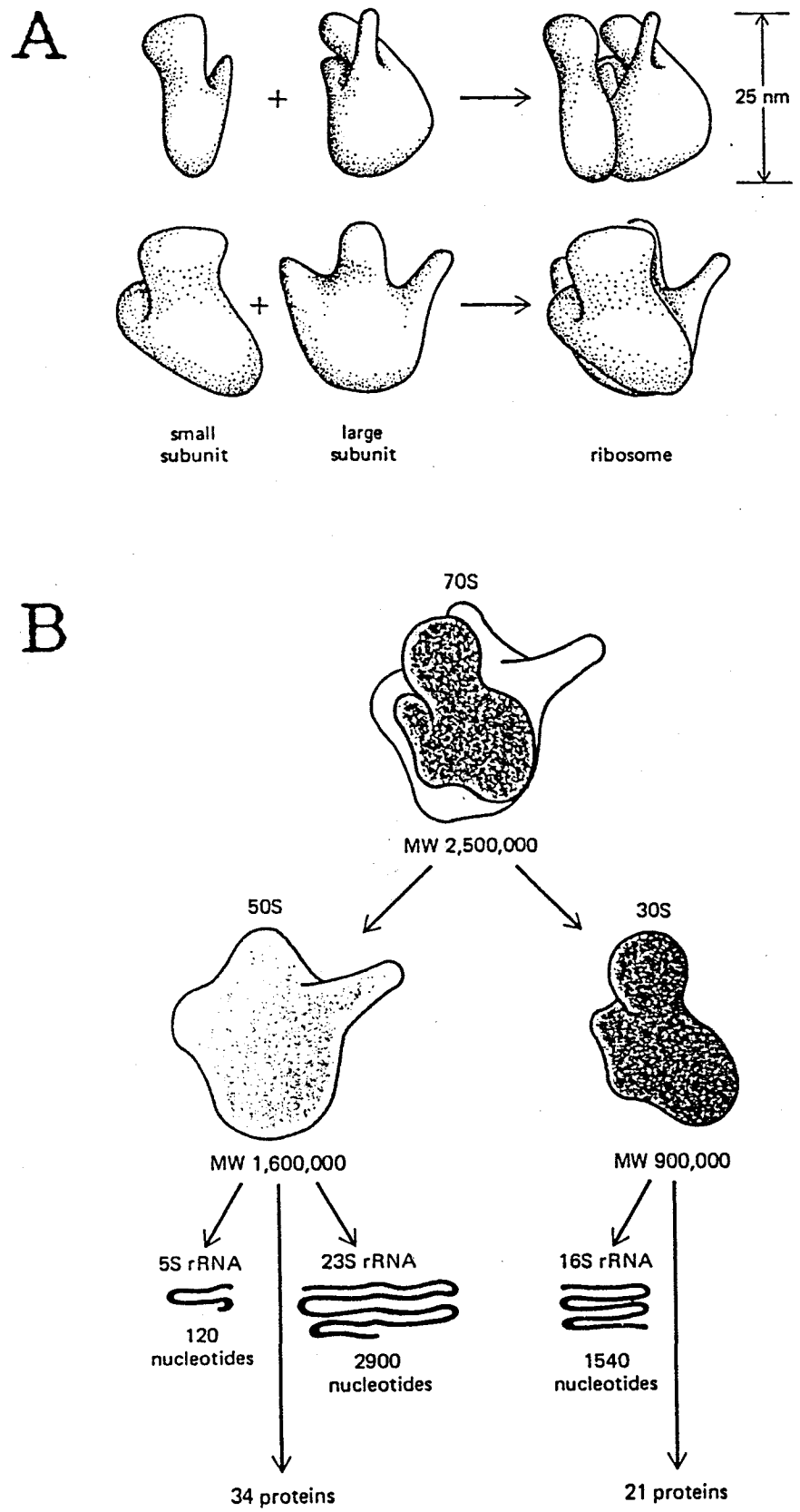

Figure II-3. (A) A three-dimensional model of the bacterial ribosome as viewed from different angles, and (B) its schematic chemical composition. (Alberts, B., Bray, D., Lewis, J., Raff, M., Roberts, K. and Watson, J. D. (1989) "*Molecular Biology of the Cell*" 2nd ed., Garland Publishing Inc., Madison Ave., New York.)

surface of ribosomes. Ribosomes are large complexes of RNA (60 %) and proteins (40 %). Eucaryotic and procaryotic ribosomes are very similar in design and function. Each is composed of one large and one small subunit (Figure II-3 A). The small subunit of procaryotic ribosome consists of one RNA with mass weight 600,000 and twenty one kinds of proteins. The total molecular weight of the small subunit is 900,000. The large subunit consists of two kinds of RNA and thirty four kinds of protein molecules. The total molecular weight of the large subunit is 1,600,000 (Figure II-3 B).

Chromatin[14, 16]

Eucaryotic DNA is tightly bound to a group of small, basic proteins called histones. Histones comprise about half of the mass of eucaryotic chromosomes, the other half being DNA. This nucleoproteins is termed chromatin. There are five types of histones called H1, H2A, H2B, H3 and H4 (and H5 in the case of chicken) (Table II-5) [17]. A striking feature of histones is their high content of positively charged side chains: about one in four residues is either lysin or arginine.

Chromatin is made up of repeating units, each consisting of 200 base pairs of DNA and of two each of H2A, H2B, H3 and H4. These repeating units are known as nucleosomes. Most of the DNA is wound around the outside of a core of histones. The remainder of the DNA, called the linker, joins adjacent nucleosomes and contributes to the flexibility of the chromatin fiber (Figure II-4). Histone H1 molecules appear to be responsible for packing nucleosomes into the 30 nm fiber. The winding of DNA around a nucleosome core contributes to the condensation of DNA.

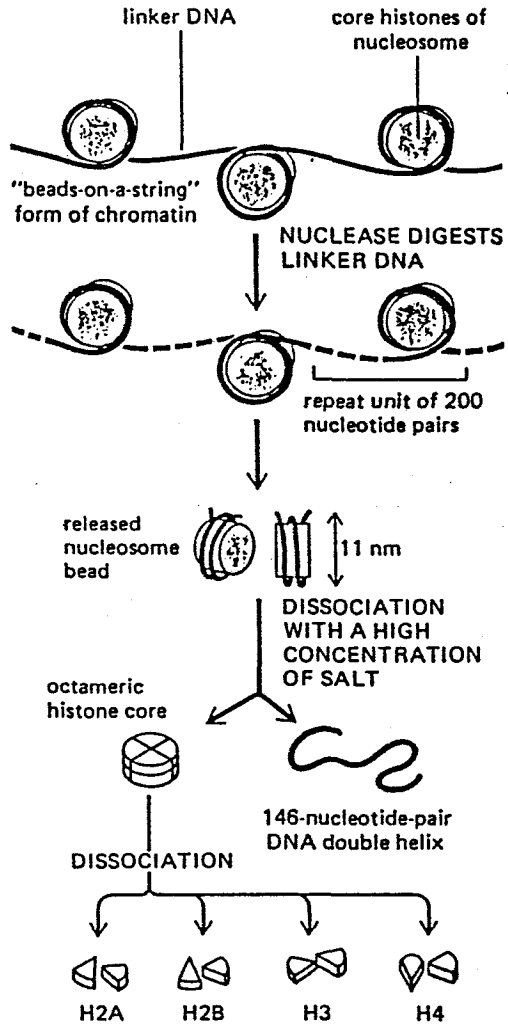

Figure II-4. Model of the structure of chromatin, and its schematic chemical composition. (Alberts, B., Bray, D., Lewis, J., Raff, M., Roberts, K. and Watson, J. D. (1989) "*Molecular Biology of the Cell*" 2nd ed., Garland Publishing Inc., Madison Ave., New York.)

Table II-5. Characteristics of histones. (Stryer, L. (1981) "*Biochemistry*" 2nd ed., W. H. Freeman and Company, New York.)

Type	*Lys/Arg ratio*	*Number of residues*	*Mass (kdal)*	*Location*
H1	20.0	215	21.0	Linker
H2A	1.25	129	14.5	Core
H2B	2.5	125	13.8	Core
H3	0.72	135	15.3	Core
H4	0.79	102	11.3	Core

II-2 Preparation of samples

A Lipid-Containing Bacteriophage, PM2, and Its Host Bacterium, Alteromonas espejiana

Purification of bacteriophage PM2 was carried out according to the modified procedure of Hinnen *et al.* [18]. All experiments were performed at 4°C. Cell debris was removed from the lysate by continuous centrifugation at 13,000 rpm (Tomy No.15S) and the phages were precipitated by incubating the lysate in the presence of 5 % (w/v) polyethyleneglycol 6,000 and 0.5 M NaCl for 48 h. The precipitate was collected by centrifugation at 9,000 rpm (Tomy RPR12-2) for 15 min. The pellet was resuspended in three volumes of buffer-B1 (1 M NaCl, 10 mM $CaCl_2.2H_2O$ and 10 mM Tris-HCl; pH 7.2 at 25°C) [18]. After a low-speed centrifugation, the suspension was layered on the top of a four-step CsCl gradient (455.4, 386.6, 322.7 and 263.3 g CsCl were added to 1 liter of buffer-B1, respectively). The phages were recovered at the interphase of the third and fourth steps after centrifugation at 24,000 rpm (Beckman SW28) for 110 min. The phage fraction was collected and its CsCl concentration was adjusted to 23.14 % (w/w) by dialysis. Then, it was centrifuged at 26,000 rpm (Beckman type 40) for 20 h to achieve the linear gradient of CsCl. The collected phage fraction was dialyzed against the solution of buffer-B1 with 2 M NaCl (buffer-B2) to remove CsCl. In order to avoid the destruction of the phage particle and suppress its rotational motion by high viscosity of solute and solvent, the dialysis was carried out in the presence of sucrose, the concentration of which was changed stepwise 10, 30 and 60 % (w/w) [19]. ^{31}P NMR spectra were measured for about 350 mg of the phage in the presence of 60 % sucrose.

A. espejiana cells were prepared as follows. 3 ml of an overnight culture of *A. espejiana* were added to 300 ml of Q-medium (0.7 g of KCl, 1.5 g of $CaCl_2 \cdot 2H_2O$, 12 g of $MgSO_4 \cdot 7H_2O$, 26 g of NaCl, 5 g of yeast extract (DIFCO) and 10 g of Bacto Tryptone (DIFCO), 1 liter of deionized water, pH 7.4) [20]. It was cultured at 25°C to the middle of the logarithmic phase. Immediately, bacterial cells were harvested at 4°C by centrifugation at

10,000 rpm (Tomy RPR12-2) for 15 min and the pellet was put into a 10 mm ϕ NMR tube. A fresh culture was used for each NMR measurement.

E. coli Phage λ and E. coli

Coli-phage λ was prepared according to the method of Yamamoto and Alberts [21]. In order to get a high concentration by volume reduction and to suppress its rotational motion, the phage preparation for the NMR measurements was dialyzed against λ-buffer (10 mM Tris, 1 mM $MgCl_2$, 0.1 M NaCl and 0.001 g gelatin; pH 7 .5) with 30 % sucrose. About 200 mg of the phage were used for the measurements. There was no difference in the spectra of the samples in the presence of 30 and 60 % sucrose.

E. coli K-12 was cultured at 37°C in YT-broth (5 g NaCl, 5 g yeast extract (DIFCO) and 8 g Bacto Tryptone (DIFCO) per 1 liter of deionized water, pH 7.2) to the middle of the logarithmic phase. The bacterial cells were harvested by centrifugation at 9,000 rpm (Tomy RPR12-2) for 15 min. and then put into 10 mm ϕ NMR tubes. They were immediately used ^{31}P NMR measurements.

Ribosomes of A. espejiana

Ribosome of *A. espejiana* were purified as described by Cox *et al.* [22]. They were finally obtained as a pellet on centrifugation at 60,000 rpm for 90 min. (Beckman Type 65). The pellet was suspended in four volumes of NTCM-buffer (0.5 M NaCl, 10 mM $CaCl_2$, 20 mM $MgCl_2$, 6 mM mercaptoethanol and 10 mM Tris-HCl, pH 7.2 at 25°C) and this suspension was dialyzed against a solution of NTCM-buffer with 60 % sucrose. These three types of samples were used for the ^{31}P NMR measurements.

Chicken Erythrocyte Chromatin

The intact chicken erythrocyte chromatins were obtained as follow [23]. At first, the chicken erythrocyte nuclei were prepared according to Olins *et al.* [24]. Nuclear envelopes were ruptured by gently suspending chicken erythrocyte nuclei in a large volume of STM-buffer (10 mM NaCl, 3 mM $MgCl_2$ and 10 mM Tris, pH 7.4). Then 1 M NaCl was added dropwise and gently up to

100 mM final concentration. The aggregated chromatins were pelleted by centrifugation at 4,000 G for 15 min, and then dialyzed against STM-buffer containing 30 % sucrose. A sample in a dialysis tubing immersed in the buffer containing 30 % sucrose was used for the NMR measurements.

Calf Thymus DNA

Calf thymus DNA was purchased from Sigma Chemical Company. Calf thymus DNA in dry state, in water (50 % (w/w)) and in buffer-A containing 60 % sucrose (35 % (w/w)) were used for ^{31}P NMR measurements.

Extracted Phospholipids of A. espejiana

The total phospholipids of PM2 phages and host cells were obtained according to the method of Bligh and Dyer [25]. They were washed with a 2 mM EDTA solution at pH 7.0 for removing divalent ions. Phosphatidylethanolamine (PE) and phosphatidylglycerol (PG) were purified from the total phospholipid fraction from the host cells by the combination of silicic acid and DEAE-52-cellulose (Whatmann) column chromatography. On silicic acid column chromatography, PE and PG were eluded with chloroform/methanol of 95/5 (v/v) and 80/20 (v/v), respectively. On DEAE-52-cellulose column chromatography, PE was eluded with chloroform/methanol of 80/20 (v/v) and PG was with chloroform/methanol/ ammonia water/ ammonium acetate (160 ml/ 40 ml/ 4 ml/ 760 mg) [26]. For NMR measurements, 300 mg of the lipids were dispersed in 1 ml of buffer-B1.

II-3 Methods of Measurements

^{31}P NMR measurements

Cross-polarization and conventional single-pulse ^{31}P NMR spectra were obtained on a JEOL FX-100 NMR spectrometer equipped with a solid-state NMR system at 40.3 MHz. The field was locked on external deuterium oxide (D_2O). A probe head specially designed for high-power and variable-temperature measurements was

used, in which the sample tube is held vertically. A 45° pulse and 3.0 to 15.0 s relaxation delays were used for the single-pulse measurements. The same relaxation delays were used for the cross-polarization pulse sequence. The proton spins were irradiated during data acquisition. Temperature calibrations for the thermal contact and proton decoupling were carried out. 4,096 data points were used for a spectral width of 50,000 Hz. ^{31}P high-resolution NMR spectra of intact *A. espejiana* cells were obtained on Bruker WM360wb NMR spectrometer without proton irradiation.

DSC measurements

Thermograms of the phospholipid dispersions were measured with a Privalov type calorimeter DASM-IV. Scan rate was 0.25 K/min. The phospholipid concentrations were 10 and 5 mg/ml for the extracted total phospholipids of the host cell and phage PM2, respectively.

References

[1] Franklin, R. M. (1974) *Current Topics in Microbiology and Immunology*, 68, 107.

[2] Conrat, H. F. and Wagner, R. R. (1978) *Comprehensive Virology*, 12, 271.

[3] Franklin, R. M., Hinnen, R., Schäfer, R. and Tsukagoshi, N. (1976) *Phil. Trans. R. Soc. London. B.*, 276, 63.

[4] Franklin, R. M., Marcoli, R., Satake, H., Schäfer, R. and Schneider, D. (1977) *Med. Microbiol. Immunol.*, 164, 87.

[5] Camerini-Otero, R. D. and Franklin, R. M. (1971) *Nature New Biology*, 229, 197.

[6] Schneider, D., Zulauf, M., Schäfer, R. and Franklin, R. M. (1978) *J. M. Biol.*, 124, 97.

[7] Espejo, R. T., Canelo, E. S. and Sinsheimer, R. L. (1971) *J. Mol. Biol.*, 56, 597.

[8] Satake, H., Kania, M. and Franklin, R. M. (1981) *Eur. J. Biochem.*, 114, 623.

[9] Marcoli, R., Pirrotta, V. and Franklin, R. M. (1979) *J. Mol. Biol.*, 131, 107.

[10] Braunstein, S. N. and Franklin, R. M. (1971) *Virology*, 43, 685.

[11] Tsukagoshi, N. and Franklin, R. M. (1974) *Virology*, 59, 408.

[12] Camerini-Otero, R. D. and Franklin, R. M. (1972) *Virology*, 49, 385.

[13] Ptashne, M. (1986) "*A Genetic Switch*", Cell Press.

[14] Alberts, B., Bray, D., Lewis, J., Raff, M., Roberts, K. and Watson, J. D. (1989) "*Molecular Biology of the Cell*" 2nd ed. Garland Publishing, Inc., Madison Ave., New York.

[15] Lake, J. A. (1985) *Ann. Rev. Biochem.*, 54, 507.

[16] Kornberg, R. D. and Klug, A. (1981) *Sci. Amer.*, 244, 48.

[17] Stryer, L. (1981) "*Biochemistry*" 2nd ed., W. H. Freeman and Company, New York.

[18] Hinnen, R., Schafer, R. and Franklin, R. M. (1974) *Eur. J. Biochem.*, 50, 1.

[19] Akutsu, H., Satake, H. and Franklin, R. M. (1980) *Biochemistry*, 19, 5264.

[20] Franklin, R. M., Salditt, M. and Silbert, J. A. (1969) *Virology*, 38, 627.

[21] Yamamoto, K. R. and Alberts, B. M. (1970) *Virology*, 40, 734.

[22] Cox, E. C., White, J. R. and Flaks, J. G. (1964) *Proc. N. A. S.*, 51, 703.

[23] Olins, A. L., Carlson, R. D., Wright, E. B. and Olins, D. E. (1976) *Nucleic Acids Res.*, 3, 3271.

[24] Nishimoto, S., Akutau, H. and Kyogoku, Y. (1987) *FEBS Lett.*, 213, 293.

[25] Bligh, E. G. and Dyer, W. J. (1959) *Can. j. Biochem. Physiolo.*, 37, 911.

[26] Law, J. H. and Essen, B. (1969) "*Methods in Enzymology*" ed. by Lowenstein, J. M., Academic Press, New York, **14**, 665.

Chapter III

Theoretical Background of Solid State NMR

Basic Principle of Cross-Polarization[1, 2]

Suppose we have a solid state system of abundant I and rare S spins i.e. $N_I >> N_S$, where N is the number of spins. The powder pattern NMR spectrum of the rare spins, which is obtained under the decoupling of heteronuclear dipolar interaction with the abundant spins, gives principal shielding values (σ_{11}, σ_{22}, σ_{33}) reflecting chemical environments and motion of the rare spins. The NMR signal of rare spin system, however, is extremely weak, because of (i) the low natural abundance, (ii) the small gyromagnetic ratio and (iii) usually a long spin lattice relaxation time. The cross-polarization pulse technique was developed by Pines *et al.* in order to obtain high resolution spectra of rare spins in solid by solving these problems. The technique involves three main steps i.e. the cooling of abundant spins, the magnetic transfer from the abundant to rare spins in the rotating frame and the decoupling of abundant spins as shown in Figure III-1.

At first a basic account on cross-polarization experiments and next the cross-polarization dynamics will be discussed.

The density matrix of the spin system defined by the temperature T is

$$\hat{\rho}=\exp(-\hat{H}/kT)/\mathrm{Tr}\{\exp(-\hat{H}/kT)\} \quad (1)$$

Here $\hat{H}$ and k represent the Hamiltonian of the spin system and Boltzman constant, respectively. By the use of $\hat{H}=\gamma\hbar\Sigma I_i B_i$ and the high temperature approximation we write for the magnetization of i direction

$$M_i=\mathrm{Tr}\{\hat{\rho}M_i\}=C\beta B_i. \quad (2)$$

Here C, B_i and β represent Curie constant, the magnetic field of i direction and the inverse temperature defined by $\beta=1/kT$, respectively. Curie constants of I and S spins are

$$C_I=(1/3)N_I\gamma_I^2\hbar^2 I(I+1), \quad (3)$$

and

$$C_S=(1/3)N_S\gamma_S^2\hbar^2 S(S+1), \quad (4)$$

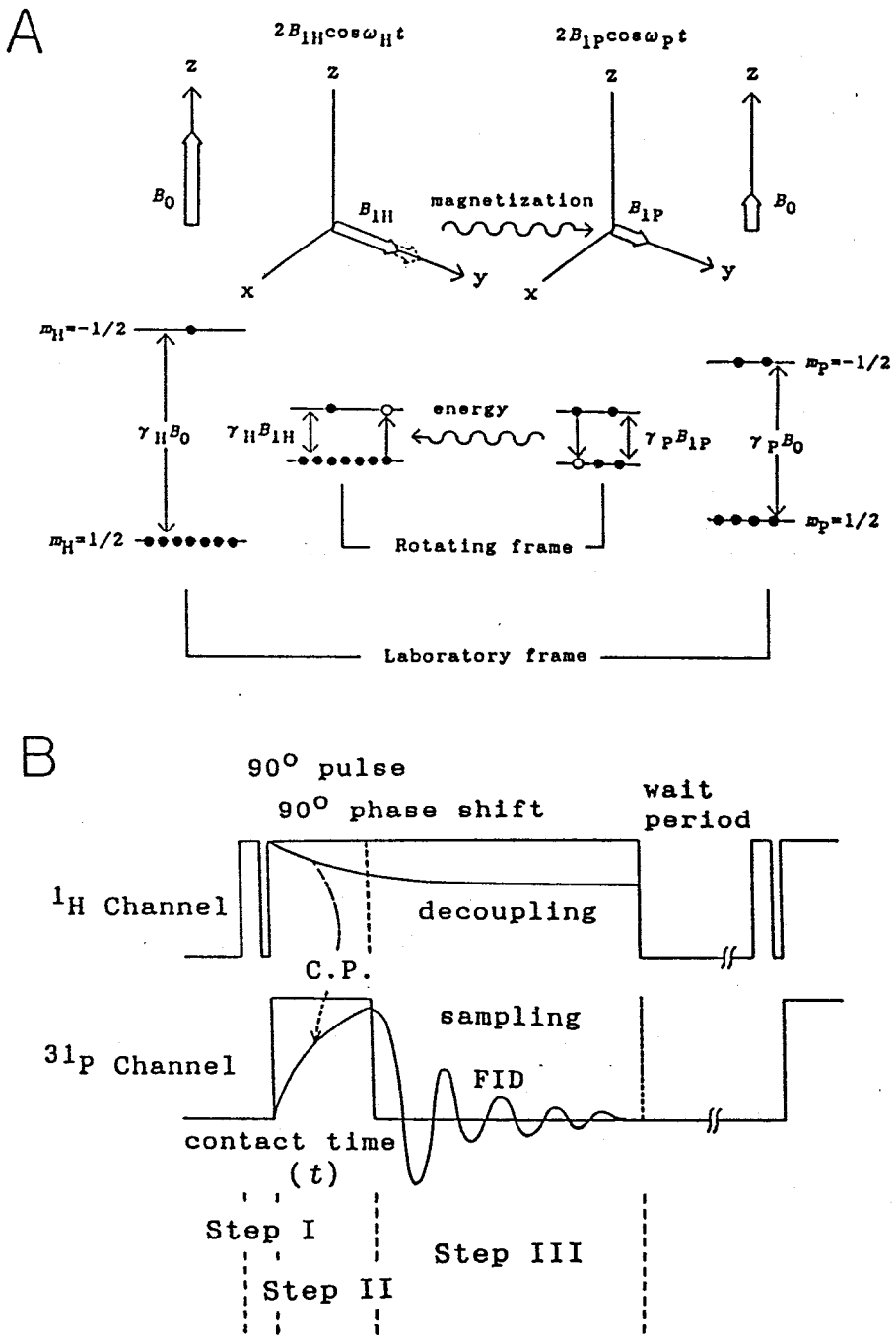

Figure III-1. (A) A scheme of ^{1}H-^{31} cross-polarization. Upper one shows magnetizations of ^{1}H and ^{31}P in their respective laboratory and rotating frames, and magnetization transfer from ^{1}H to ^{31}P spin systems in their rotating frames. Lower one shows energy levels of ^{1}H and ^{31}P in their respective laboratory and rotating frames, and energy transfer from ^{31}P to ^{1}H spin systems in their rotating frames with magnetization transfer. (B) ^{1}H-^{31}P cross-polarization pulse sequence.

respectively. Here, γ, $\hbar$, I and S represent gyromagnetic ratio, universal constant and spin quantum number of I and S spins, respectively. When a sample is in the static magnetic field B_0 and the spin systems are in the thermal equilibrium with the lattice, the magnetizations of I and S spins are

$$M_{0I}=\beta_L C_I B_0, \tag{5}$$

and $$M_{0S}=\beta_L C_S B_0, \tag{6}$$

respectively. Here β_L is the inverse lattice temperature. Abundant spin I with a large gyromagnetic ratio generally has the magnetization enough for measurements. But rare spin S with a small gyromagnetic ratio has only small magnetization. Therefore, it is desirable to amplify the magnetization of the rare spin by transferring the large magnetization of the abundant spin to the rare spin system. The effective transfer of the magnetization from I to S spin system can be performed through two processes i.e. cooling of the abundant I spin system and bringing I and S spin systems into contact.

The cooling of the abundant I spin system can be achieved as mentioned below. The magnetization of abundant spins M_{0I} in equilibrium with the lattice is turned to the y-axis of the rotating frame by a $\pi/2$ pulse of the oscillating magnetic field $2B_{1I}\cos\omega_I t$, ($\omega_I=-\gamma_I B_0$), which gives the static magnetic field B_{1I}, along the x-axis in the rotating frame. And immediately after the $\pi/2$ pulse, M_{0I} is spin-locked along the y-axis of the rotating frame by shifting the phase of the r.f. field by $\pi/2$. In the rotating frame, the magnetization of spin I, M_I, can be described as follows, using the inverse spin temperature in the rotating frame, β_I.

$$M_I=\beta_I C_I B_{1I}. \tag{7}$$

Since $M_I=M_{0I}$ in this case, equations (5) and (7) give

$$\beta_I=\beta_L B_0/B_{1I}. \tag{8}$$

In this case, since $B_{1I}<<B_0$ is hold, I spin system has a very low spin temperature in the rotating frame.

When we irradiate the r.f. magnetic field $2B_{1S}\cos\omega_S t$, ($\omega_S=-\gamma_S B_0$), to the rare spin S, the spin temperature of the S spin system in the rotating frame is infinitively high, because the magnetization of S spins is zero at the beginning. At this

point, if the Hartmann-Hahn condition, equation (9), is fulfilled, the energy difference between the two quantized states of I and S spin systems in their respective rotating frames are equal to each other. Thus, the energy transfer from the S to I spin systems can be induced by the flip-flop term in the dipolar Hamiltonian.

$$\gamma_S B_{1S} = \gamma_I B_{1I}. \tag{9}$$

Namely, the polarization transfer from the abundant to rare spin systems occurrs under the Hartmann-Hahn condition and their spin temperatures become equal to each other, β_f, under total energy conservation.

In the high temperature approximation, the energy of spin system can be described as

$$E = \mathrm{Tr}\{\hat{\rho}\hat{H}\} = -\beta C B^2. \tag{10}$$

Therefore, from the total energy conservation through whole processes in the thermal contact between I and S spins,

$$\beta_I(t) C_I B_{1I}^2 + \beta_S(t) C_S B_{1S}^2 = \beta_f (C_I B_{1I}^2 + C_S B_{1S}^2). \tag{11}$$

As $\beta_S(0)=0$ at $t=0$, equation (11) leads to

$$\beta_f/\beta_I(0) = (1+\varepsilon)^{-1}, \tag{12}$$

Where $\varepsilon = (C_S B_{1S}^2)/(C_I B_{1I}^2)$ is the ratio of the heat capacities of the S and I spins.

If the Hartmann-Hahn condition is fulfilled, we obtain the following relationship from equations (3) and (4), and $N_I >> N_S$.

$$\varepsilon = \{N_S S(S+1)\}/\{N_I I(I+1)\} << 1. \tag{13}$$

With $M_I^{(f)} = \beta_f C_I B_I$ and $M_S^{(f)} = \beta_f C_S B_S$, the final I and S spin magnetizations reach

$$M_I^{(f)} = (1+\varepsilon)^{-1} M_I(0) \fallingdotseq M_I(0), \tag{14}$$

and $$M_S^{(f)} = (\gamma_I/\gamma_S)(1+\varepsilon)^{-1} M_{0S} \fallingdotseq (\gamma_I/\gamma_S) M_{0S}, \tag{15}$$

respectively. Where $M_I(0)$ is the initial magnetization of the I spins and M_{0S} is the Zeeman magnetization of the S spins.

If the magnetic ratio γ_I of abundant spin I is bigger than that of rare spin S, the magnetization of S spin is amplified by cross-polarization. The magnetization of rare spins is observed as FID after switching off B_{1S}. Here, the r.f. magnetic field B_{1I} is utilized for polarization transfer during the cross-polarization and is used for decoupling of I spins during the observation of FID of rare spin S.

Next, let's consider a phenomenological approach to describe the variation of the inverse spin temperatures β_I and β_S of the I and S spins, respectively.

We assume that the Hartmann-Hahn condition is fulfilled between I and S spin systems and that the systems interact not only with each other but also with the lattice, as shown schematically in Figure III-2. Here, the time constants of energy transfer between I and S spins, between I and lattice and between S and lattice are expressed by T_{IS}, $T_{1\rho}(I)$ and $T_{1\rho}(S)$, respectively. If we invoke energy conservation in the rotating frame, we can write

$$d\beta_I/dt+\varepsilon' d\beta_S/dt=0, \tag{16}$$

where $\varepsilon'=\varepsilon\alpha^2$. Here $\varepsilon=\{N_S S(S+1)\}/\{N_I I(I+1)\}$, $\alpha=(\gamma_S B_{1S})/(\gamma_I B_{1I})$. The S spin temperature β_S is relaxed with the time constant T_{IS} towards the instantaneous I spin-temperature which results in the following coupled differential equations:

$$d\beta_S/dt=-T_{IS}(\beta_S-\beta_I)-T_{1\rho}(S)^{-1}\beta_S, \tag{17}$$

and

$$d\beta_I/dt=-(\varepsilon'/T_{IS})(\beta_I-\beta_S)-T_{1\rho}(I)^{-1}\beta_I, \tag{18}$$

where the last term in equations (17) and (18) have been added to account for spin-lattice relaxations of I and S spins. These coupled differential equations are straightforwardly solved in the ordinary manner under the initial conditions

$$\beta_S(0)=0 \text{ and } \beta_I(0)=\beta_{0I}, \tag{19}$$

resulting in

$$\beta_S(t)=\beta_{0I}(a_+-a_-)^{-1}[\exp(-a_- t/T_{IS})-\exp(-a_+ t/T_{IS})], \tag{20}$$

and

$$\beta_I(t)=\beta_{0I}(a_+-a_-)^{-1} \times[(1-a_-)\exp(-a_- t/T_{IS})-(1-a_+)\exp(-a_+ t/T_{IS})], \tag{21}$$

where $a_+=a_0[1+(1-b/a_0^2)^{1/2}]$, $a_-=a_0[1-(1-b/a_0^2)^{1/2}]$, $a_0=[(1+\varepsilon\alpha^2+T_{IS}/T_{1\rho}(I)+T_{IS}/T_{1\rho}(S)]/2$, $\alpha=\gamma_S B_{1S}/\gamma_I B_{1I}$ and $\varepsilon=N_S/N_I$.

According to equation (21), the magnetization of the rare spins $M_S(t)$ at contact time t is expressed as

$$M_S(t)=C_S B_{1S}\beta_S(t), \tag{22}$$

and the magnetization of the rare spins at equilibrium with lattice in the static magnetic field B_0 is

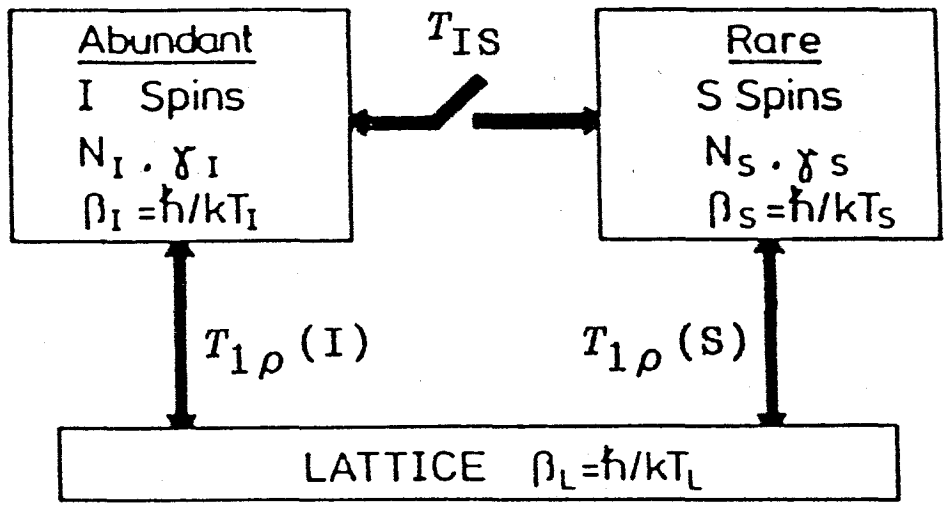

Figure III-2. Schematic representation of an abundant I spin reservoir and a rare S spin reservoir, which are coupled to the lattice as expressed by their spin lattice relaxation times T_{1I} and T_{1S}. The coupling between the two reservoirs as represented by the cross relaxation time T_{IS} can be varied at the experimenters discretion by a suitable application of rf fields. (Mehring, M. (1983) "*Principles of High Resolution NMR in Solids*", Springer-Verlag, Berlin.)

A

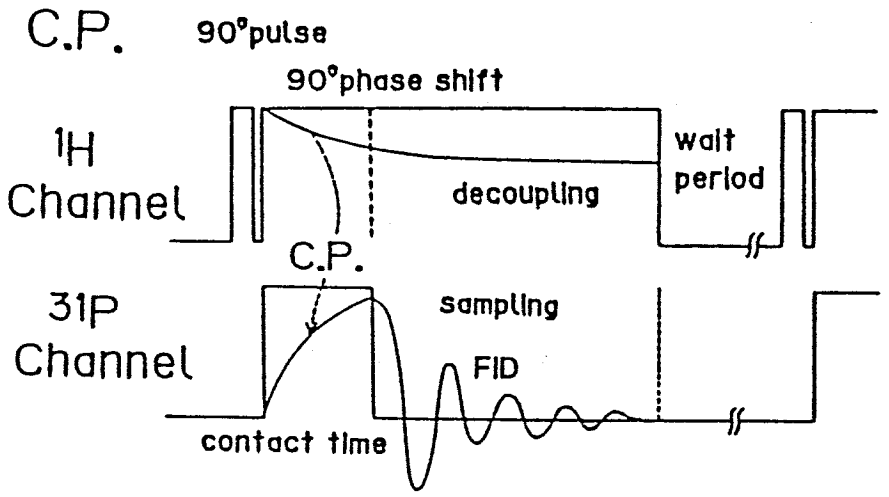

B

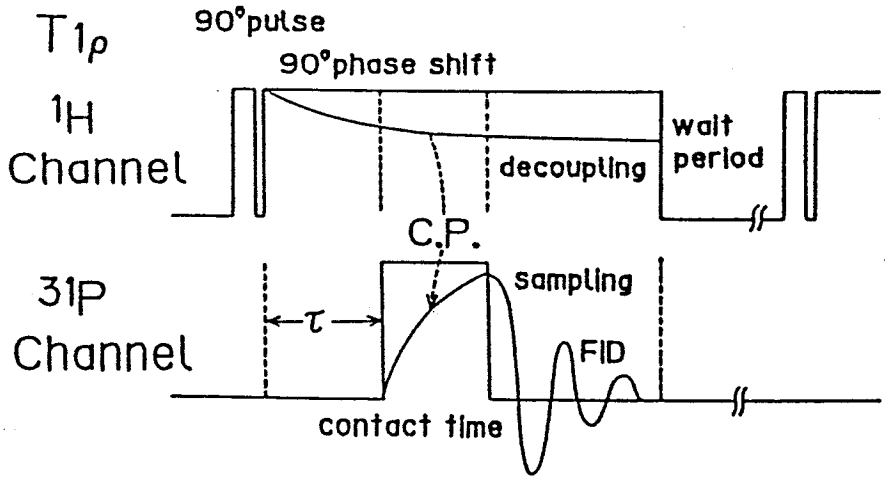

Figure III-3. ^{1}H-^{31}P cross-polarization pulse sequences used for the measurement for (A) contact time dependence of spectral total intensity and (B) spin lattice relaxation time of proton in the rotating frame. Here t and τ represent variables in the pulse sequences of (A) and (B), respectively.

$$M_{0S}=\beta_L B_0 C_S. \quad (23)$$

Equations (22) and (23) lead to

$$M_S(t)=(B_{1S}/B_0)(\beta_S(t)/\beta_L)M_{0S}$$
$$=\alpha(\gamma_I/\gamma_S)(\beta_S(t)/\beta_{0I})M_{0S}, \quad (24)$$

where the transform from second to third term is done by the use of $\alpha=\gamma_S B_{1S}/\gamma_I B_{1I}$.

Combining equations (20) and (24), we obtain

$$M_S(t)=\alpha(\gamma_I/\gamma_S)(a_+-a_-)^{-1}[\exp(-a_- t/T_{IS})-\exp(-a_+ t/T_{IS})]M_{0S} \quad (25)$$

for the normal cross-polarization pulse sequence (Figure III-3 A).

If $(\varepsilon\alpha^2)^2<<1$, $T_{IS}/T_{1\rho}(S)<<1$ and the Hartmann-Hahn condition is fulfilled, equation (25) becomes

$$M_S(t)=K(1+\alpha\varepsilon^2-T_{IS}/T_{1\rho}(I))^{-1}$$
$$\times[\exp(-t/T_{1\rho}(I))-\exp(-t(1+\varepsilon\alpha^2)/T_{IS})] \quad (26)$$

with $K=\alpha(\gamma_I/\gamma_S)M_{0S}$. This equation can be used for the analysis of the contact time dependence of the intensity of a cross-polarization signal.

The spin-lattice relaxation time of abundant spins in the rotating frame can be determined by changing $\beta_I(0)$. In this case, $\beta_I(0)$ is not equal to β_{0I} any more. Instead of equation (26), we get

$$M_S(t,\tau)=\varepsilon\alpha(\gamma_S/\gamma_I)(1+\varepsilon\alpha^2-T_{IS}/T_{1\rho}(I))^{-1}$$
$$\times[\exp(-t/T_{1\rho}(I))-\exp(-t(1+\varepsilon\alpha^2)/T_{IS})]M_I(0,\tau) \quad (27)$$

with $M_I(0,\tau)=M_I\exp(-\tau/T_{1\rho}(I))$. On fixing t, this leads to

$$M_S(\tau)=C_t\exp(-\tau/T_{1\rho}(I)), \quad (28)$$

where C_t is constant. Equation (28) can be used for the analysis of the direct measurement of $T_{1\rho}(H)$. The pulse sequence is shown in Figure III-3 B [3].

Line Shape of NMR spectra of Solid Samples[2, 4, 5, 6]

There are many biological macromolecules and supramolecules which are difficult or impossible to be crystallized. In the case of molecules in a suppressed motion, their spectrum shows a

very broad and characteristic line shape, powder-type pattern. For example, ^{31}P NMR spectra of dry DNA or phospholipids show the powder-type pattern reflecting their respective dynamic structures under the proton decoupling. These powder-type spectra are mainly explained by the next three factors. (i) Since the electron density around ^{31}P nuclei is not isotropic but depends on the bonding pattern, the electronic shielding is smallest along the axis with the lowest electron density and largest along the molecular axis with the highest electron density. (ii) Non-oriented samples are distributed to all directions statistically. (iii) Rapid motions of molecules overage the interaction tensor, giving rise to a characteristic powder type pattern. Namely, powder type pattern spectra contain the information about the structures and dynamic states of molecules. What is important for us, is how to get high-resolutional or useful information from such spectra. Therefore, in this section we derive the relationship between the powder patterns and the structure or dynamic states of molecules.

The shielding Hamiltonian of the spin can be expressed as coupling of the spin I with the magnetic field B_0 via the shielding tensor $\tilde{\sigma}$ in the laboratory frame, whose z-axis is selected to be B_0 direction:

$$\begin{aligned}\hat{H}_S &= \gamma\hbar\hat{I}\tilde{\sigma}B_0 \\ &= \gamma\hbar(I_x\ I_y\ I_z)\begin{pmatrix}\sigma_{11}' & \sigma_{12}' & \sigma_{13}' \\ \sigma_{21}' & \sigma_{22}' & \sigma_{23}' \\ \sigma_{31}' & \sigma_{32}' & \sigma_{33}'\end{pmatrix}\begin{pmatrix}0 \\ 0 \\ B_0\end{pmatrix} \\ &= \gamma B_0\hbar(\sigma_{13}'I_x+\sigma_{23}'I_y+\sigma_{33}'I_z). \qquad (29)\end{aligned}$$

The Kubo-Tomita theorem suggests that perturbation Hamiltonian, which do not commute with Zeeman energy term, give little influence to shift and strength of absorption within second-order perturbation approximation, and line broadening or the increase in the second moment are caused by perturbations which commute with Zeeman energy. As only third term in equation (29) is commutational with Zeeman energy, NMR spectra of solid samples are mainly determined by the third term. This suggests that chemical shift observed for solid samples is 3-3 component (σ_{33}') of second rank chemical shift tensor in the laboratory

frame.

On the other hand, the chemical shift tensor ($\tilde{\sigma}_p$) in the principal coordinate system is expressed as

$$\tilde{\sigma}_p=\begin{pmatrix}\sigma_{11} & 0 & 0\\ 0 & \sigma_{22} & 0\\ 0 & 0 & \sigma_{33}\end{pmatrix}, \tag{30}$$

where σ_{11}, σ_{22} and σ_{33} are principal components of the tensor and we use the convention: $\sigma_{11}<\sigma_{22}<\sigma_{33}$. σ_{11} and σ_{33} represent the directions of the lowest and highest electron density, respectively. σ_{22} is perpendicular to the plane involving σ_{11} and σ_{33}.

Suppose $\tilde{\sigma}_p$ is a second rank tensor expressed in the principal axis system (Figure III-4) and $\tilde{\sigma}$ is the same tensor expressed in the laboratory frame system which is related to the principal axis system by a unitary transformation $\tilde{R}(\alpha, \beta, \gamma)$ with the Euler angles (α, β, γ) (Figure III-5). Then,

$$\tilde{\sigma}=\tilde{R}\tilde{\sigma}_p\tilde{R}^{-1}, \tag{31}$$

where

$$\tilde{R}(\alpha, \beta, \gamma)=\begin{pmatrix}\cos\gamma\cos\beta\cos\alpha-\sin\gamma\sin\alpha & \cos\gamma\cos\beta\sin\alpha+\sin\gamma\cos\alpha & -\cos\gamma\sin\beta\\ -\sin\gamma\cos\beta\cos\alpha-\cos\gamma\sin\alpha & -\sin\gamma\cos\beta\sin\alpha+\cos\gamma\cos\alpha & \sin\gamma\sin\beta\\ \sin\beta\cos\alpha & \sin\beta\sin\alpha & \cos\beta\end{pmatrix}. \tag{32}$$

From equations (29), (30), (31) and (32), we get the following relationship:

$$\sigma_{33}'=\sigma_{11}\cos^2\alpha\sin^2\beta+\sigma_{22}\sin^2\alpha\sin^2\beta+\sigma_{33}\cos^2\beta. \tag{33}$$

The observed frequency ω of a spectral line can be expressed by the Euler angles (α,β) which relate the principal axes of the tensor $(\omega_{11}, \omega_{22}, \omega_{33})$ to the laboratory frame as

$$\omega=\omega_{11}\cos^2\alpha\sin^2\beta+\omega_{22}\sin^2\alpha\sin^2\beta+\omega_{33}\cos^2\beta. \tag{34}$$

If $I(\omega)$ is the intensity of the NMR signal at the frequency ω and $P(\Omega)d\Omega$ is the probability of finding the tensor orientation in the range between the solid angle Ω and $\Omega+d\Omega$,

$$P(\Omega)d\Omega=I(\omega)d\omega. \tag{35}$$

In a powder, all angles of Ω are equally probable i.e. $P(\Omega)=1/4\pi$, it leads to

$$I(\omega)=(1/4\pi)\ d\Omega/d\omega, \tag{36}$$

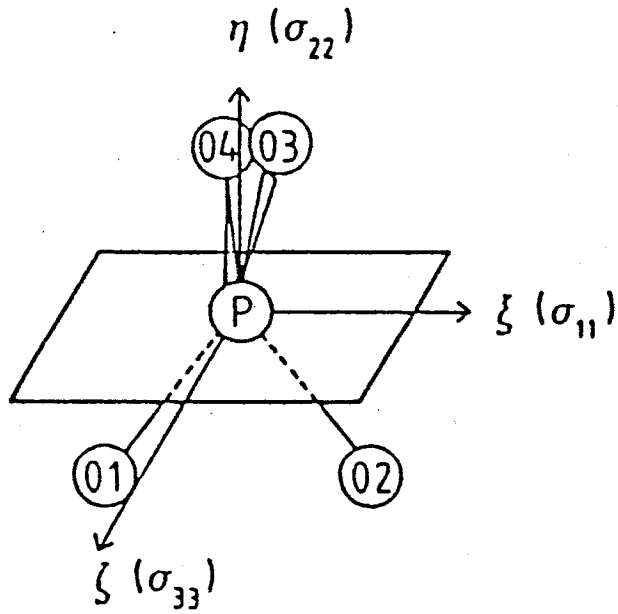

Figure III-4. Orientation of the ^{31}P chemical shift tensor (principal components σ_{ii}) in the molecular frame of the phosphate segment. O(3) and O(4) are the two nonesterified oxygens. O(1) and O(2) connect the phosphate group with the glycerol back bone and the head group residue, respectively, of the phospholipid molecule. (Seelig, J. (1978) *Biochim. Biophys. Acta* **515**, 105.)

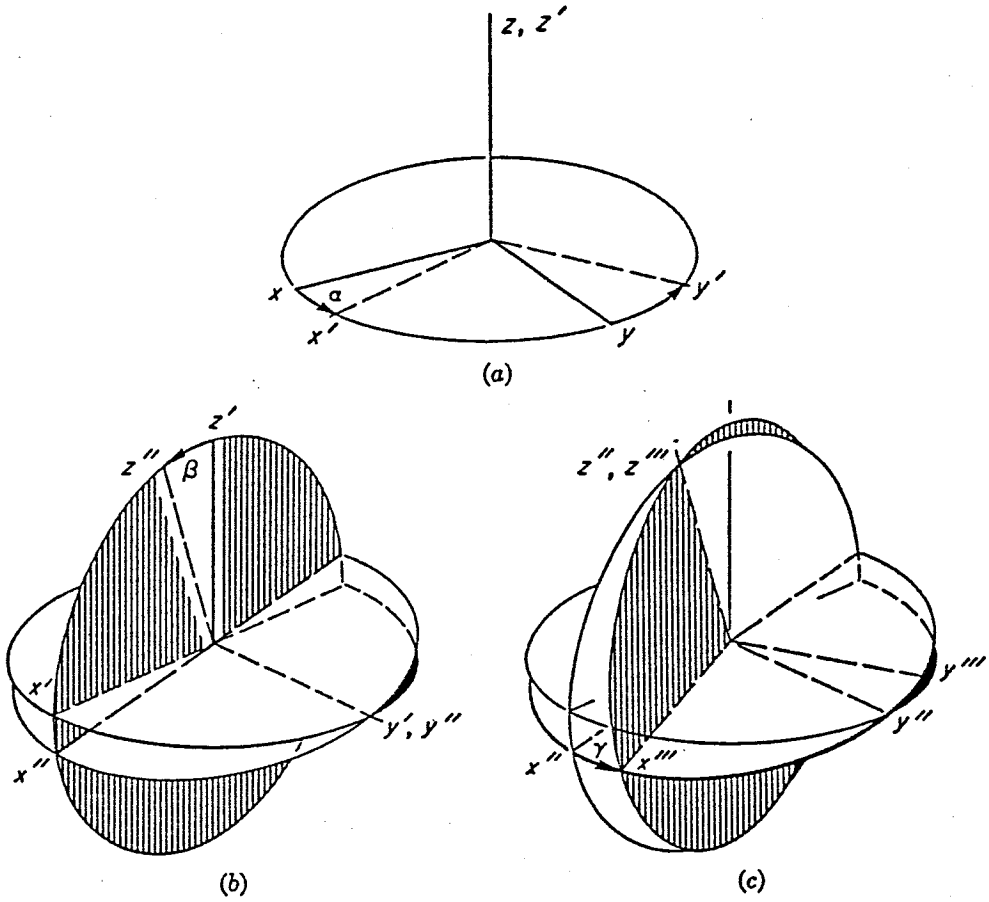

Figure III-5. The Euler angles α, β and γ and the three Euler rotations which carry the initial (x, y, z) coordinate system into the final (x''', y''', z''') coordinate system. (Rose, M. E. (1967) "*Elementary Theory of Angular Momentum*", J. Wiely, New York.)

where $d\Omega = \sin\beta\, d\beta\, d\alpha$.

In the case that the tensor has the axial symmetry i.e. $\omega_{//} = \omega_{33}$ and $\omega_{\perp} = \omega_{11} = \omega_{22}$, equation (34) becomes

$$\omega = (\omega_{//} - \omega_{\perp})\cos^2\beta + \omega_{\perp}. \tag{37}$$

Using equations (35) and (36) so obtained the line shape function as

$$I(\omega) = (1/2)[(\omega_{//} - \omega_{\perp})(\omega - \omega_{\perp})]^{-1/2}. \tag{38}$$

The general case with $\omega_{33} > \omega_{22} > \omega_{11}$ is more complicated and the line shape function is expressed as

$$I(\omega) = \pi^{-1}(\omega - \omega_{11})^{-1/2}(\omega_{33} - \omega_{22})^{-1/2}K(m) \tag{39a}$$

with

$$m = (\omega_{22} - \omega_{11})(\omega_{33} - \omega)/(\omega_{33} - \omega_{22})(\omega - \omega_{11})$$

for

$$\omega_{33} > \omega > \omega_{22},$$

and

$$I(\pi) = {}^{-1}(\omega_{33} - \omega)^{-1/2}(\omega_{22} - \omega_{11})^{-1/2}K(m) \tag{39b}$$

with

$$m = (\omega - \omega_{11})(\omega_{33} - \omega_{22})/(\omega_{33} - \omega)(\omega_{22} - 1\,1)$$

for

$$\omega_{22} > \omega > \omega_{11}.$$

$I(\omega) = 0$ in case $\omega > \omega_{33}$ and $\omega < \omega_{11}$.

$K(m)$ is the complete elliptic integral of the first kind

$$K(m) = \int_0^{2\pi} d\phi\,[1 - m\sin^2\phi\,]^{-1/2}. \tag{40}$$

The line shapes according to equations (38) and (39) are plotted in Figure III-6. Usually, a residual line broadening is taken into account by convention of $I(\Omega)$ with a broadening function (Lorentzian or Gaussian).

$\Delta\sigma = \sigma_{33} - \sigma_{11}$ and $\Delta\sigma = \sigma_{//} - \sigma_{\perp}$, which are called chemical shielding anisotropy, give the information on the dynamic states of molecules. For example, in the case that fluctuation as shown Figure III-7 is added to the molecular motions and the fluctuation is more rapid than the time scale of NMR, spins cannot distinguish different environments, i.e., the chemical shielding anisotropy becomes partially averaged, leading to a smaller residual chemical shielding anisotropy. It is evident from Figure III-6 and the corresponding formula for the powder spectrum how the principal shielding components (σ_{11}, σ_{22}, σ_{33}) can be obtained directly

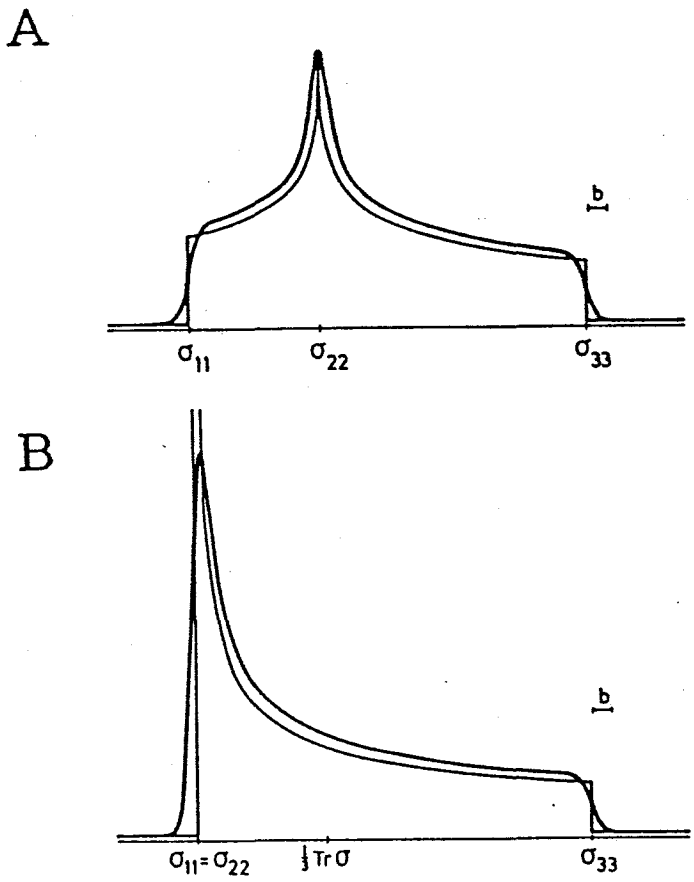

Figure III-6. Schematic representation of theoretical powder line shapes for second rank tensor interactions. The theoretical curves are convoluted with Lorentzian broadening functions, whose width b is indicated. (A) Arbitrary second rank tensor, (B) axially symmetric second rank tensor. (Mehring, M. (1983) "*Principles of High Resolution NMR in Solids*" 2nd ed., Springer-Verlag, Berlin.)

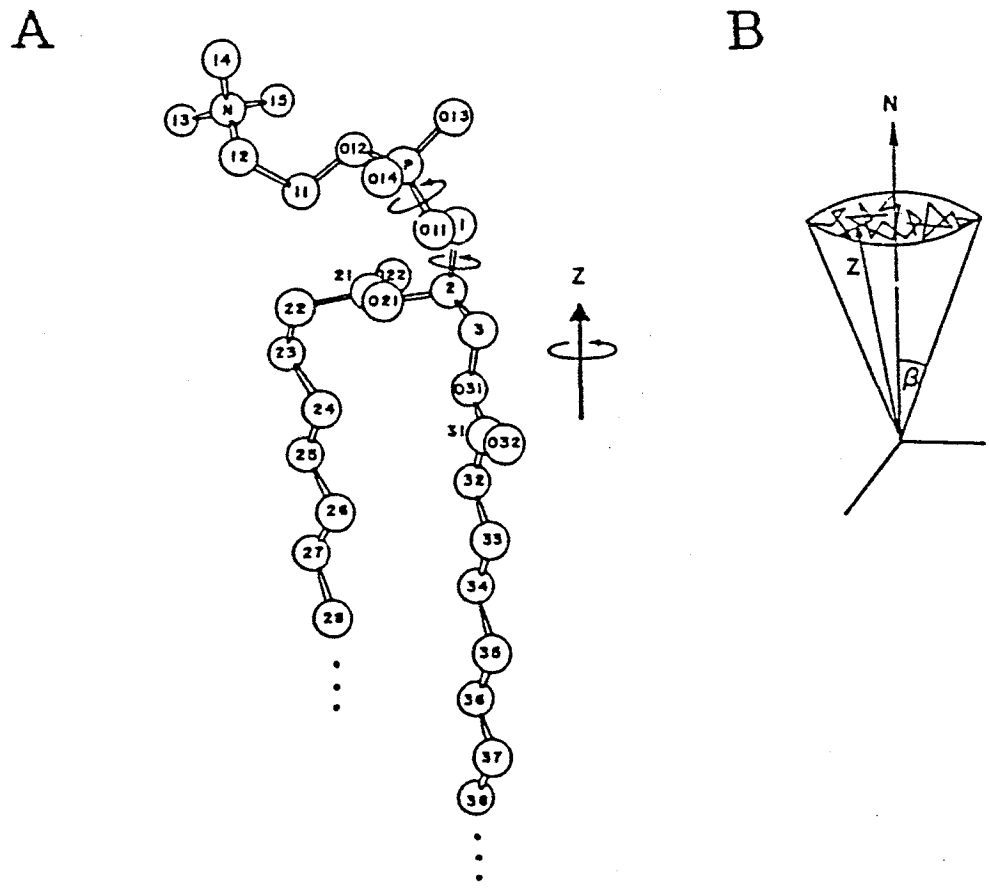

Figure III-7. Motions used in the formulation of the model of head-group motion. A truncated DPPC molecule is drawn in a and the rotations about P-O11, C1-C2, and the molecular z axis are indicated. Rotation about O11-CI was also considered, but could not be shown on the figure. The labeling of the atoms is consistent with that used in the x-ray crystallographic work on dilauroyl PE. The wobble motion is schematically drawn in b. The molecular z axis executes a random walk with in a cone centered on the bilayer normal N. Variation of the angle β changes the area over which z may execute the walk. (Kohler, S. J. and Klein, M. P. (1977) *Biochemistry* 16, 519.)

from the spectrum.

References

[1] Akutsu, H. (1986) *J. Magn. Reson.*, **66**, 250.

[2] Mehring, M. (1983) "*Principles of High Resolution NMR in Solids*", Springer-Verlag, Berlin

[3] Stejskal, E. O., Schaefer, J., Sefcik, M. D. and MacKay, R. A. (1981) *Macromolecules*, **14**, 275

[4] Kubo, R and Tomita, K. (1954) *J. Phys. Soc. Japan*, **9**, 888.

[5] Rose, M.E. (1967) "*Elementary Theory of Angular Momentum*", J. Wiley, New York

[6] Seelig, J. (1978) *Biochim. Biophys. Acta*, **515**, 105.

Chapter IV

Cross-Polarization Method for Detection of the Dynamic State of Each Component in Supramolecular Systems

Summary

A method to get a ^{31}P NMR spectrum of a particular supramolecular structure in an intact biological system was developed by applying the ^{1}H-^{31}P cross-polarization technique to a lipid-containing bacteriophage PM2 and its host bacterium, *A. espejiana*. It was shown that ^{31}P NMR spectra of nucleic acids and lipid bilayers can be obtained separately with short and long thermal contacts, respectively.

IV-1. Introduction

Solid-state ^{31}P NMR is one of the most powerful tools for studies of phosphorus containing molecules undergoing limited motion such as phospholipids in biomembranes and nucleic acids in chromosome complexes or ribosome particles. The conventional single pulse technique, however, cannot be used for the studies of complicated systems such as an intact cell, since the resonances of all phosphorus containing molecules overlap with one another in the spectrum because of the extraordinarily broad line width of suppressed molecules. To get meaningful information, the signal of interest should be observed separately. For this purpose, the ^{1}H-^{31}P cross-polarization technique has been shown to be promising [1, 2]. By the use of this technique, the ^{31}P NMR spectra of chromatins in intact chicken erythrocytes [2] and nucleic acids in intact bacterial cells [3] were observed selectively.

In this work, we developed this method to get information on the biomembranes and suppressed supramolecular nucleic acids in intact biological systems. A lipid-containing bacteriophage,

PM2, and its host cell, *A. espejiana*, were used for this purpose. *A. espejiana* is a marine bacterium, the optimal growth temperature of which is in the range of 20 - 25°C [4]. The phage PM2 was extensively investigated by the use of biochemical and biophysical methods [5, 6, 7]. It consists of four kinds of proteins (73.1 % by dry weight), lipids (12.6 %) and a circular double-stranded DNA (14.3 %) [7]. There are only two different phosphorus-containing molecular species, namely, phospholipids and DNA. Because of the simplicity of the components, the intact phage was investigated by conventional ^{31}P NMR which gave rise to an overlap of two powder patterns from phospholipids and DNA [8]. In contrast, the host cell has a much more complicated system. It consists of many kinds of metabolite molecules and a variety of RNAs in addition to the thousands of proteins, lipids and DNA. Therefore, the phage PM2 and its host cell provide good model systems to exploit a new method to investigate supramolecular systems *in vivo*.

Our results showed that ^{1}H-^{31}P cross-polarization method can be used to get the membrane and the supramolecular nucleic acid spectra selectively even in such a complicated system as a cell.

IV-2. Results

^{1}H-^{31}P Cross-Polarization spectra of Bacteriophage PM2.
Bacteriophage PM2 is a good model system to study the membrane in the intact state because of its simple composition. Figure IV-1 A shows a ^{31}P NMR spectrum of PM2 in buffer-B2 containing 60% sucrose measured by the conventional single-pulse mode at 5°C. All phosphorus-containing compounds in the phage particular contribute to this spectrum. This spectrum was interpreted in terms of the asymmetric and axially symmetric powder patterns [8]. The phage has only two phosphorus-containing compounds, namely, phospholipids in its lipid bilayer and DNA packaged in its core. The asymmetric and axially symmetric powder patterns were assigned to the DNA and lipid bilayer, respectively. For an extensive investigation, however, it is desirable to get each signal

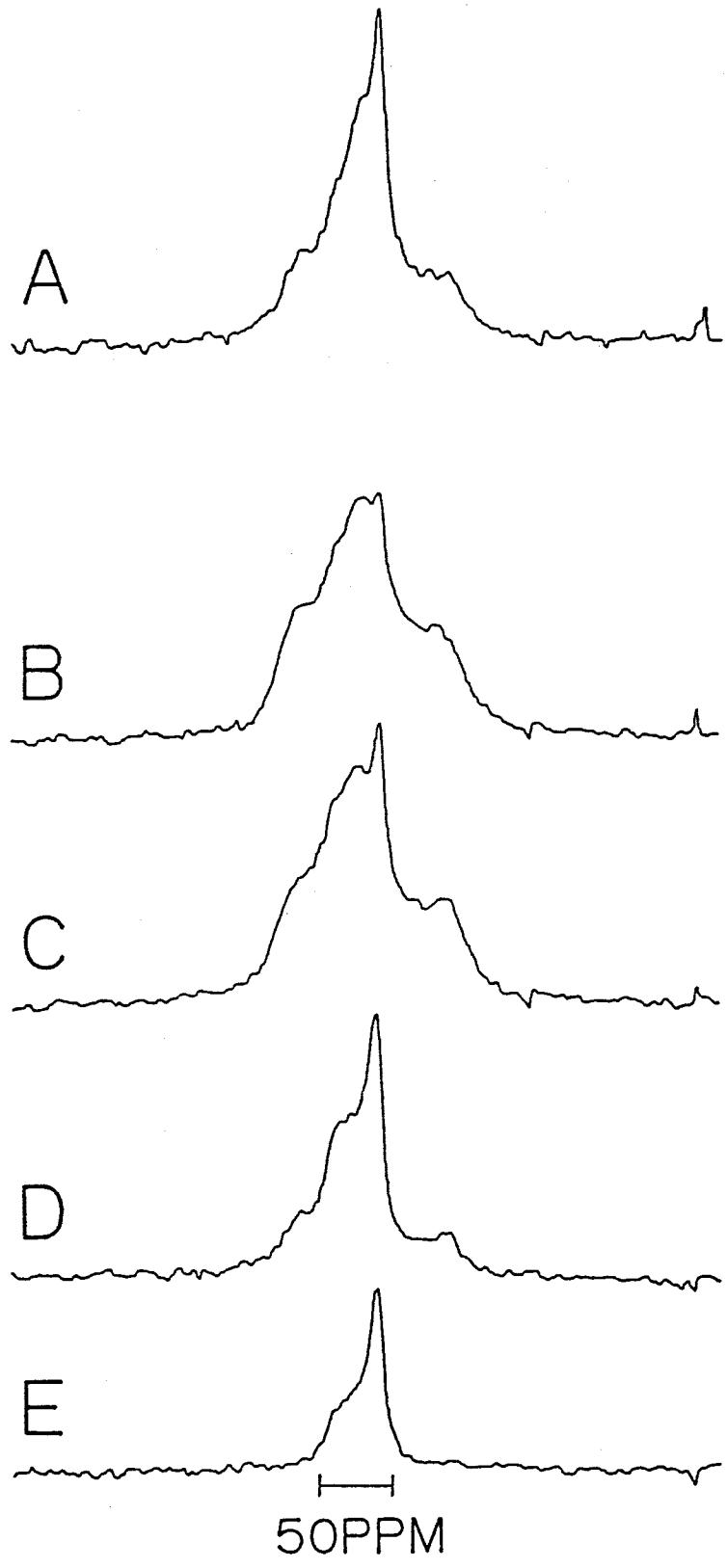

Figure IV-1. ^{31}P NMR spectra of intact bacteriophage PM2 in Buffer-B2 containing 60 % sucrose at 5°C. (A) Single-pulse spectrum with accumulation of 20,000 free induction decays. B, C, D and E were cross-polarization spectra with 0.7, 1.0, 3.0 and 6.0 ms thermal contacts, respectively. 8,000, 8,000, 20,000 and 28,000 transients were accumulated for B, C, D and E, respectively. The 90° pulse width was 13.5 μs. An exponential window function with a 100 Hz broadening factor and a pulse delay of 3.6 s were used.

separately. For that purpose, the cross-polarization technique was applied to this system. The efficiency of cross-polarization is given by the time dependent magnetization ($M_P(t)$) of the proton system after a contact time t, which is a function of the spin-lattice relaxation time of protons in the rotating frame ($T_{1\rho}(H)$) and the cross relaxation time (T_{HP}) between the proton and phosphorus as shown in equation (1),

$$M_P(t)=K(1+\varepsilon\alpha^2-T_{HP}/T_{1\rho}(H))^{-1}[\exp(t/T_{1\rho}(H))-\exp(-t(1+\varepsilon\alpha^2)/T_{HP})], \quad (1)$$

where $\alpha=\gamma_P B_{1P}/\gamma_H B_{1H}$, $\varepsilon=N_P/N_H$ and $K=\alpha(\gamma_H/\gamma_P)M_{P0}$. Here t, γ, B, N and M_{P0} represent the contact time, the gyromagnetic ratio, the amplitude of the rotating magnetic field, the number of spins and the Zeeman magnetization of phosphorus spins, respectively. The efficiency is dominated by T_{HP} and $T_{1\rho}(H)$ at short and long thermal contact times, respectively. These time constants are closely connected with the modes of molecular motions [1]. Since phospholipids and DNA in the phage particle are undergoing quite different types of motions, the contact time dependence of the cross-polarization efficiency is expected to be different for them. Thus, we have measured the cross-polarization ^{31}P NMR spectra of the intact bacteriophage PM2 at a variety of contact times, which are presented in Figure IV-1 B, C, D and E. The spectrum obtained at 0.7 ms contact time (Figure IV-1 B) showed a typical asymmetric powder pattern, which corresponds to the broader component in the single-pulse spectrum. The principal values of its chemical shift tensor (σ_{11}, σ_{22}, σ_{33}) were 70, 6 and -68 ppm. Its chemical shift anisotropy ($\Delta\sigma=\sigma_{33}-\sigma_{11}$) was -138 ppm. This is close to the value estimated from the overlapped spectrum [8]. With a longer thermal contact, a narrow component was coming up at the expense of the asymmetric powder pattern. The spectrum ended up as a simple axially symmetric powder pattern with the chemical shift anisotropy ($\Delta\sigma=\sigma_{//}-\sigma_{\perp}$) of -44 ppm at 6.0 ms contact time (Figure IV-1 E). This accounted for the narrow component in the single-pulse spectrum. These results support the explanation of the single-pulse spectrum in the earlier paper [8]. In order to confirm the assignments, the cross-polarizaton characteristics of DNA in phage particles and

phospholipid bilayer were examined.

Efficiency of The Cross-Polarization Studied on Model Liposomes and λ Phage. Phosphatidylglycerol (PG) and phosphatidylethanolamine (PE) purified from the host cells were mixed at the ratio of 64/27 (w/w), which is the phospholipid composition in PM2 [5]. The cross-polarization spectrum of the liposomes of this lipid mixture was measured at variety of contact times at 5°C. They showed axially symmetric powder patterns, one of which is given in the insert of Figure IV-2 A. The intensity minimum in the spectrum can be explained by weak dipolar interactions in the magic angle orientation [9]. The minimum disappeared at longer contact times because of the lateral diffusion and/or tumbling motions of the vesicles. The integrated intensity of the spectrum is plotted as a function of contact time in Figure IV-2 A. T_{HP} and $T_{1\rho}(H)$ were obtained by nonlinear least-squares fitting using equation (1), which gave 0.8 and 25.1 ms, respectively. The best-fit curve is shown by the solid line. λ Phage was used as a model of DNA packaged in a virus particle, since DNA is the single source of phosphorus in this phage. The cross-polarization spectrum of the intact λ phage is given in the insert of Figure IV-2 B, which shows an asymmetric powder pattern. Its integrated intensity is plotted as a function of contact time in Figure IV-2 B. T_{HP} and $T_{1\rho}(H)$ were obtained in a similar way as for phospholipids and were 0.5 and 3.1 ms, respectively.

Both from the type of powder patterns and the cross-polarization characteristics, we can definitely assign the asymmetric and axially symmetric powder patterns in Figure IV-1 to DNA and phospholipid bilayer, respectively. On the basis of the results of Figure IV-2, however, more contribution of DNA signal to the spectrum at 6.0 ms contact time would be expected, while the contribution is hardly seen in Figure IV-1 E. This fact suggests that the real T_{HP} and $T_{1\rho}(H)$ of DNA and phospholipid bilayer in PM2 may be a little different from the values obtained from Figure IV-2. Now we can conclude that the spectra of lipid bilayers and DNA can be obtained separately in such a simple system as PM2 phage by choosing an optimum contact time.

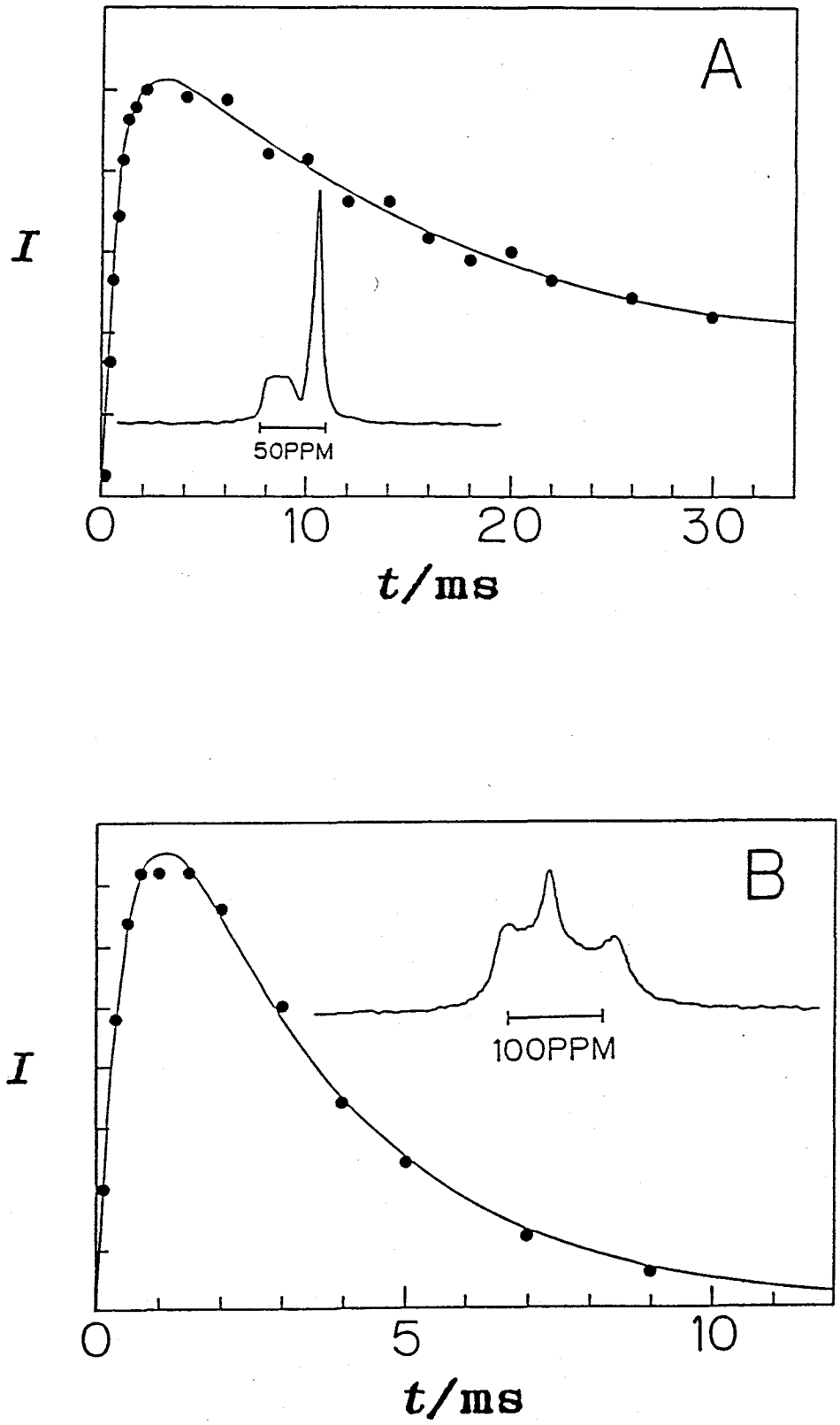

Figure IV-2. Contact time (t) dependence of the integrated intensity (I) of the cross-polarization ^{31}P NMR spectra at 4°C. (A) Liposomes of the semi PM2 total phospholipid, which is the mixture of PE and PG from *A. espejiana* at the same ratio as in the lipid composition of PM2 phage. (B) Intact λ phage in λ-buffer with 30 % sucrose. The solid curves were obtained by nonlinear least-squares fitting. The spectra at 6.0 ms (A) and 0.7 ms (B) contact times are presented in the inserts.

^{1}H-^{31}P Cross-Polarization Spectra of Intact Cells of A. espejiana. The application of the cross-polarization technique was extended to a more complicated system, a bacterial cell, to check the general feasibility of this method. Figure IV-3 A is the ^{31}P NMR spectrum of *A. espejiana* cells at 4°C measured by the conventional single-pulse mode, which includes the contributions from all phosphorus-containing molecules in a cell. Phosphorus nuclei are located in DNA, RNA, phospholipids and many metabolites such as ATP and sugar phosphate in a bacterial cell. The sharp and symmetrical peak at the center comprises signals originating from small soluble molecules. Since an exponential window function with a 100 Hz broadening factor was used, the signals were not resolved. Actually, well resolved signals were obtained in a ^{31}P high-resolution NMR spectrum as can been seen in Figure IV-3 B [10]. The broad components in Figure IV-3 A can be attributed to supramolecular systems undergoing limited motions such as phospholipids in the biomembrane, DNA in the chromosome complex and RNA in the ribosomes and so on. The cross-polarization pulse technique is expected to get rid of the contributions from at least small molecules. Figure IV-4 A, B, C and D show the cross-polarization ^{31}P NMR spectra of intact *A. espejiana* cells obtained at 0.7, 3.0, 5.0 and 7.0 ms contact times, respectively. In any of these cross-polarization spectra, the sharp peak at the center was hardly seen as expected. The pattern of the cross-polarization spectrum changed with the contact time as in the case of PM2. In spite of the complexity of the system, the observed spectrum was rather simple. The cross-polarization spectrum with a 0.7 ms thermal contact (Figure IV-4 A) showed an asymmetric powder pattern. This spectrum corresponds to the broadest component in the single pulse spectrum and its chemical shift anisotropy is about -160 ppm. In spite of its large anisotropy, the principal values of the chemical shift tensor are not evident, suggesting a broad distribution of the motions. The spectrum with a 7.0 ms thermal contact gives rise to a pure axially symmetric powder pattern as in the case of PM2. The chemical shift anisotropy was -44.7 ppm. The spectra observed at 3.0 and 5.0 ms contact times can be interpreted by an

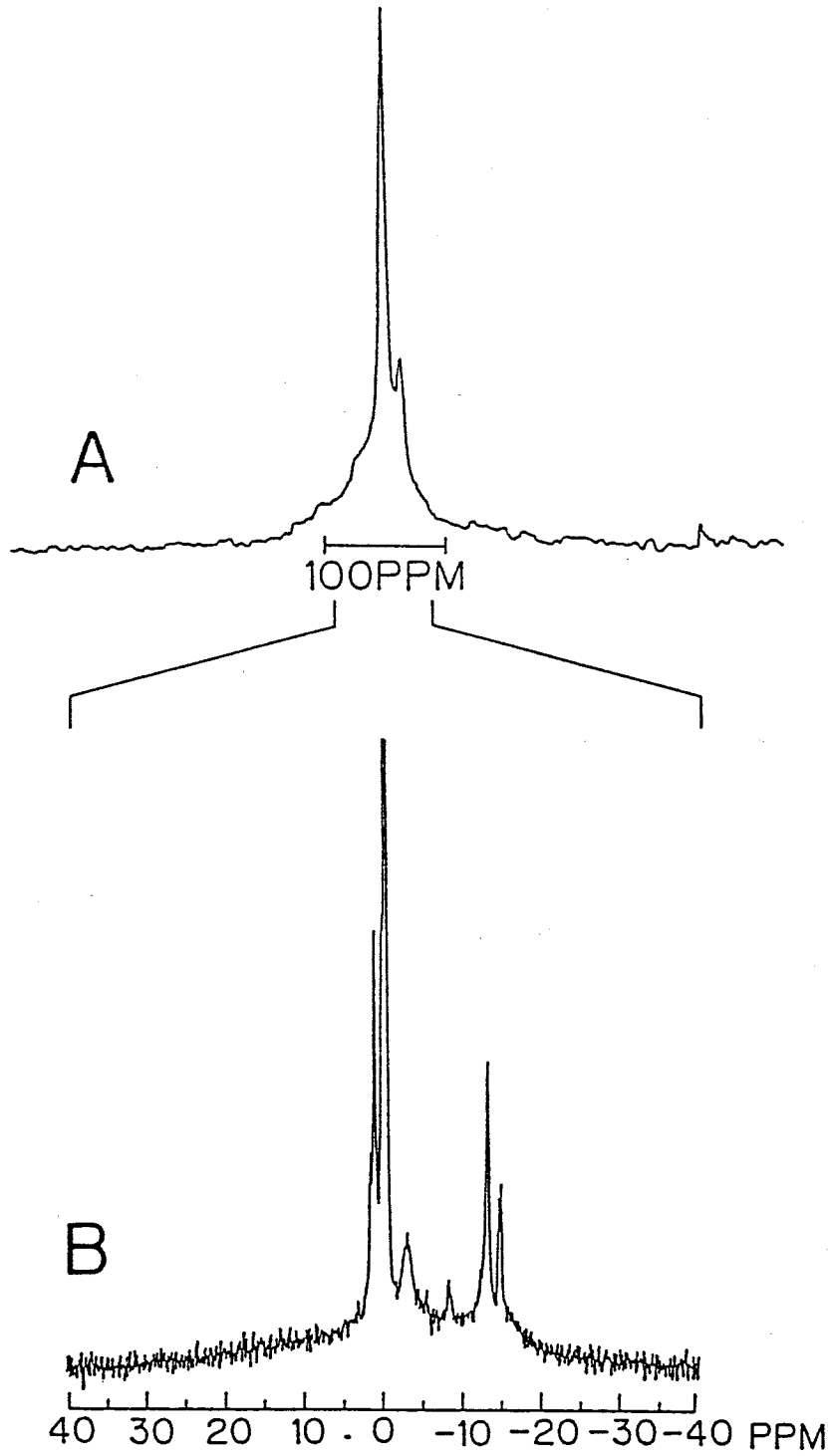

Figure IV-3. ^{31}P NMR spectra of intact *A. espejiana* cells measured by the single-pulse mode at 4°C. (A) A single-pulse broadline at 40.3 MHz with proton-noise-decoupling and a pulse delay of 3 s. 3,000 transients were accumulated and an exponential window function with a 100 Hz broadening factor was used. (B) A high-resolution spectrum with a pulse delay of 0.3 s and an exponential window function with a 3 Hz broadening factor. 45,000 transients were accumulated.

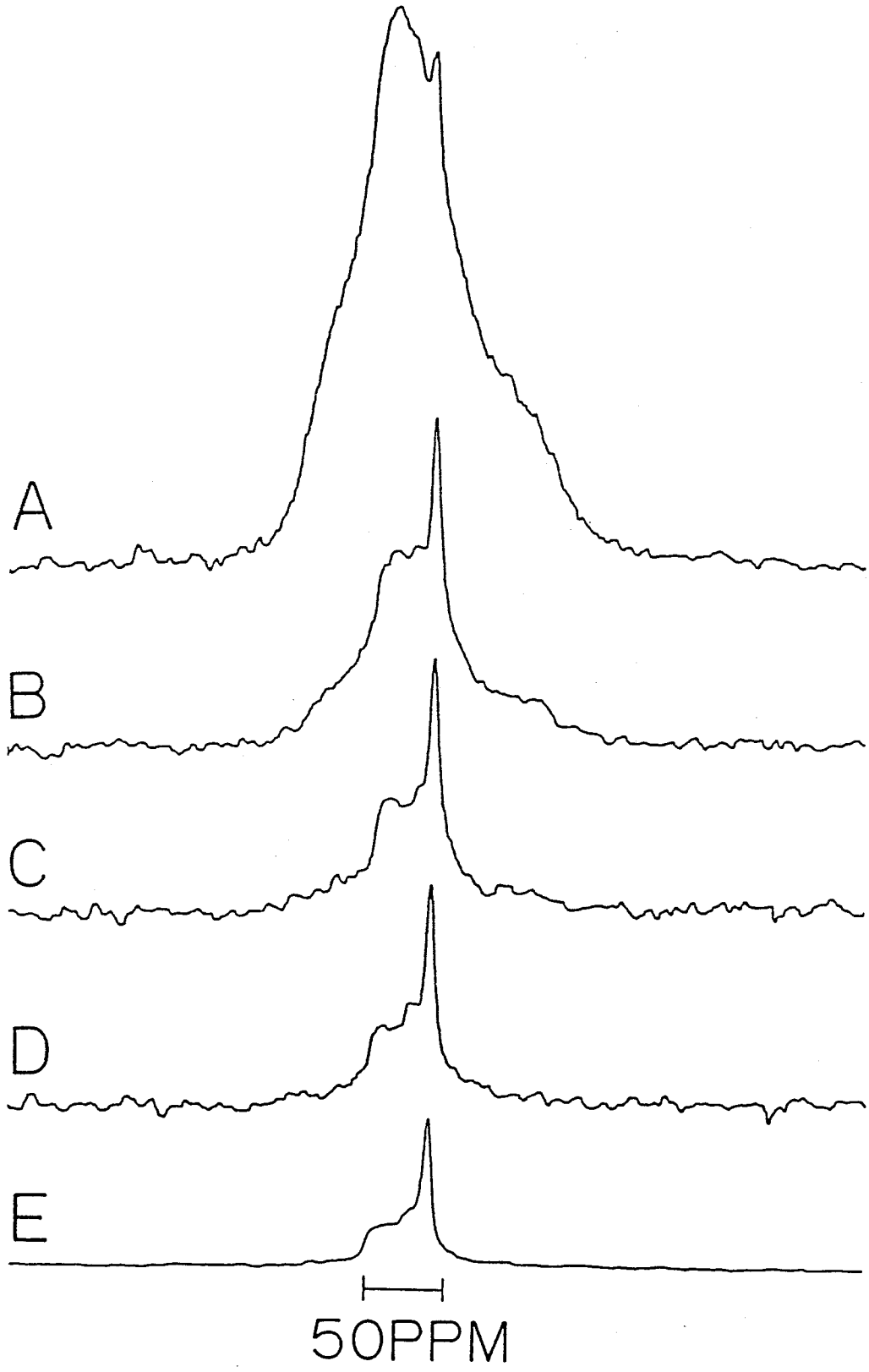

Figure IV-4. Cross-polarizarion ^{31}P NMR spectra of intact *A. espejiana* cells at 4°C. A, B, C and D were measured at 0.7, 3.0, 5.0 and 7.0 ms contact times, respectively, with the accumulation of 3,000 free induction decays. E was measured at a contact time of 7 .0 ms with the accumulation of 12,000 scans. The 90° pulse width was 10.3 μs. A pulse delay of 3 s and an exponential window function with a 100 Hz broadening factor were used.

overlapping of the powder patterns at 0.7 and 7.0 ms contact times at different ratios. These results show that the weak sharp peak on the right in the single-pulse spectrum (Figure IV-3 A) is an overlapping of the perpendicular component of the axially symmetric powder pattern and signals of soluble molecules.

Comparison of The Cross-Polarization Efficiency between Liposomes and Ribosomes. The major supramolecular structures containing phosphorus in a bacterial cell are nucleic acids and the biomembrane. In the former, ribosomal RNA and DNA are known to be the most and second most major species [11]. To identify the origins of the two powder patterns, ^{31}P cross-polarization spectra were examined for purified ribosomes and the liposomes of the total phospholipid fraction extracted from the cells. The latter again showed an axially symmetric powder pattern. The ribosomes in NTCM-buffer with 60 % sucrose gave rise to an asymmetric powder pattern with the principal values of the chemical shift tensor of 88, 17 and -117 ppm as show in the insert of Figure IV-5 B. The spectral intensity was plotted as a function of contact time in Figure IV-5. Nonlinear least squares fitting was carried out by using equation (1). Solid lines represent best fitting curves. The obtained T_{HP} and $T_{1\rho}(H)$ of the phospholipid bilayer were 0.9 and 38.2 ms at 4°C and 2.1 and 1,300 ms at 30°C, respectively. As can been seen later (Chapter V), the bilayer of the total phospholipid fraction is in a broad phase transition at 4°C and in the liquid-crystalline state at 30°C. $T_{1\rho}(H)$ of the protons became longer with an increase in the motions of the phospholipids, suggesting that the dominant correlation time is in the fast motional regime. The maximum intensity was obtained at 3.0 and 7.0 ms contact times at 4 and 30°C, respectively. Similar results were reported for synthetic phosphatidylcholine bilayers [1]. On the other hand, the maximum intensity of the cross-polarization spectra of the purified ribosomes in NTCM-buffer with 60 % sucrose was observed at 0.7 ms contact time and the intensity decreased to the one twentieth of the maximum at 7.0 ms contact time. T_{HP} and $T_{1\rho}(H)$ obtained by nonlinear least-square fitting were 0.3 and 2.3 ms, respectively. In order to imitate the situation in the cell, the purified

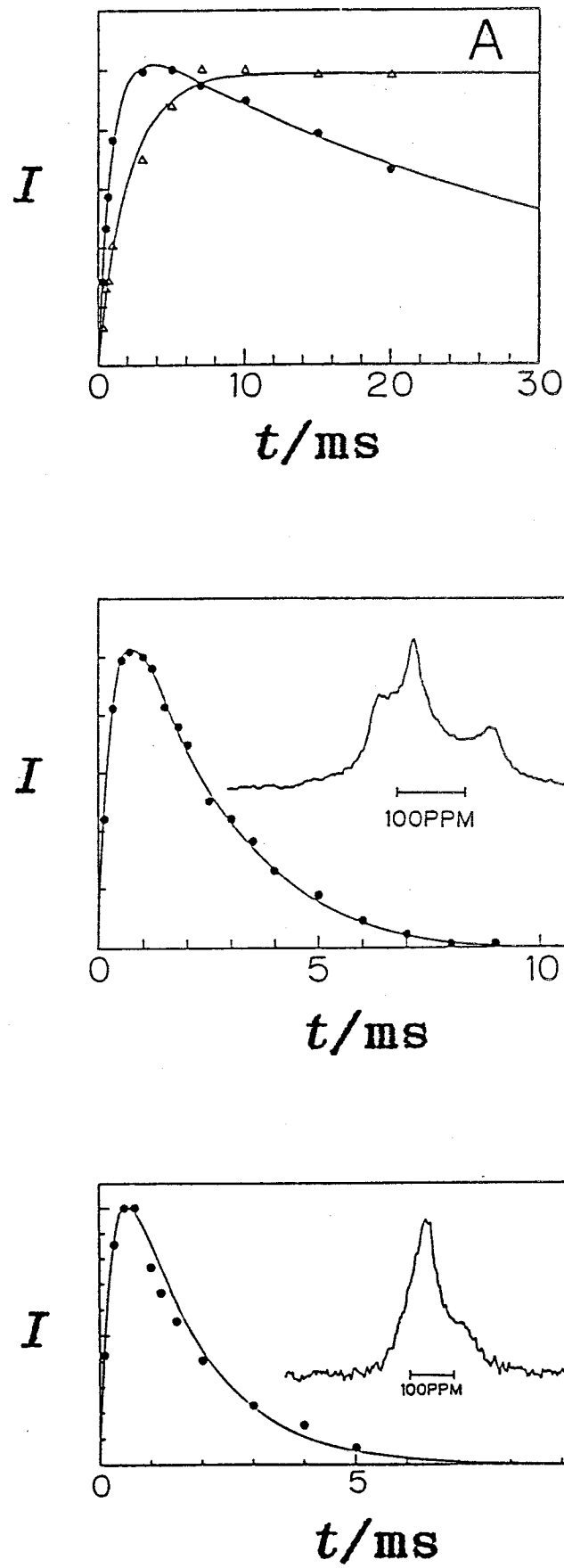

Figure IV-5. Contact time (t) dependence of the integrated intensity (I) of the cross-polarization spectra. A: Liposomes of total phospholipids of *A. espejiana* at 4°C (●) and at 30°C (△). The 90° pulse width was 10.2 μs. B, C: Purified ribosomes of *A. espejiana* at 4°C suspended in about five volumes of NTCM-buffer with 60 % sucrose (B), and suspended in four volumes of NTCM-buffer (C). The 90° pulse width was 10.3 μs. A pulse delay of 3 and 4 s was used for liposomes and ribosomes, respectively. The spectra of ribosomes at a thermal contact time of 0.7 ms are given in the inserts.

ribosomes suspended in four volumes of NTCM-buffer was also examined at 4°C. The result is given in Figure IV-5 C. Its spectrum is similar to the cross-polarization spectrum of the intact host cells with 0.7 ms thermal contact. The chemical shift anisotropy was -170 ppm. The maximum intensity was obtained with 0.6 ms thermal contact. While the contact time dependence of the ribosomes was similar to that of DNA, the contact time at its intensity maximum was shorter than that of DNA because of shorter T_{HP} and $T_{1\rho}(H)$.

These results allow us to assign the spectra at 0.7 and 7.0 ms contact times to the nucleic acids and biomembrane of *A. espejiana* cell, respectively. In the former, the contribution of ribosomal RNA should be dominant because of its major presence. Actually, the intensity maximum of the cross-polarization spectrum of the host cells was observed at 0.7 ms contact time, which is in good agreement with that at the maximum for the purified ribosomes. This fact also supports the major contribution of the ribosomes. The contribution of DNA is expected to be one sixth according to the composition in *E. coli* [11]. Therefore, it cannot be ignored as well. This complexity might be the reason for the rather featureless powder pattern of Figure IV-4 A.

Although the supramolecular systems of nucleic acids can be observed in *in vivo* by the cross-polarization method, it turned out to be difficult to extract more specific information on the chromosome complex, ribosomes and so on unless one component was overwhelmingly dominant. In contrast, the information on the biomembrane is clear regardless of the complexity of the biosystems.

IV-3. Discussion

^{1}H-^{31}P cross-polarization was shown to be useful for the investigation of lipid bilayers [1, 12] and the chromatin in intact chicken erythrocyte cells [2]. Both of them are, however, very extreme cases. In the former, the origin of the spectrum is self-evident, and in the latter, the contributions from RNA and

lipid bilayer were negligible or very small. It was shown in this work that the feasibility of this method is more general. The selectivity of the information is especially high for the biomembranes. A pure lipid bilayer spectrum could be obtained from intact bacterial cells. In the case of nucleic acids, the assignments are not straightforward. Nevertheless, the major contribution should come from DNA and/or ribosomes. The contact time dependence of the spectral intensity can give an idea of which one is dominant. A chemical composition surely helps the analysis.

The separation of the spectra of nucleic acids and lipid bilayer is not accidental. The lipid bilayer has much more freedom of motion because it is composed of small lipid molecules which undergo rapid axially symmetric motions [13, 14]. Double stranded DNA in a chromosome complex and RNA in ribosomes are much more rigid. Thus, the cross-relaxation time, T_{HP}, is longer for lipid bilayers than for nucleic acids. The correlation time of the proton motion in the lipid bilayers in the gel and liquid-crystalline states falls in the fast motional regime in the rotating frame [1], while that of chromatin DNA is in the slow motional regime [2]. Since $T_{1\rho}(H)$ of nucleic acids is close to its minimum (Akutsu *et al.*, unpublished), it is usually shorter than $T_{1\rho}(H)$ of lipid bilayers. The longer T_{HP} and $T_{1\rho}(H)$ of lipid bilayers as compared to those of nucleic acids permit the selective observation of their spectra. However, a longer cross-correlation time leads to a lower signal to noise ratio in the spectrum of the lipid bilayers. Another interesting point is that the abnormal intensity minimum observed in the extracted lipids did not appear in the intact biological system. This suggests that the mode of fluctuation of the polar groups is different for the simple lipid bilayers and intact biomembranes [9]. Thus, it was shown that the application of this method to PM2 and its host cell was satisfactory.

References

[1] Akutsu, H. (1986) *J. Magn. Reson.*, **66**, 250.

[2] Nishimoto, S., Akutsu, H. and Kyogoku, Y. (1987) *FEBS Letters*, **213**, 293.

[3] Odahara, T., Akutsu, H. and Kyogoku, Y. , submitted.

[4] Espejo, R. T. and Canelo, E. S. (1968) *J. Bacteriolo.*, **95**, 1877.

[5] Mindich, L. (1987) "*Comprehensive Virology*" ed. by Fraenkel-Conrat, H. and Wagner, R. R., **12**, 271.

[6] Franklin, R. M., Hinnen, R., Schäfer, R. and Tsukagoshi, N. (1976) *Phil. Trans. R. Soc. London. B.*, **276**, 63.

[7] Franklin, R. M. (1974) *Current Topics in Microbiology and Immunology*, **68**, 107.

[8] Akutsu, H., Satake, H. and Franklin, R. M. (1980) *Biochemistry*, **19**, 5264.

[9] Frye, J., Albert, A. D., Selinsky, B. S. and Yeagle, P. L. (1985) *Biophys. J.*, **48**, 547.

[10] Seelig, J. (1986) "*Physics of NMR Spectroscopy in Biology and Medicine*" ed. by Maraviglia, N., 3849-411, North-Holland Physics Publishing, 1000 AC Amsterdam.

[11] Watson, J. D. (1975) "*Molecular Biology of the Gene*" 3rd ed., p69, W. A. Benjamin INC, Menlo Park, California.

[12] Akutsu, H. and Kyogoku, Y. (1984) *Biochim. Biophys. Acta*, **774**, 293.

[13] Kohler, S. J. and Klein, M. P. (1977) *Biochemistry*, **16**, 519.

[14] Seelig, J. (1978) *Biochim. Biophys. Acta*, **515**, 105.

Chapter V

Studies of the Phase State of Phospholipids Membranes by ^{1}H-^{31}P Cross-Polarization Method

Summary

The temperature dependence of the chemical shift anisotropy ($\Delta\sigma=\sigma_{//}-\sigma_{\perp}$) was examined for the selectively observed cross-polarization spectra of membrane of intact PM2 phage and its host bacterium, *A. espejiana*. Referring to the thermal analysis and ^{31}P NMR spectra of the bilayers of the extracted phospholipids, the phase transition of the biomembrane was identified for PM2 phage and its host cell. The dynamic state of the biomembrane of intact bacteria was directly monitored for the first time. The result for PM2 is in good agreement with the reported one [1]. It turned out that the phase behavior of the intact biomembrane is different from the bilayer of the extracted lipids for both PM2 and its host cell. Namely, the terminal temperatures of the phase transition of the host cell and PM2 membranes were lower and higher than those of the extracted phospholipids, respectively.

V-1. Introduction

Many of the important reactions in a cell are taking place on biological membranes. Biomembranes are generally made up of lipids and proteins as highly ordered supramolecular structures [2], which play one of key roles in organizing the concerted activities in a biological system. Therefore, information on the biomembrane of an intact cell would be very important in the investigation of *in vivo* systems.

A lipid containing bacteriophage, PM2, which infects a marine bacterium, *Alteromonas espejiana*, is a suitable system for the study of intact biomembranes, because of the simple structure

and chemical composition of its bilayer. Namely, the phage has a lipid bilayer with four kinds of membrane proteins [3, 4]. In the case of studying biomembranes being highly ordered supramolecular structures, ^{31}P solid-state NMR method is one of the powerful method, by which the information on the structure and the dynamics of molecules are obtained. By the use of the ^{1}H-^{31}P cross-polarization method, ^{31}P NMR spectra of the biomembranes of intact PM2 and *A. espejiana* were observed selectively at 6 and 7ms of thermal contact, respectively, as shown in Chapter IV [5]. Therefore, by the use of this advantage, in order to investigate their dynamic states and phase behaviors, temperature dependence of the chemical shift anisotropy ($\Delta\sigma=\sigma_{//}-\sigma_{\perp}$) was examined for those selectively measured spectra.

V-2. Results

Phase Transition of The Phospholipid Bilayers in The Intact Biomembranes of PM2 and A. espejiana In Chapter IV, It was shown that the lipid bilayer of intact PM2 phage and its host cell, *A. espejiana*, were separately observed at 6 and 7 ms contact times by the use of ^{1}H-^{31}P cross-polarization method. We took advantage of this in exploring the dynamic nature of their biomembranes *in vivo*. In order to see the correlation between the chemical shift anisotropy and phase behavior, the temperature dependence of the chemical shift anisotropy and the thermogram of the bilayer of total-phospholipid fraction extracted from *A. espejiana* cells and PM2 phage were examined. The results are presented in Figure V-1. Figure V-1 A shows the thermogram of *A. espejiana* total phospholipid bilayers. The phase transition started from below 5°C and finished at 24.5°C. This asymmetric profile of the transition is characteristic of PE-rich lipid bilayers [6]. ^{31}P chemical shift anisotropy of the same phospholipid bilayers is plotted as a function of temperature in Figure V-6 B. The absolute value of the ^{31}P chemical shift anisotropy decreased gradually from about 0°C to about 23°C, which is in good agreement with the phase transition range in the thermogram.

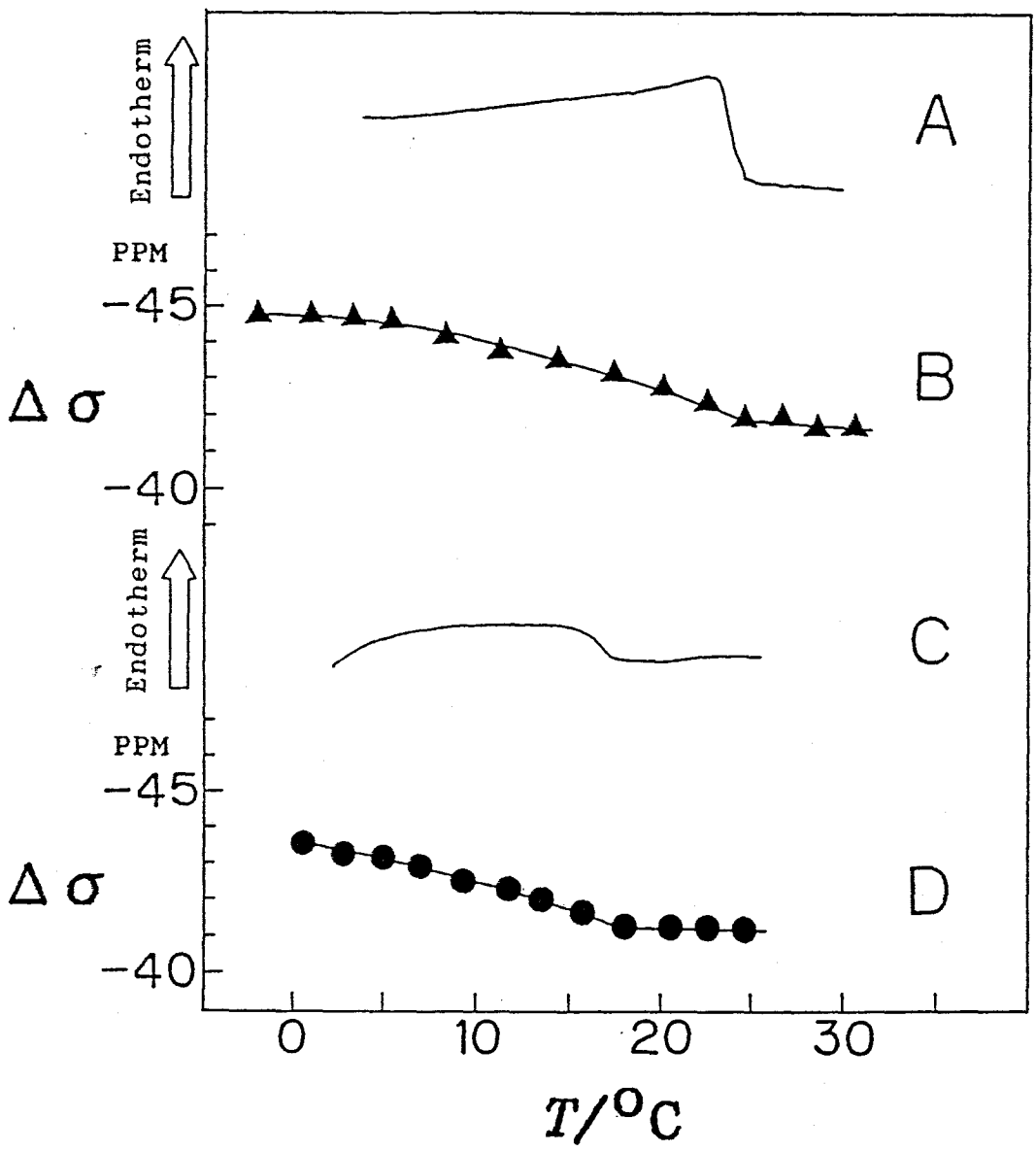

Figure V-1. Thermograms (A and C) and temperature (T) dependence of the ^{31}P chemical shift anisotropy ($\Delta\sigma=\sigma_{//}-\sigma_{\perp}$) (B and D) of total phospholipid liposomes of PM2 phage and *A. espejiana*. (A) and (B) *A. espejiana* total-phospholipids. (C) PM2 total phospholipids and (D) semi PM2 total phospholipids (see the legend of Figure IV-2).

The results show that the *A. espejiana* total phospholipid bilayer is in the liquid-crystalline state above 24.5°C, and in a process of a broad phase transition in the range 0°C to 24.5°C, where the liquid-crystalline and gel states coexist.

Presented in Figure V-1 C is the thermogram of the liposomes of the total phospholipid fraction extracted from PM2 phage. The thermogram indicates that the phase transition started from below 5°C and finished at about 17°C. Thus, it can be said that the PM2 total phospholipid bilayer is in the liquid-crystalline state at above 17°C, and in the process of a broad transition below 17°C. The different profile of the thermogram from that of *A. espejiana* total phospholipid fraction can be attributed to the low fraction of phosphatidylethanolamine (27 %) in PM2. Since the amount of the total phospholipids of PM2 phage was not enough for the measurement of a ^{31}P NMR spectrum, the temperature dependence of the ^{31}P chemical shift anisotropy was examined for the semi PM2 total phospholipid bilayer (the mixture of PE and PG from the host cells). The result is given in Figure V-1 D. The absolute value of the ^{31}P chemical shift anisotropy decreased gradually up to about 18°C and settled down at above that temperature. This also shows a good correlation with the result of the thermal analysis. The reflective point represents the end of the phase transition. This coincidence shows in turn that the semi PM2 total phospholipid bilayer well reflects the nature of the genuine one.

Since the correlation between the phase behavior and ^{31}P chemical shift anisotropy was substantiated, *A. espejiana* and PM2 phage were examined. The cross-polarization ^{31}P NMR spectra of intact *A. espejiana* cells at 7.0 ms contact time were obtained at several temperatures. Every measurement was performed with a fresh culture. All the spectra gave rise to axially symmetric powder patterns (Figure V-3). The chemical shift anisotropy of the spectrum was plotted as a function of temperature in Figure V-2 A. The chemical shift anisotropy was -45 ppm at 0°C and its absolute value decreased with the increase of temperature from 4°C to 30°C. However, the slope of the plot above 11°C is different from that in the range from 0°C to about 11°C. The slope

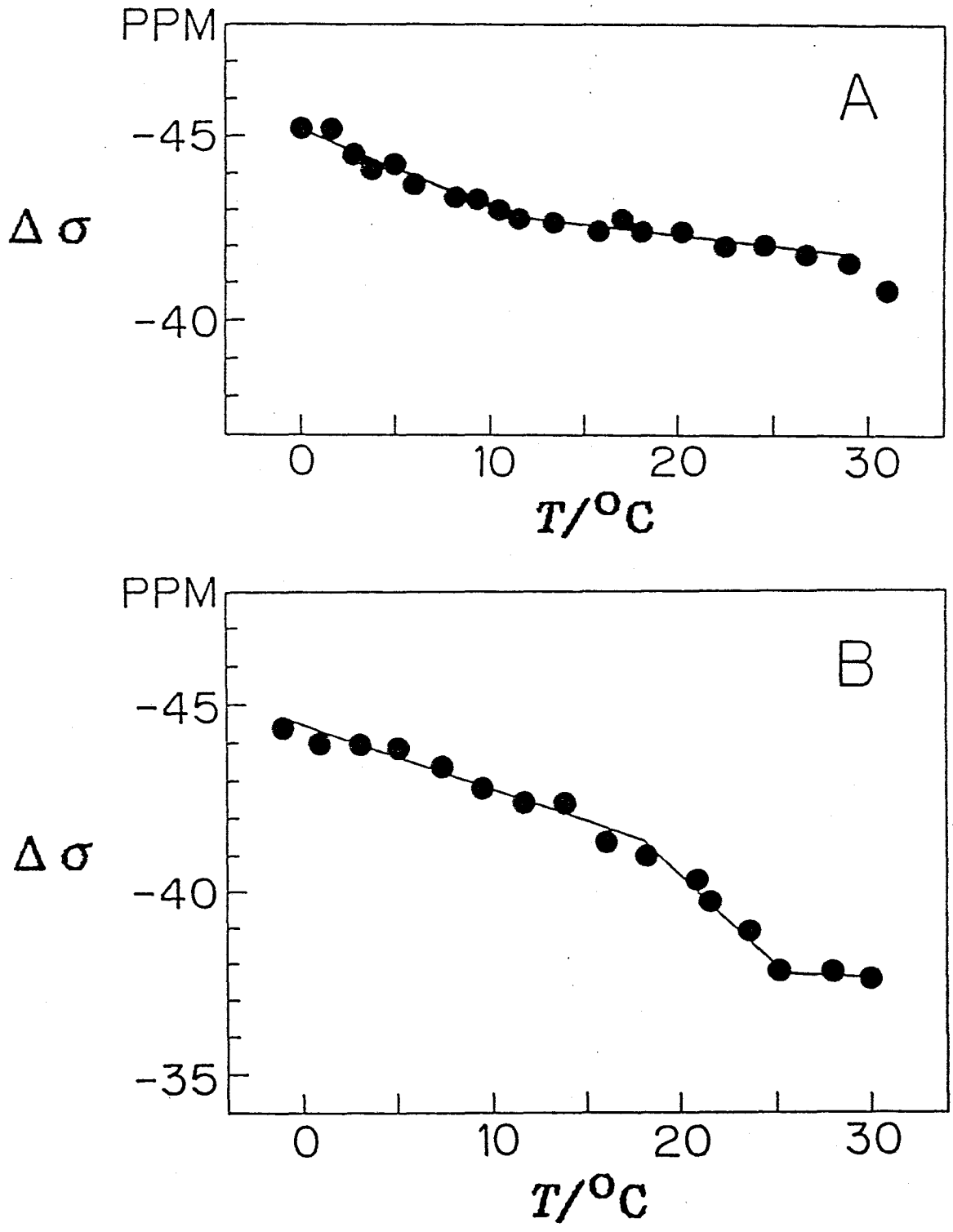

Figure V-2. Temperature (T) dependence of the ^{31}P chemical shift anisotropy ($\Delta\sigma=\sigma_{//}-\sigma_{\perp}$) of biomembranes *in vivo*. (A) Intact *A. espejiana* cells. A fresh culture was used for each measurement. (B) Intact PM2 phage in buffer-B2 with 60 % sucrose. The Hartmann-Hahn condition was redetermined for every measurement.

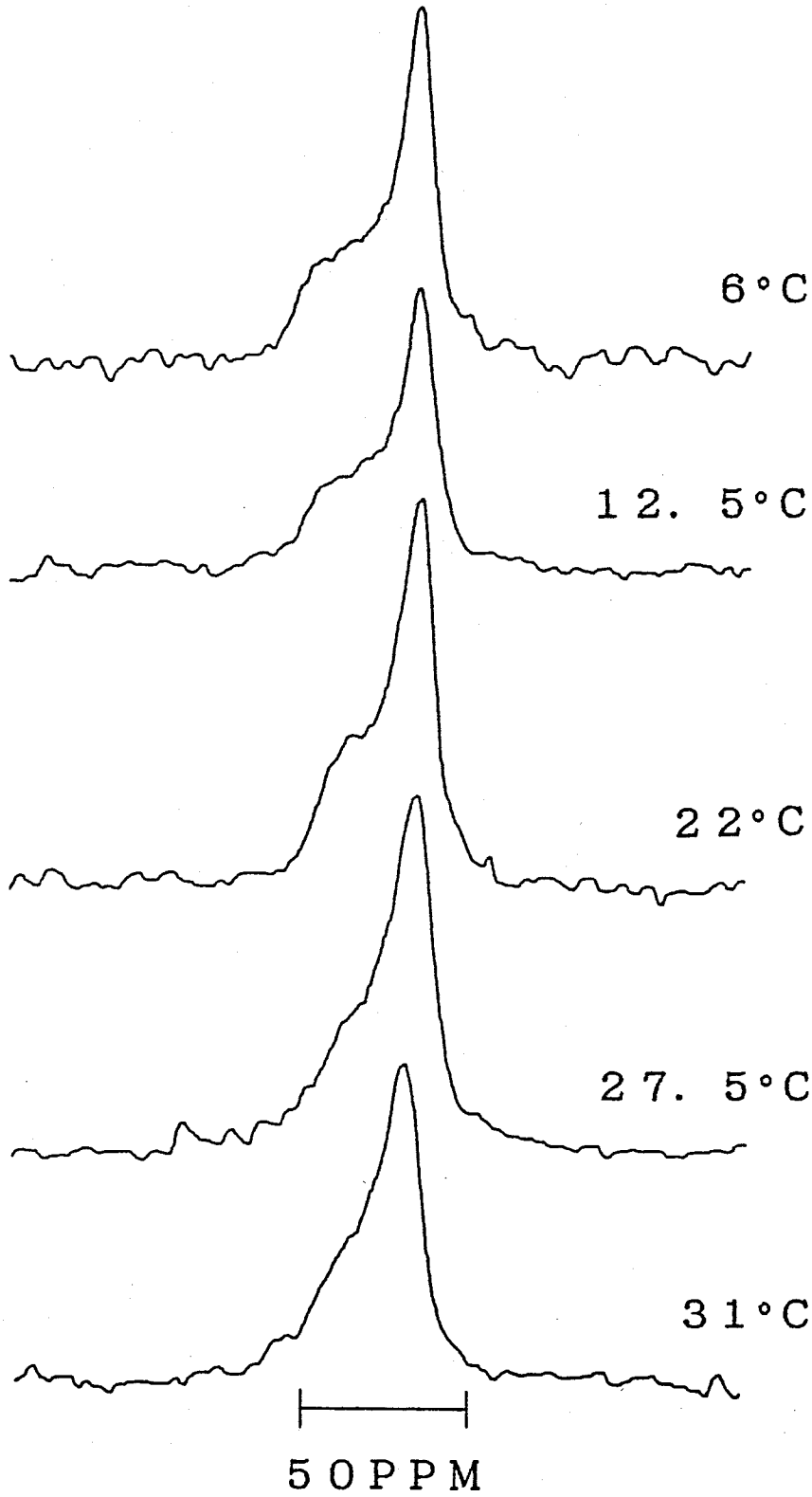

Figure V-3. Temperature dependence of ^{31}P NMR spectrum of intact PM2 phage in buffer-B2 with 60 % sucrose. Spectra were obtained at a thermal contact time of 6.0 ms by the ^{1}H-^{31}P cross-polarization method. An exponential window function with a 100 Hz broadening factor and a pulse delay of 3.6 s were used.

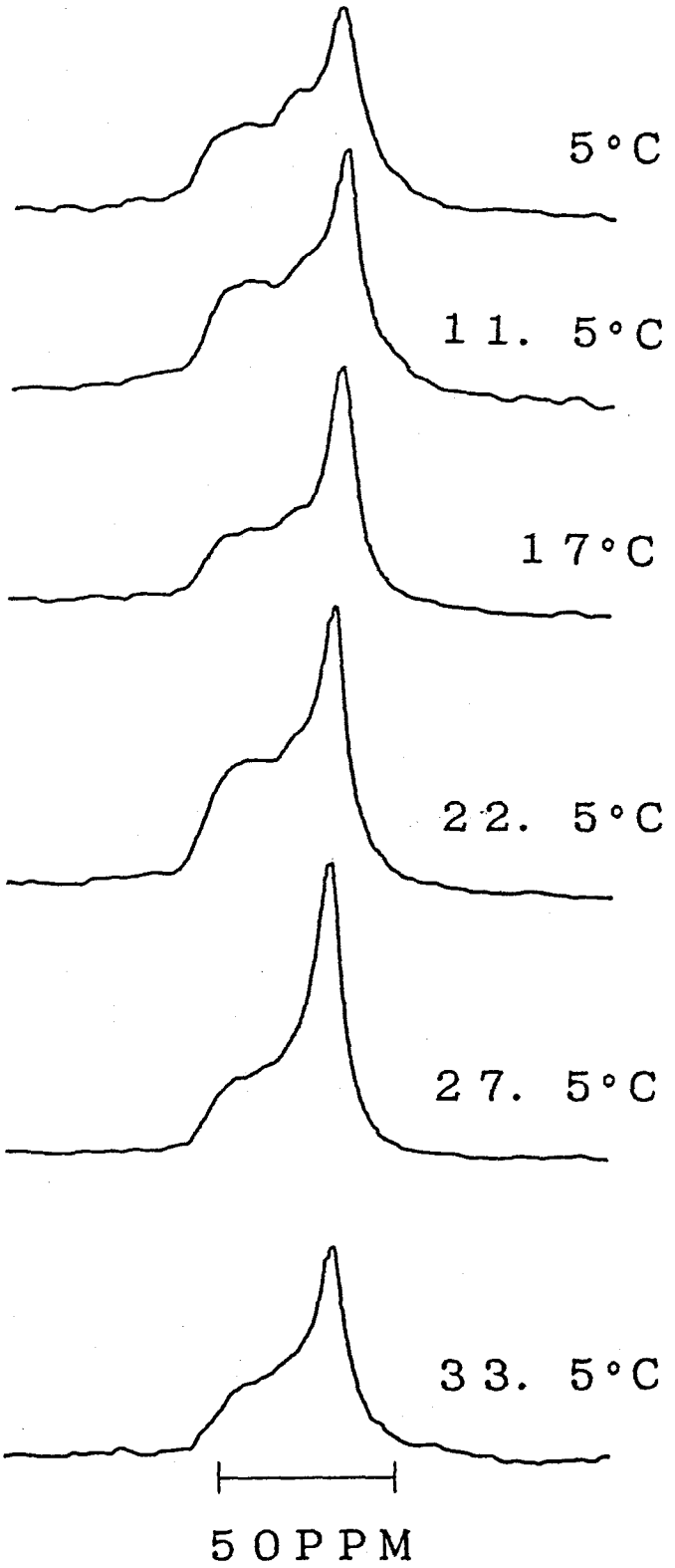

Figure V-4. Temperature dependence of ^{31}P NMR spectrum of intact *A. espejiana* cells. Spectra were obtained at a thermal contact time of 7.0 ms by the ^{1}H-^{31}P cross-polarization method. A pulse delay of 3 s and an exponential window function with a 100 Hz broadening factor were used.

in the lower temperature range is steeper, giving a break point at about 11°C. This bacterium is known to die above 30°C [7], which is reflected in the measured point at extreme right of chemical shift anisotropy (Figure V-2) at the highest temperature. The ^{31}P chemical shift anisotropy of the membrane of intact PM2 phage is plotted as a function of temperature in Figure V-2 B. All the cross-polarization spectra of intact PM2 at 6.0 ms contact time were also axially symmetric powder patterns (Figure V-4). The ^{31}P chemical shift anisotropy was -44 ppm at about 0°C. Its absolute value decreases gradually up to about 17°C followed by a large change and settled down at about 25°C.

V-3. Discussion

In Chapter IV, it was shown that the application of ^{1}H-^{31}P cross-polarization method to PM2 phage and its host cell, *A. espejiana*, was satisfactory. Thermal analyses and phosphorus chemical shift measurements of extracted lipids showed a good correlation. These results provided the firm base for the analysis of the intact biological system. Although the phase behaviors of the lipids extracted from *A. espejiana* cells and PM2 phage were investigated by ESR [8] and NMR [1], respectively, no clear conclusion was obtained. The present work clearly showed that both lipid bilayers have broad phase transitions. They are in the liquid-crystalline state at above 17°C for PM2 phage and at above 24.5°C for the host cells. The difference between two temperatures can be attributed to the difference in the phospholipid composition, since the fatty acid composition is expected to be similar [9]. The phospholipid composition is 27 % phosphatidylethanolamine (PE), 64 % phosphatidylglycerol (PG) for PM2 phage [10, 11] and 72 % PE, 23 % PG for the host cell [12]. Since the phase transition temperature of phosphatidylglycerol bilayers is generally lower than that of phosphatidylethanolamine, the difference in the phase transition temperature mentioned above is reasonable.

A phase behavior of the biomembranes of intact cells was reported for the first time. To our knowledge, no other method can provide such information. The phase transition of *A. espejiana* membrane took place between lower than 4 and 11°C. The phase behavior of the purified membranes of this bacterium was investigated by ESR using spin label reagent [8]. The phase transition temperature determined from the reflection point was 12°C. Our result agrees with this, provided that this is the end of the phase transition. However, the end point of the phase transition is different from that of extracted lipid bilayers by about 13°C. This is rather surprising because many reports showed that the phase behavior is more or less similar both in the biomembranes and extracted lipid bilayers. However, this is reasonable from the biological point of view in this case, since the biomembrane should be in the liquid-crystalline state at physiological temperature (20-25°C). The difference in the phase behavior should be attributed to the organization of biomembranes. The exact reason could not be identified at this stage.

The change in the chemical shift anisotropy of PM2 phage was larger than those of the extracted phospholipids and the intact host cells, resulting in a smaller absolute value at a higher temperature. This suggests that some motions averaging the chemical shift tensor are involved. Since the diameter of this virus is about 60 nm [13], either lateral diffusion or/and rotation of the particle can cause the averaging. No averaging was observed up to 32°C in the presence of 60 % sucrose [1]. Thus, the smaller value of the chemical shift anisotropy in this work may be attributed to the rotation of the particle due to its lower concentration, which resulted in a lower viscosity of the solution. A part of the gradual change in Figure V-2 can be attributed to the increase of the rotational motion with the increase of temperature. The change between 17 and 25°C, however, cannot be explained by such motions. Consequently, it can be ascribed to the phase transition of the lipid bilayer of PM2 phage. This coincides with the conclusion obtained in the previous work [1]. The temperature range of the phase transition of the PM2 membrane is much narrower than that of the extracted

lipids. Furthermore, the temperature at the end of the phase transition of PM2 is higher than that of the extracted lipids by 8°C in contrast to the case of *A. espejiana* cells. Since the structure of this virus was well established, we may discuss these features in more detail. In PM2 phage, phospholipid are located in an asymmetrical manner, namely, most of phosphatidylethanolamine are located inside and most of phosphatidylglycerol are outside of the nucleocapsid membrane [14]. The nucleocapsid was covered by coat proteins (Protein II), which are basic (pI 9-12.3) [15]. Furthermore, half of the space of the nucleocapsid membrane is occupied by the capsid proteins (Protein III) [16]. The squeezing out of phosphatidylglycerol from the inner leaflet of the bilayer would raise its phase transition temperature. And the interaction between phosphatidylglycerol and basic coat proteins would also raise the phase transition temperature of the outer leaflet. Protein-protein interaction within the capsid proteins and between the capsid proteins and coat proteins may affect the dynamic state of the lipid bilayer as well. These interactions can introduce cooperative nature to a greater extent in the dynamic structure of the lipid bilayer, which would result in a sharper phase transition. Thus, the increase of the phase transition temperature and the sharper transition in PM2 membrane are consistent with the proposed structural model of the phage [1, 4].

In the previous paper [1], the early event of the infection of PM2 phage to the host cell was examined as a function of temperature (Figure V-5). An enhancement of the infectivity was observed in the temperature region from 15 to 13°C. It was concluded that the change in the dynamic state of the phage membrane might be involved in this early event. The results of this work supports this conclusion. In the first place, it was confirmed that the phase transition of the cell membrane of the host bacterium takes place in a quite different temperature range from the above one. Thus, the alteration of the dynamic state of the host cell biomembrane cannot be directly correlated with the infectivity of PM2. Secondly, it was confirmed that the phase transition of the phage membrane occurs in the same temperature

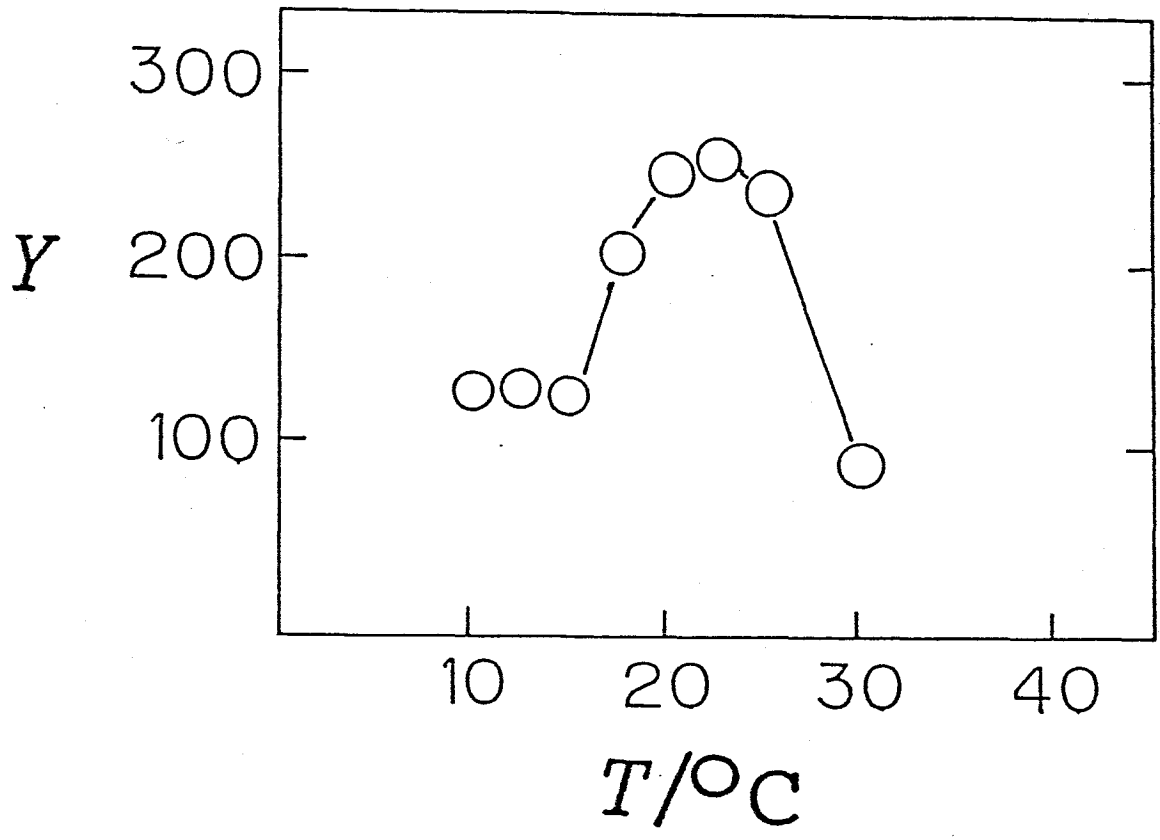

Figure V-5. Yield (Y) of PM2 phage in plaque forming unit ($x10^8/cm^3$) as a function of temperature (T) during the first 5min of incubation. (Akutsu *et al.* (1980) *Biochemistry* **19**, 5264.)

range as shown above. Consequently, it is reasonable to ascribe one of the main factors for alteration of the phage infectivity to the dynamic structure of the phage particle.

References

[1] Akutsu, H., Satake, H. and Franklin, R. M. (1980) *Biochemistry*, **19**, 5264.

[2] Singer, S. J. and Nicolson, G. L. (1972) *Science*, **17**, 720.

[3] Franklin, R. M., Hinnen, R., Schäfer, R. and Tsukagoshi, N. (1976) *Phil. Trans. R. Soc. London. B.*, **276**, 63.

[4] Franklin, R. M. (1974) *Current Topics in Microbiology and Immunology*, **68**, 107.

[5] Odahara, T., Akutsu, H. and Kyogoku, Y., submitted.

[6] Jackson, M. B. and Sturtevant, J. M. (1977) *J. Bio. Chem.*, **252**, 4749.

[7] Espejo, R. T. and Canelo, E. S. (1968) *J. Bacteriol.*, **95**, 1887.

[8] Tsukagoshi, N., Peterson, M. H., Huber, U., Franklin, R. M. and Seelig, J. (1976) *Eur. J. Biochem.*, **62**, 257.

[9] Camerini-Otero, R. D. and Franklin, R. M. (1972) *Virology*, **49**, 385.

[10] Braunstein, S. and Franklin, R. M. (1971) *Virology*, **43**, 685.

[11] Tsukagoshi, N., Kania, M. N. and Franklin, R. M. (1976) *Biochim. Biophys. Acta*, **450**, 131.

[12] Diedrich, D. L. and Cota-Robles, E. H. (1974) *J. Bacteriol.*, **119**, 1006.

[13] Silbert, J. A., Salditt, M. and Franklin, R. M. (1969) *Virology*, **39**, 666.

[14] Schäfer, R. and Franklin, R. M. (1975) *J. Mol. Biol.*, **97**, 21.

[15] Schäfer, R., Hinnen, R. and Franklin, R. M. (1974) *Eur. J. Biochem.*, **50**, 15.

[16] Schneider, D., Zulauf, M., Schäfer, R. and Franklin, R. M. (1978) *J. Mol. Biol.*, **124**, 97.

Chapter VI

Dynamics of Phospholipid Membranes of PM2 and *A. espejiana* as monitored by $T_{1\rho}$(H)

Summary

The temperature dependence of spin-lattice relaxation time of proton in the rotating frame ($T_{1\rho}$(H)) was examined for the lipid membranes of intact PM2 phage, its host cell, *A. espejiana*, and the extracted phospholipids (phosphatidylethanolamine, *A. espejiana* total phospholipid [1, 2], semi PM2 total phospholipid [3], and phosphatidylglycerol). The results revealed that the all lipid bilayers were in the fast-motional regime and that the dynamic state of the intact biomembranes were considerablly different from those of the extracted phospholipid bilayers. Namely, the motion of the intact biomembranes is more suppressed than that of the extracted phospholipid bilayers, and the former do not reflect the dynamic state expected from the phospholipid composition.

VI-1. Introduction

In Chapter IV, we have successfully shown the selective observation of ^{31}P NMR spectra of their biomembranes *in vivo* by applying ^{1}H-^{31}P cross-polarization pulse technique to a lipid-containing bacteriophage, PM2, and its host bacterium, *A. espejiana*. The temperature dependence of the chemical shift anisotropy obtained from selectively observed spectra provided the information on their phase behaviors. Thus, it was shown that ^{1}H-^{31}P cross-polarization method is a powerful tool for the study of dynamic states of biomembranes in intact biological systems, which usually carry a lot of phosphorus-containing molecules in different dynamic states.

This chapter is devoted to the exploration of more quanti-

tative information on their dynamic states. It was carried out by measuring the spin-lattice relaxation time of protons in the rotating frame ($T_{1\rho}$(H)) of the lipid membranes, because it is one of the important parameters in the ^{1}H-^{31}P cross-polarization dynamics. $T_{1\rho}$(H) is a function of the correlation time of motions, and Akutsu [4] reported that $T_{1\rho}$(H) is such a good parameter that reflects the phase behavior of DPPC bilayers. Thus, the measurement of $T_{1\rho}$(H) is expected to be promising for the quantitative analysis of the dynamic state of the biomembranes in intact systems.

VI-2. Results

$T_{1\rho}$(H) of a system containing only one phosphorus component such as extracted phospholipid bilayers can be obtained by the analysis of the contact time dependence of integrated intensity of cross-polarization spectrum as shown in Chapter IV. However, this method cannot be used to get $T_{1\rho}$(H) of each component in an intact system, which contains more than two phosphorus components, because of the overlapping the contributions from different components. In such a complicated system, we should take advantage of the separately observed spectrum of the component of interest to obtain $T_{1\rho}$(H). For this purpose, the cross-polarization pulse sequence proposed by Stejskal *et al.* [5] was used, because a constant contact time, which can guarantee the condition for the separate observation of each component, is used in this pulse sequence. The detailed description on this pulse sequence is given in Chapter III.

The cross-polarization spectra of the intact and the extracted-lipid bilayers were observed by varying the time (τ) of spin-locking without thermal contact. The integrated intensity of the cross-polarization spectrum of the bilayers of intact PM2 phage and *A. espejiana* cell is plotted as a function of τ in Figure VI-1 A and B, respectively. The powder pattern of the spectrum did not change with the increase of τ. A single exponential was assumed because semilogarithmic plots showed good

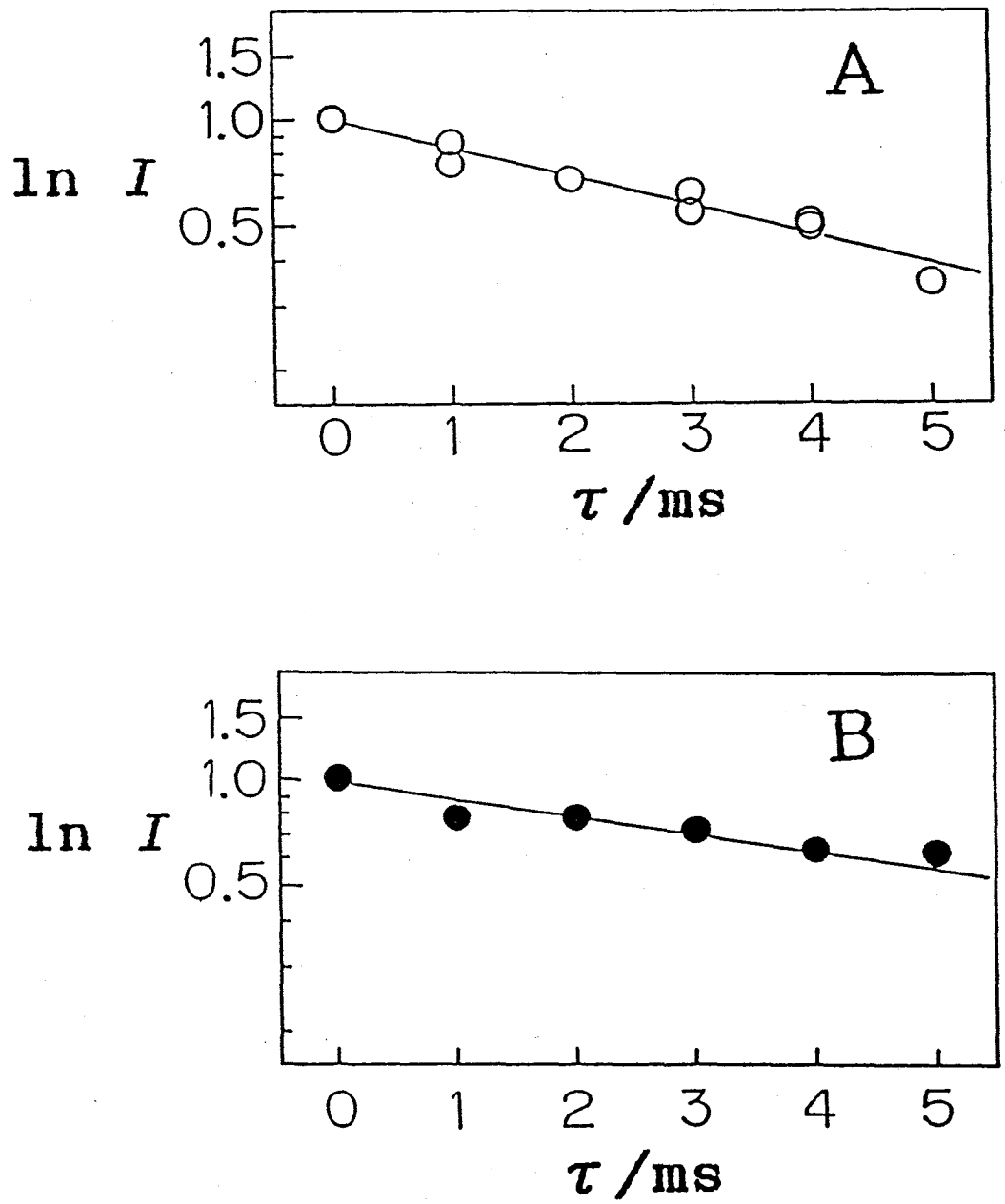

Figure VI-1. The interval (τ) dependence of the integrated intensity (I) of the cross-polarization ^{31}P spectrum at 4°C. (A) The lipid bilayer of intact PM2, and (B) the biomembrane of intact *A. espejiana* cells. The solid straight lines were obtained by least-squares fitting.

linearity for most observations. This suggests that the heat reservoir of the proton spins in the biomembranes is simple in spite of its heterogeneous composition. The change of the integrated intensity of the cross-polarization spectra of PM2 and *A. espejiana* was analyzed by the use of Equation (1) [4].

$$M_P(\tau)=C\exp(-\tau/T_{1\rho}(H)), \quad (1)$$

where $M_P(\tau)$ is the magnetization transferred by cross-polarization with the delay of τ s, and C is constant. The best fit lines are shown by the solid ones. Obtained $T_{1\rho}(H)$ of the bilayers of intact PM2 and *A. espejiana* at 4°C were 4.8 and 8.6 ms, respectively, at 4.7×10^{-4} T of effective magnetic field in the rotating frame, which corresponds to 12.5 μs of 90° pulse (Table 1).

For comparison, $T_{1\rho}(H)$ of the extracted-phospholipid bilayers was examined at 4°C for phosphatidylethanolamine (PE), *A. espejiana* total phospholipid (PE/PG=75/23), semi PM2 total phospholipid (PE/PG=23/64), and phosphatidylglycerol (PG). Their results are shown in Figure VI-2 A, B, C and D. A single exponential was also assumed in these cases, because semilogarithmic plots showed good linearity for the most observations. The best fit lines were shown in the figures. Their $T_{1\rho}(H)$ at about 6.0×10^{-4} T of effective field in the rotating frame are summarized in Table 1. The PE bilayers showed the shortest $T_{1\rho}(H)$ among the extracted phospholipid bilayers. And that $T_{1\rho}(H)$ became longer with the increase of PG content. Another remarkable point is that all of the extracted-phospholipid bilayers showed longer $T_{1\rho}(H)$ than the intact bilayers. This result well explains the disappearance of local minimum in the powder pattern of the cross-polarization spectra of the intact bilayers, and is in good agreement with the results reported by Frye *et al* [6].

Akutsu [4] showed that $T_{1\rho}(H)$ is sensitive to the phase transition of DPPC bilayers. And it is known that $T_{1\rho}(H)$ in the fast-motional regime becomes longer with the enhancement of the motion under the constant effective field in the rotating frame. Therefore, the temperature dependence of $T_{1\rho}(H)$ was examined for the intact and the extracted lipid bilayers. The $T_{1\rho}(H)$ of the intact PM2 phage is plotted as a function of temperature in

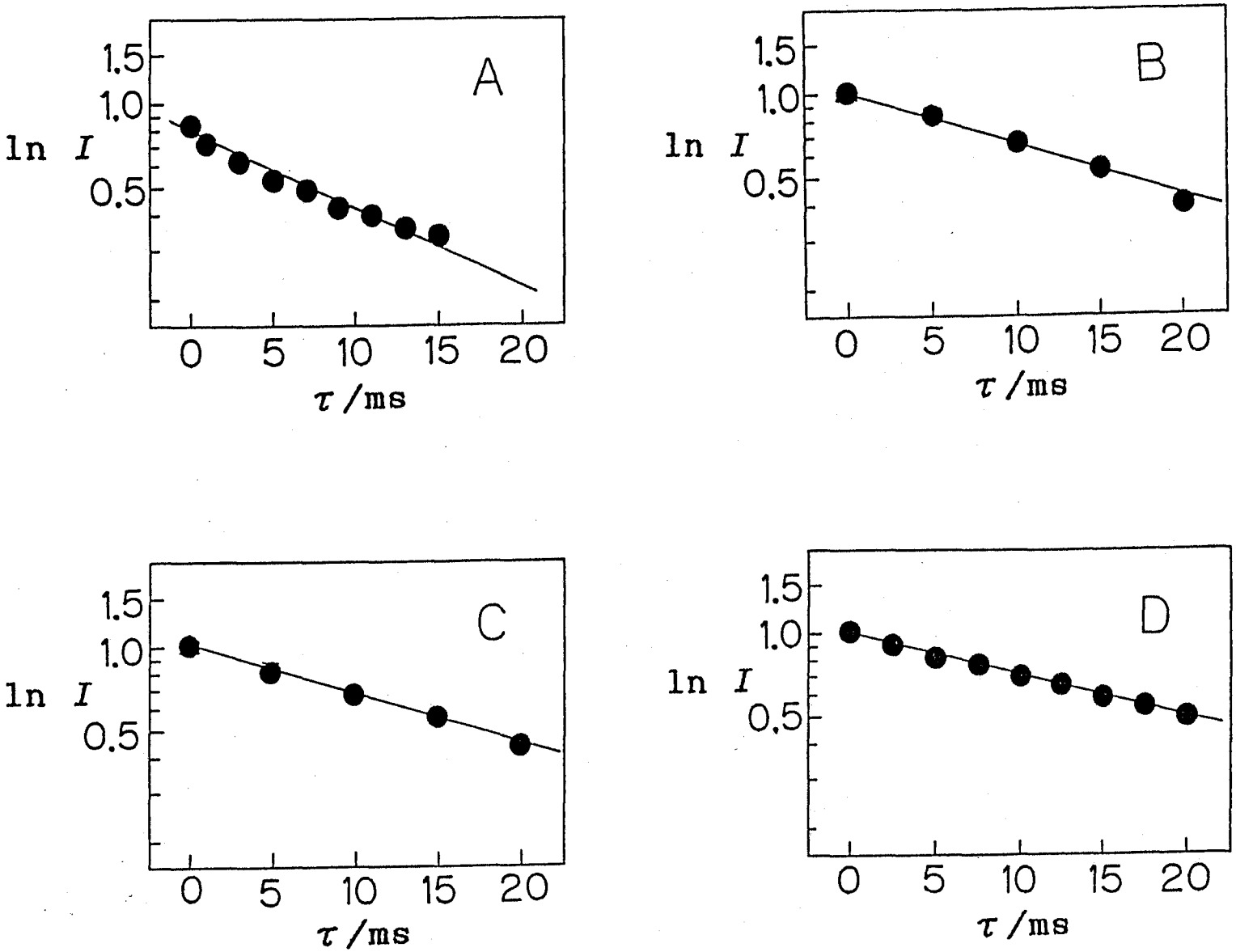

Figure VI-2. The interval (τ) dependence of the integrated intensity (I) of the cross-polarization ^{31}P spectrum at 4°C. (A) PE, (B) *A. espejiana* total phospholipid, (C) semi PM2 total phospholipid, and (C) PG. The solid straight lines were obtained by least-squares fitting.

Table VI-1. Spin-lattice relaxation time ($T_{1\rho}$(H)) of proton in the rotating frame.

Sample	90° pulse/μs	$B_{1H}/10^{-3}$T	$T_{1\rho}$(H)/ms
Intact PM2	12.5	0.47	4.8
Intact *A. espejiana*	12.5	0.47	8.6
PE	10.2	0.58	11.4
A. espejiana total (PE/PG=75/23)	10.2	0.58	22.1
Semi PM2 total (PE/PG=23/64)	9.6	0.61	25.1
PG	9.5	0.62	31.3

Figure VI-3. It was 4.0 ms at 0.5°C, and became longer very gradually with the increase of temperature, namely, with the increase of the motion, up to about 18°C, suggesting that the relevant motion of the bilayer is in the fast-motional regime. The $T_{1\rho}$(H) significantly changed from 18 to 22°C, and did not change above 22°C, suggesting that the change of the dynamic state of the bilayer occurred from 18 to 22°C. This result is in good agreement with the temperature dependence of chemical shift anisotropy shown in Figure VI-2B [3]. On the other hand, $T_{1\rho}$(H) of the bilayer of intact *A. espejiana* was 9.8 ms at 10°C, which is longer than that at 4°C, under 4.7×10^{-4} T of effective field in the rotating frame. It can be concluded that the relevant motion of the bilayer of intact *A. espejiana* is also in the fast-motional regime.

$T_{1\rho}$(H) of the extracted-phospholipid bilayers is plotted as a function of temperature in Figure VI-4. PE showed 10 ms of $T_{1\rho}$(H) at 0°C, and became longer very gradually with the increase of temperature, and reached 23 ms at 24°C. *A. espejiana* and semi PM2 total phospholipid bilayers showed similar temperature dependence of $T_{1\rho}$(H) to each other. Namely, $T_{1\rho}$(H) of *A. espejiana* and semi PM2 total phospholipid bilayers were 17 and 18 ms at 0°C, respectively, became longer linearly with the increase of temperature to 72 and 74 ms at 32°C, respectively. The PG bilayer showed the largest change of $T_{1\rho}$(H) in the extracted phospholipid bilayers. The $T_{1\rho}$(H) increased from 22 to 133 ms with the temperature change from 0 to 34°C. All of their $T_{1\rho}$(H) became longer with the increase of temperature, showing that the relevant motions are in the fast-motional regime in this temperature range. Although the reflection point according to the phase transition was recognized in the temperature dependence of $T_{1\rho}$(H) for intact PM2 bilayer, it was not clear in that for the extracted-phospholipid bilayers. This also suggests that the phase behavior of the intact PM2 bilayer is different from that of the extracted-phospholipid bilayers.

Moreover, since all of $T_{1\rho}$(H) of the intact and extracted-lipid bilayers are in the fast-motional regime, we can compare their mobility by referring to $T_{1\rho}$(H) at the same temperature.

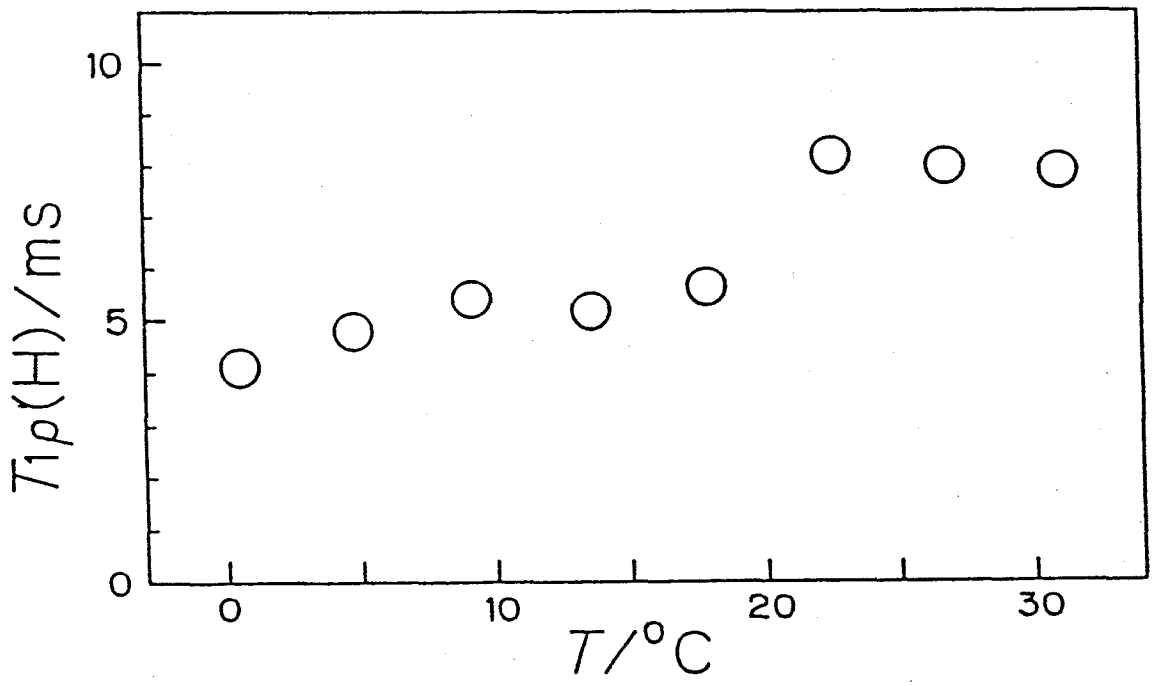

Figure VI-3. The temperature (T) dependence of spin lattice relaxation time of proton in the rotating frame ($T_{1\rho}$(H)) of PM2 bilayers *in vivo*. Intact PM2 phage was in buffer-B2 with 60 % sucrose.

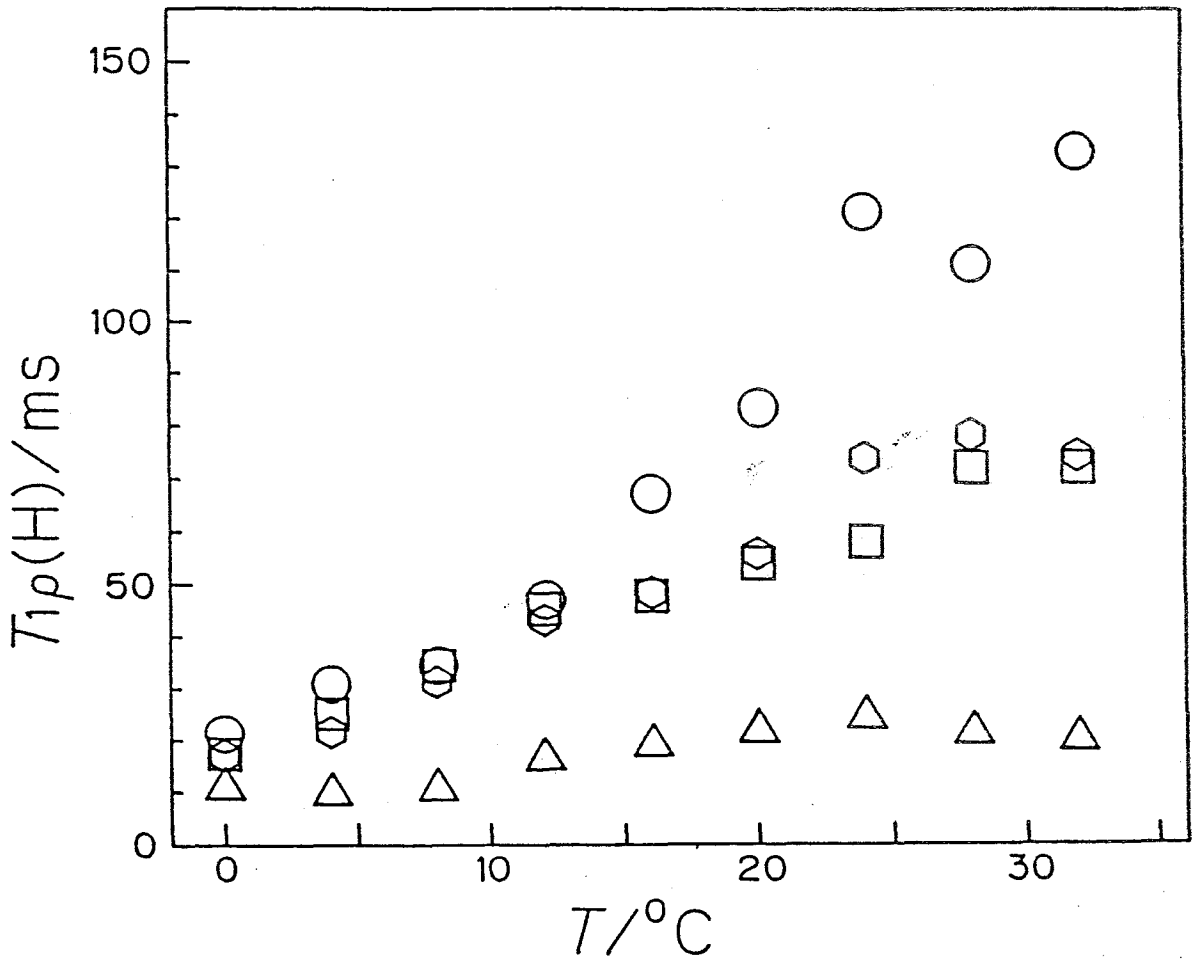

Figure VI-4. The temperature (T) dependence of spin-lattice relaxation time of proton in the rotating frame ($T_{1\rho}$(H)) of the extracted phospholipid bilayers. PE (△), *A. espejiana* total phospholipid (□), semi PM2 total phospholipid (⬡), and PG (○).

Of course, the effective field in the rotating frame should be also taken into account, since $T_{1\rho}$(H) depends on it. Now, we can conclude from the results summarized in Table 1 that the motion of the bilayer of intact PM2 phage is most suppressed among these lipid bilayers, and that the mobility increases in the order of intact PM2, intact *A. espejiana*, PE, *A. espejiana* total phospholipid, semi PM2 total phospholipid and PG. This order suggests that the intact bilayers undergo more suppressed motions than the extracted phospholipid bilayers.

VI-3. Discussion

In Chapter IV [3], it was shown that ^{31}P NMR spectra of the biomembranes of PM2 phage and *A. espejiana in vivo* were separately observed by the application of the ^{1}H-^{31}P cross-polarization method. This enabled us to measure directly spin-lattice relaxation time of proton in the rotating frame ($T_{1\rho}$(H)) of their biomembranes, which can provide a new insight into their dynamics.

The temperature dependence of the $T_{1\rho}$(H) indicated that all of the intact and extracted phospholipid bilayers were in the fast-motional regime ($\tau_c < 1.7\times10^{-6}$ s) above 0°C. This is reasonable, because the axially and semi-axially symmetric powder patterns of ^{31}P NMR spectra shown in Chapter IV [3] mean that phospholipid molecules in the bilayers undergo rapid axially symmetric rotations [7, 8]. Campbell *et al.* [9] reported the relationship between total lineshape of ^{31}P NMR spectrum and the correlation time of polar head group of phospholipid. They estimated that the correlation time of the rotational motion of the polar head group is shorter than 2×10^{-6} s. Thus, both time ranges are in good agreement with each other. It was indicated that the motion which dominates $T_{1\rho}$(H) is not necessarily restricted to the polar head group, because proton spin temperature is common in almost the entire region of the molecules [4]. However, our results suggest that the rotational motion of the phospholipid molecules is responsible for the $T_{1\rho}$(H).

The measurement of $T_{1\rho 1}$(H) revealed that the mobility increased in order of the intact PM2, intact *A. espejiana*, PE, *A. espejiana* total phospholipid (PE/PG=75/23), semi PM2 total phospholipid (PE/PG=23/64) and PG. The result on the extracted-phospholipid bilayers is reasonable. It is known that PE, which is a neutral phospholipid, forms salt bridges through hydrogen bonding among the polar head groups. In contrast, PG has a negative charge in its head group so that the electrostatic repulsion is working between their head groups. Therefore, if fatty acid composition is the same, PE bilayers are expected to be more rigid than PG bilayers, which is actually evidenced by the higher phase transition temperature of PE than PG. Judging from Figure VI-4, the electrostatic repulsion between the head groups of PG molecules is eased by the increase of neutral PE. On the other hand, it was shown that the intact PM2 bilayer was more rigid than the intact *A. espejiana* bilayer in spite of a high PG content of the former than the latter. The biomembrane of intact *A. espejiana* cell has so complicated chemical composition that we cannot discuss the relationship between the structure and the dynamic state in detail at this stage. However, the simple structure and chemical composition of PM2 phage allows [1, 2] us to discuss it. Schafer *et al.* [11] reported that the arrangement of the lipid bilayer in the phage was asymmetric, namely, most of PG are located in the outer leaflet of the bilayer. And, Franklin *et al.* [1, 2] proposed a model for the phage structure in which the basic coat protein (II) interacts with the acidic phosphatidylglycerol of the bilayer to stabilize the membrane. Since $T_{1\rho}$(H) reflects the dynamic state of the entire region of the molecules [4], the influence of proteins III and IV should be taken into account. In particular, protein III is an integral membrane protein and enbeded in the lipid bilayer at a very high content. Even if phospholipids do not strongly interact with these proteins, such interaction in addition to the protein-protein interactions could impose a cooperative restriction on the motion of the phospholipid molecules [12]. The difference between the dynamic states of PM2 phage and *A. espejiana* intact membranes should be attributed to their biological

functions, although the detail of them is not yet clarified. An important conclusion of this work is that the dynamic state of the intact biomembranes cannot be simply anticipated from the phospholipid composition.

References

[1] Franklin, R. M. (1974) "*Current Topics in Microbiology and Immunology*", **68**, 107.

[2] Franklin, R. M., Hinnen, R., Schäfer, R. and Tsukagoshi, N. (1976) *Phil. Trans. R. Soc. Lond. B.*, **276**, 63.

[3] Odahara, T., Akutsu, H. and Kyogoku, Y., submitted.

[4] Akutsu, H. (1986) *J. Magn. Reson.*, **66**, 250.

[5] Stejskal, E. O., Schäfer, J., Sefcik, M. D. and McKay, R. A. (1981) *Macromolecules*, **14**, 275.

[6] Frye, J., Albert, A. D., Selinsky, B. S. and Yeagle, P. L. (1985) *Biophys. J.*, **48**, 547.

[7] Kohler, S. J. and Klein, M. P. (1977) *Biochemistry*, **16**, 519.

[8] Rajan, S., Kang, S-Y., Gutowsky, H. S. and Oldfield, E. (1981) *J. Biol. Chem.*, **256**, 1160.

[9] Campbell, R. F., Meirovitch, E. and Freed, J. H. (1979) *J. Phys. Chem.*, **83**, 525.

[10] Schneider, D., Zulauf, M., Schäfer, R. and Franklin, R. M. (1978) *J. Mol. Biol.*, **124**, 97.

[11] Schäfer, R., Hinnen, R. and Franklin, R. M. (1974) *Eur. J. Biochem.* , **50**, 15.

[12] Akutsu, H., Satake, H. and Franklin, R. M. (1980) *Biochemistry*, **19**, 5264.

Chapter VII

Dynamic Structure of Nucleic Acids and Their Protein Complexes Studied by ^{1}H-^{31}P Cross-Polarization NMR

Summary

^{31}P solid-state NMR spectra were measured to investigate the dynamic structures of nucleic acid molecules in six different types i.e. calf thymus DNA, ribosome of *A. espejiana*, chicken erythrocyte chromatin, *E. coli* phage λ, $\lambda\Delta$ mutant phage and PM2 phage. The addition of water to calf thymus DNA showed that the second hydration induced the transition from A to B form DNA and increased drastically the mobility of nucleic acid molecules. From the experiment of heat denaturation of the proteins in the complexes, it was shown that the coat proteins of λ phage do not directly interact with the DNA in the core as same as T4 phage [1], and that there are direct interactions between the nucleic acids and proteins in ribosome and PM2 phage particles. The temperature dependence of ^{31}P chemical shift anisotropy showed that the change in the mobility of nucleic acids with the increase of temperature in order of intact chicken erythrocyte chromatin, ribosome of *A. espejiana*, *E. coli* phage λ, $\lambda\Delta$ mutant phage and PM2 phage and calf thymus DNA. Moreover, the measurements of the spin-lattice relaxation time of proton in the rotating frame ($T_{1\rho}(H)$) revealed that the intact systems and calf thymus DNA were classified into two different categories of dynamics, respectively.

VII-1. Introduction

Nucleic acid molecules play important roles in the conservation of species and the activity of life. DNA, being a gene itself, has information on heredity and RNA plays key roles in such as transcription and translation. Extensive works on the

structure of nucleic acid molecules have been carried out by X-ray, high-resolution NMR and other physicochemical methods. However, there have been not so many works about the dynamic state in the intact system in spite of its importance.

We examined the dynamic states of five kinds of nucleic acids interacting with proteins in different ways, namely, calf thymus DNA, chicken erythrocyte chromatins, ribosomes of *A. espejiana*, *E. coli* phage λ, $\lambda\Delta$ mutant phage and lipid-containing bacteriophage PM2. Calf thymus DNA does not contain proteins. In the chicken erythrocyte chromatin, the double-stranded DNA is extensively condensed by the interaction with histon proteins [2, 3]. In the case of λ and $\lambda\Delta$ mutant phages, a double-stranded DNA is thought to be tightly packaged in the head without any direct protein-nucleic acid interaction. It was suggested that PM2 phage has a DNA-binding protein (protein-IV) anchoring itself in the inner leaflet of its bilayer membrane [4, 5, 6]. The motion of PM2 DNA was suggested to be coupled with the changes in membrane fluidity through protein-IV [1]. Ribosomes are large complexes of RNAs and proteins. The RNAs are expected to interact directly with ribosomal proteins [7]. Those nucleic acid molecules form so huge structure that their motions are significantly suppressed.

To investigate the dynamic states of the huge systems with phosphorus in suppressed motion, the ^{1}H-^{31}P cross-polarization was shown to be promising in the previous chapters (Chapter IV, V, VI). The method is particularly advantageous for such complicated systems as PM2 phage and its host, which have more than two rigid phosphorus components, because this method allows us to observe the different dynamic components separately.

Therefore, we applied the ^{1}H-^{31}P cross-polarization method to the five systems mentioned above, and investigated the relationship between the structures and the dynamic states of nucleic acid molecules.

VII-2. Results

Cross-Polarization Spectra of DNA at Different Conditions.

In order to investigate the dynamic states of nucleic acid molecules in different types of protein-nucleic acid complexes, it is necessary to know the dynamics of nucleic acid molecules themselves without proteins. We examined ^{31}P NMR spectra of calf thymus DNA under several different conditions by the use of single-pulse and ^{1}H-^{31}P cross-polarization methods. Their spectra at 5°C are shown in Figure VII-1. Figure VII-1 A is a single-pulse spectrum of the dry DNA. The spectrum showed a typically asymmetric powder pattern characteristic of rigid molecules, and the principal components of chemical shift tensor (σ_{11}, σ_{22}, σ_{33}) are 98.3, 24.8 and -124.1 ppm, respectively. The chemical shift anisotropy ($\Delta\sigma=\sigma_{33}-\sigma_{11}$), which is a parameter relating to the motion of the DNA, is -222.4 ppm.

In actual biological systems, water is abundantly present and plays a key role in the function of biomolecules. In order to see the influence of water, we examined ^{31}P NMR spectra of DNA with different water contents. Figures VII-1 B, C and D are the spectra of the DNA samples kept at 71, 87 and 92 % of relative humidities at 25°C for a few days, respectively. The chemical shift anisotropies of B, C and D are -188.5, -165.4 and -156.5 ppm, respectively. The absolute value of chemical shift anisotropy ($|\Delta\sigma|$) decreased with the increase of water content. And, the principal components of the chemical shift tensor suddenly became unclear above 87 % of relative humidity. It is known that the A form DNA transforms into the B form in the range from 84 to 92 %, namely, DNA is in the A form at a low relative humidity but takes on the B form in the physiological condition [8]. Figure VII- 1 E is a cross-polarization spectrum of the DNA sample prepared by adding 0.1 ml of water to 0.1 g of dry DNA. There was no difference in the single-pulse and cross-polarization spectra of the sample. The spectrum showed a Gaussian type symmetric pattern characteristic of the isotropic motion. The spectral width is extremely narrow in comparison with those in Figures VII-1 B - D, and is 37.2 ppm. These results mean that

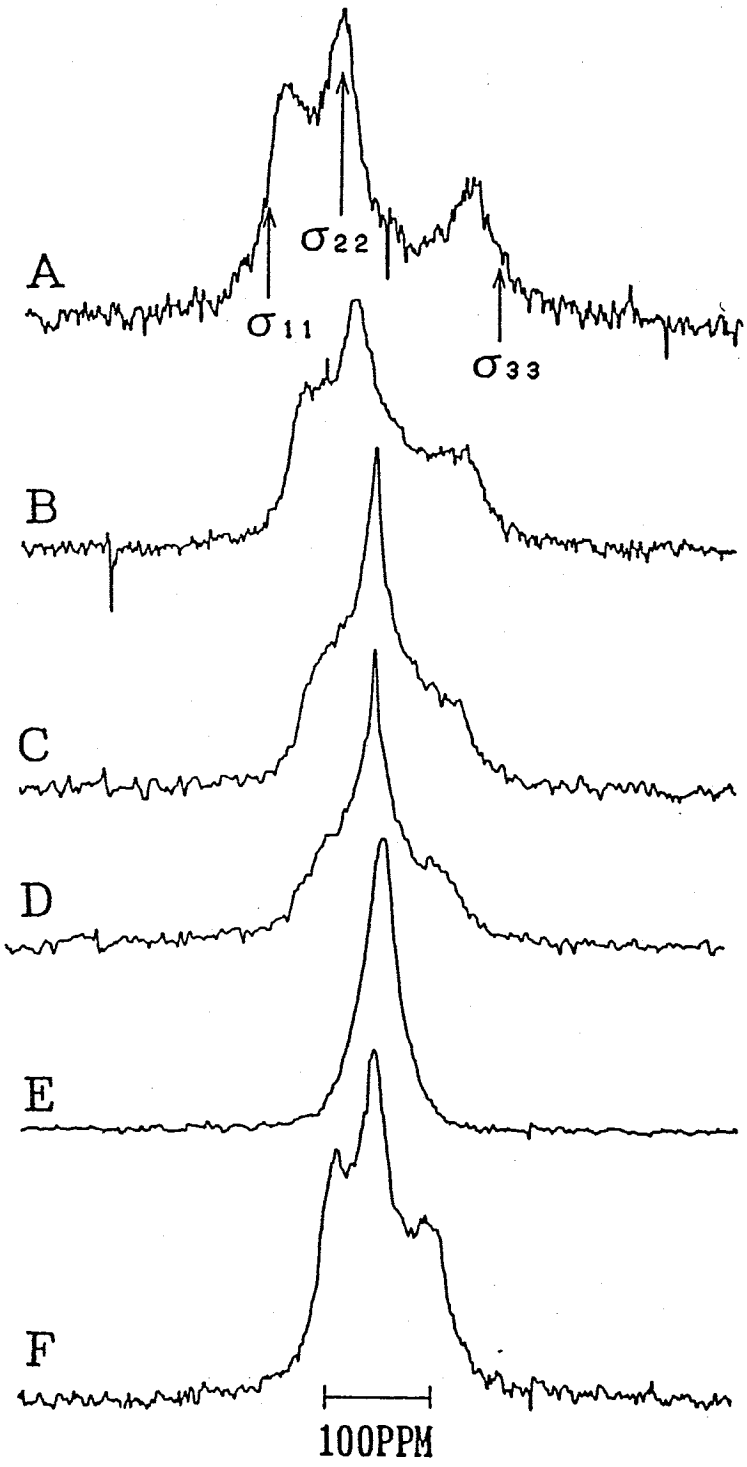

Figure VII-1. ^{31}P NMR spectra of calf thymus DNA at 5°C. (A) Single pulse spectrum of dry DNA with a pulse delay of 20 s; (B) cross-polarization spectrum of DNA kept in 71 % of relative humidity at 25°C with a pulse delay of 3 s; (C) single pulse spectrum of DNA kept in 87 % of relative humidity at 25°C with a pulse delay of 3 s; (D) single pulse spectrum of DNA kept in 92 % of relative humidity at 25°C with a pulse delay of 3 s; (E) cross-polarization spectrum of DNA sample prepared by adding 0.1 ml of water to 0.1 g of dry DNA with a pulse delay of 3 s; and (F) cross-polarization spectrum of the DNA sample prepared by adding 0.2 ml of buffer-A solution with 60 % sucrose to 0.1g of dry DNA with a pulse delay of 4 s. 600, 2,000, 2,000, 2,000 1,000 and 2,000 transients were accumulated for A, B, C, D, E and F, respectively. The 90° pulse was used both for cross-polarization and for single pulse modes. An exponential window function with a 50 Hz broadening factor was used.

the existence of water in the DNA drastically influences the mobility of DNA molecules. We also measured ^{31}P NMR spectra of DNA in sucrose-containing buffer-A solution, because the spectra of intact chicken erythrocyte chromatin, λ, $\lambda\Delta$ and PM2 phages were measured in the presence of sucrose as shown later. Figure VII-1 F is a cross-polarization spectrum of the sample obtained by adding 0.2 ml of buffer-A solution with 60 % of sucrose to 0.1 g of dry DNA. The principal components are clearly recognized at 67.2, 5.0 and -66.9 ppm. The chemical shift anisotropy is -134.1 ppm. There was no difference in the spectra of the DNA in the presence of 30 and 60 % sucrose. σ_{11} and σ_{33} in Figure VII-1 C and D are more indistinct than those of Figure VII-1 F, in spite of larger anisotropy of the formers than that of the latter, suggesting that the motion of DNA in the solution with 60 % sucrose is either more uniform or more restricted than those in the figures at 87 and 92 % of relative humidity.

Cross-Polarization Spectra of Nucleic Acids-Proteins Complexes ^{1}H-^{31}P cross-polarization technique was applied to five different kinds of protein-nucleic acid complexes. ^{31}P NMR spectra of them, namely, the purified ribosome of *A. espejiana*, the intact chicken erythrocyte chromatin, *E. coli* phage λ, $\lambda\Delta$ mutant phage and lipid-containing bacteriophage PM2, are shown in Figure VII-2 A, B, C, D and E, respectively. All DNAs in the complexes mentioned above are double-stranded ones. In particular, Figure VII-2 E is the selectively observed spectrum of the DNA packaged in PM2 core, which became possible to be observed only by the use of cross-polarization method. In order to suppress the rotational motions and to get high concentrations by volume reduction, the ribosome was prepared as pellet by centrifugation at 60,000 rpm (Beckman Type 65), wild type and deletion mutant of λ phages were dialyzed against a λ-buffer solution with 30 % sucrose, the intact chicken erythrocyte chromatin was dialyzed against a STM-buffer solution with 30 % sucrose and PM2 phage was subjected to stepwise dialysis against a buffer-B2 solutions with 10, 30 and 60 % sucrose, respectively. All spectra showed typical asymmetric powder patterns with clear principal components of ^{31}P chemical shift tensor, suggesting that the

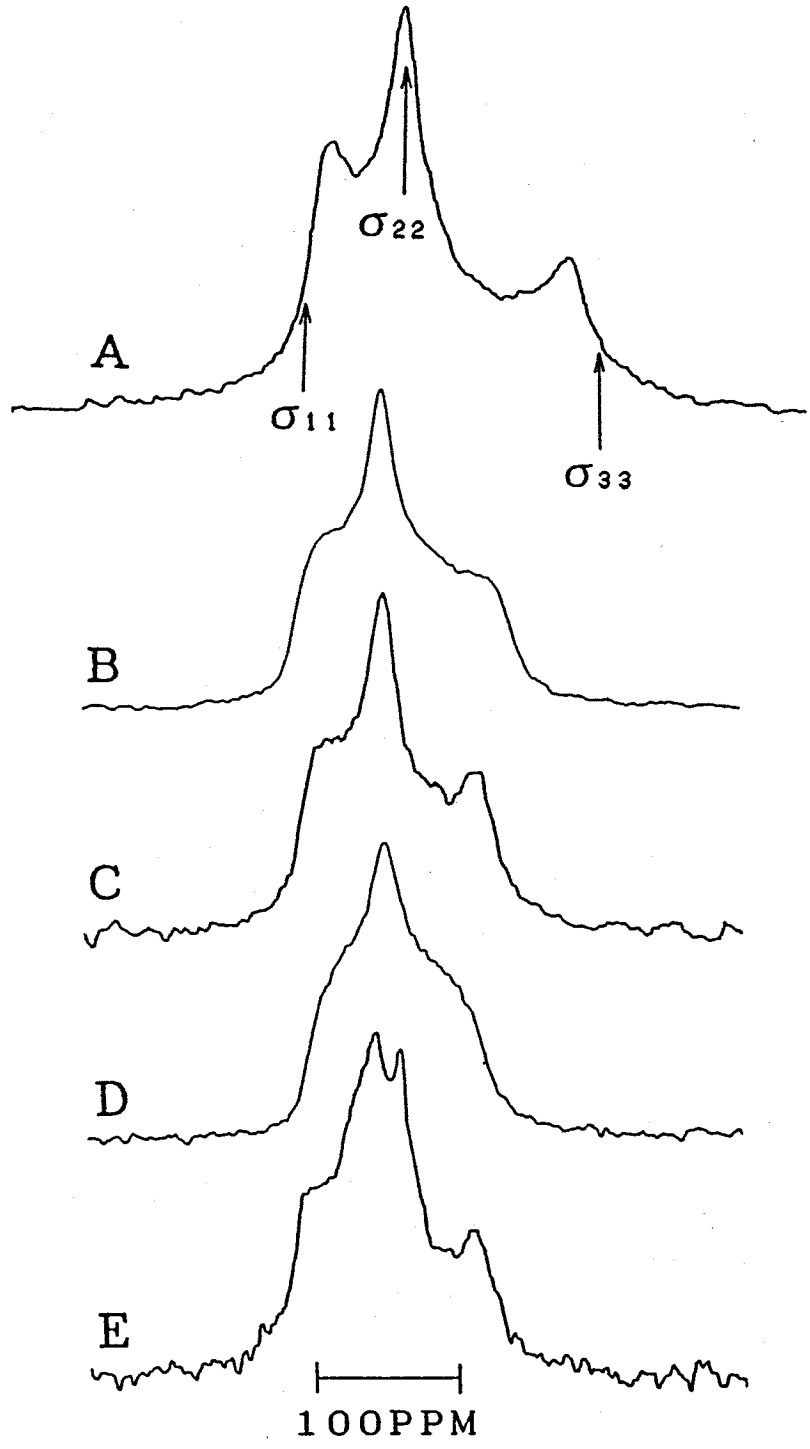

Figure VII-2. Cross-polarization ^{31}P NMR spectra of (A) purified ribosome pellet of *A. espejiana*, (B) intact chicken erythrocyte nuclei in STM-buffer solution with 30 % sucrose, (C) intact λ phage, (D) $\lambda\Delta$ mutant phage in λ-buffer solution with 30 % sucrose and (E) PM2 phage in buffer-B2 solution with 60 % sucrose, with a thermal contact time of 0.7 ms at 5°C. 1,600, 8,000, 1,000, 2,000 and 8,000 transients were accumulated for A, B, C, D and E, respectively. The 90° pulse for the ribosome, the chromatin, λ, $\lambda\Delta$ mutant and PM2 phages was 10.8, 6.6, 8.0, 7.0 and 12.5 μs, respectively. An exponential window-function with a 100 Hz broadening factor was used.

motions of phosphorus are uniformly suppressed. ^{31}P chemical shift anisotropies of nucleic acid molecules of the ribosome, the chromatin, λ phage, $\lambda\Delta$ mutant phage and PM2 phage at 5°C were -210, -155, -141, -127.6 and -139 ppm, respectively. The spectra of the chromatin and λ phage did not change on the increase of sucrose concentration from 30 to 60 %. This suggests that the presence of 30 % sucrose in a buffer solution was enough to suppress the rotational or overall motions of these complexes.

Spectra of the Heat Treated Complexes. In order to see the nature of the interactions between protein and nucleic acid molecules, the ribosome pellet, λ phage in λ-buffer solution with 30 % of sucrose and PM2 phage in buffer-B2 solution with 60 % of sucrose, each of which was incubated at 65°C for 5 h, were examined. ^{31}P NMR spectra of the incubated samples were taken at 5°C and are shown in Figures VII-3 A, B and C. The chemical shift anisotropies of the ribosome and PM2 phage are -176 and -125 ppm, respectively. Although the chemical shift anisotropies of the heat-treated ribosome and PM2 phage were smaller than those of intact ones and the principal components were unclear, the cross-polarization spectra still could be characterized as the asymmetric powder patterns. This suggests that the nucleic acid molecules in the complexes have something to interact with them and that the interactions are not uniform. In contrast, the spectrum λ phage drastically changed by heat treatment and showed a sharp signal at the center. The linewidth at the half height of the signal is 12.4 ppm. This is similar to the result on T4 phage reported by Akutsu *et al* [1]. Cross-polarization spectrum would not be taken under any conditions, suggesting that the DNA is in rapid motion. This is consistent with the narrow line shape of the signal.

Temperature Dependence of the Chemical Shift Anisotropy of DNA under Different Conditions. The temperature dependence of chemical shift anisotropy is more sensitive to the flexibility of the structure than the value of the chemical shift anisotropy itself, because the latter could depend on the state of sample. At first, we examined the temperature dependence of chemical shift anisotropy of calf thymus DNA. ^{31}P chemical shift aniso-

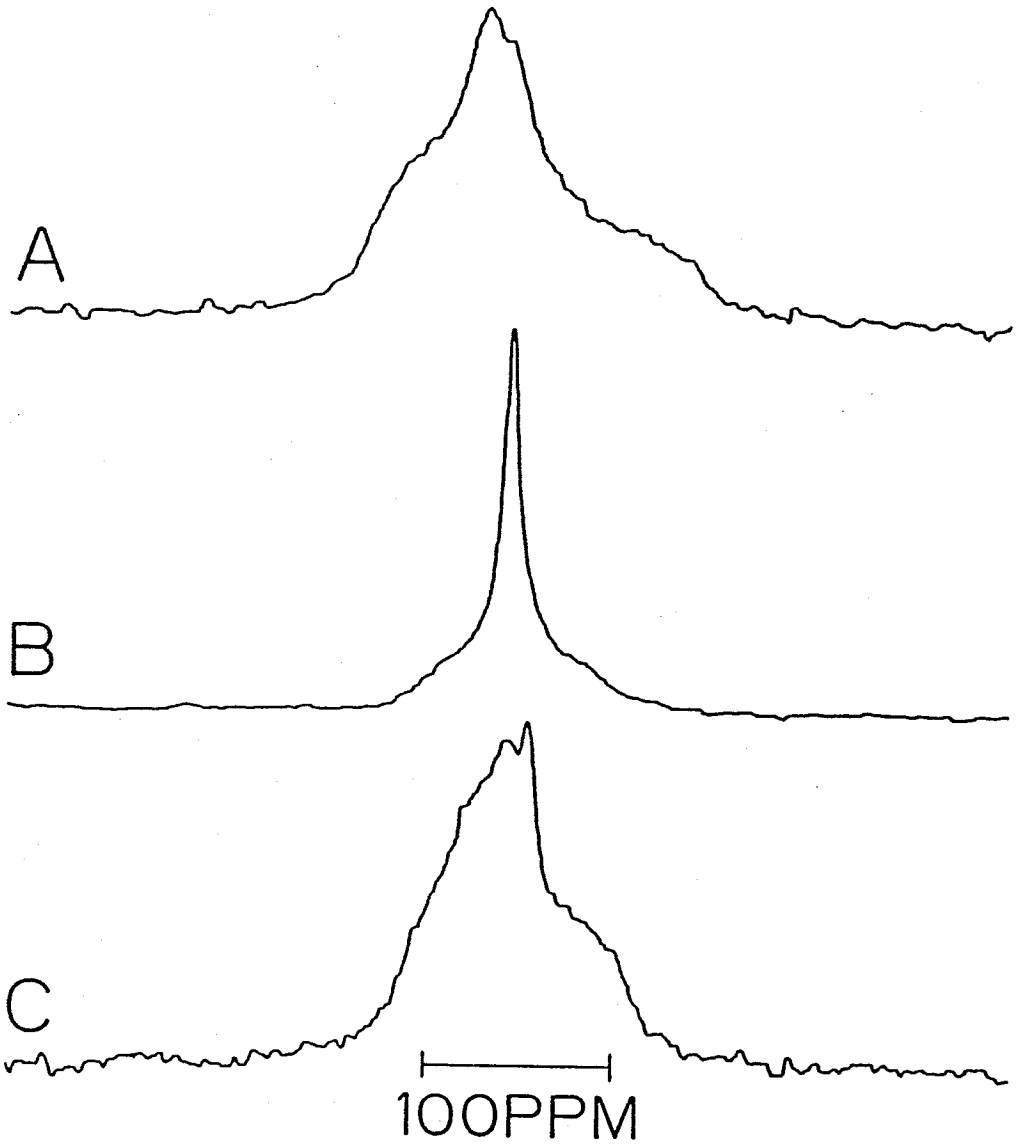

Figure VII-3. ^{31}P NMR spectra of purified ribosome pellet of *A. espejiana*, λ phage in λ-buffer solution with 30% sucrose and PM2 phage in buffer-B2 solution with 60 % sucrose at 5°C after being heated at 65°C for 5 h. (A) Ribosome of *A. espejiana*, measured by the cross-polarization method at a thermal contact time of 0.7 ms; (B) λ phage, measured by the single-pulse method; and (C) PM2 phage, measured by the cross-polarization method at a thermal contact time of 0.7 ms. 1,200, 1,200 and 10,000 transients were accumulated for A, B and C, respectively. The 90° pulse width was 10.8, 10.0 and 12.5 μs for A, B and C, respectively. The 45° pulse was used for the single pulse spectrum of λ phage. An exponential window-function with a 100 Hz broadening factor was used.

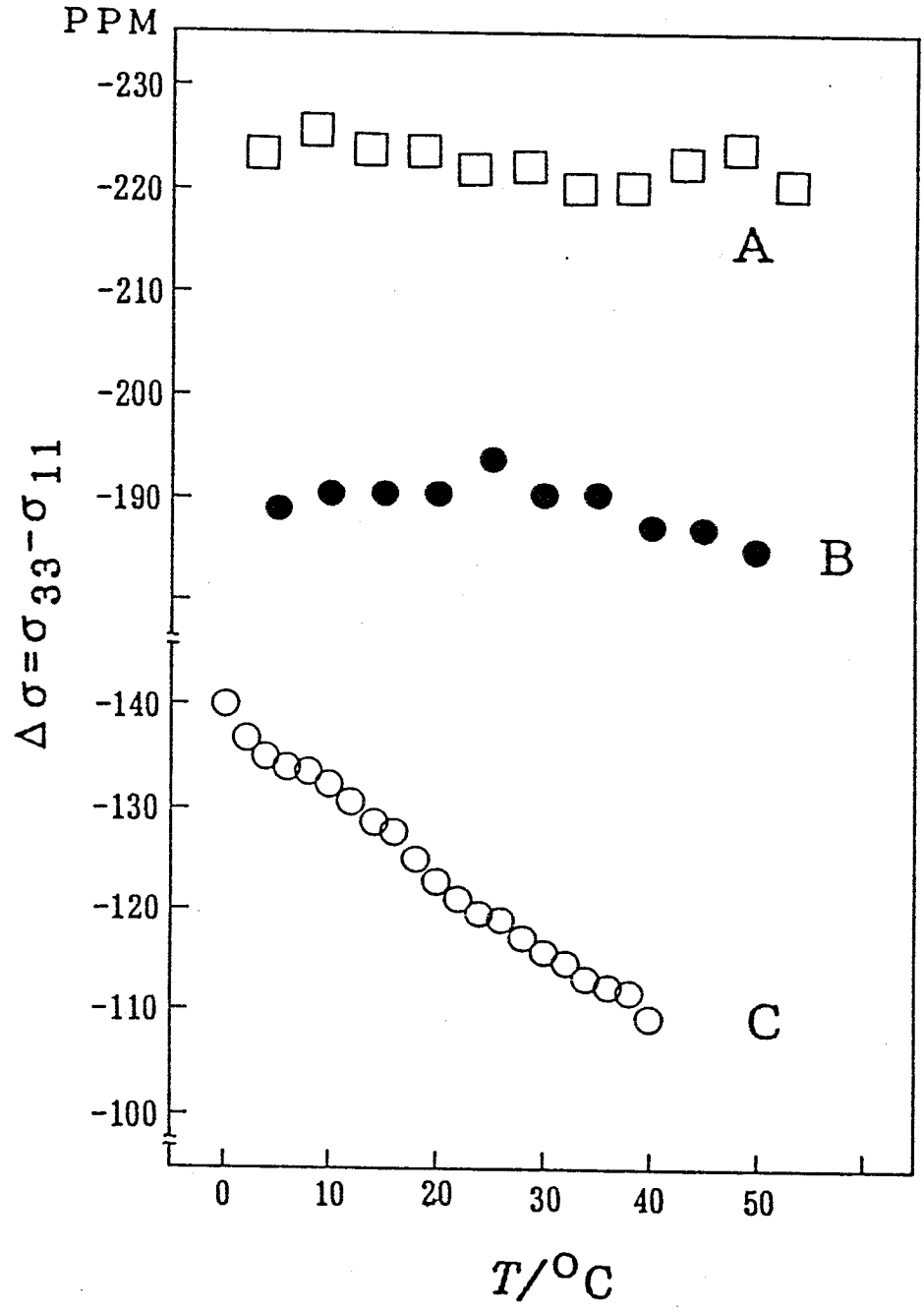

Figure VII-4. Temperature (T) dependence of the ^{31}P chemical shift anisotropy ($\Delta\sigma=\sigma_{33}-\sigma_{11}$) of calf thymus DNA. (A) Dry DNA; (B) the DNA kept in 71 % of relative humidity at 25°C; and (C) the DNA sample prepared by adding 0.2 ml of buffer-A solution with 60 % sucrose to 0.1 g of dry DNA.

tropies of DNA in dry state, kept at 71 % of relative humidity and in buffer-A solution with 60 % sucrose are plotted as a function of temperature in Figures VII-4 A, B and C, respectively. The chemical shift anisotropy of dry DNA was -223 ppm at 5°C and no change was observed in both chemical shift anisotropy and powder pattern of the spectra in the temperature range examined. The DNA at 71 % of relative humidity showed -190 ppm of chemical shift anisotropy at 5°C and hardly changed up to 45°C. However, σ_{11} and σ_{33} of the spectrum began to become unclear above 45°C, and vanished at all at 70°C. These results showed that the water effectively caused segmental motions of DNA above 45°C, because a rapid overall motion was not expected for its very large molecular size. The chemical shift anisotropy of the DNA in buffer-A solution with 60 % of sucrose was -139 ppm at 0°C, and its absolute value decreased linearly with an increase of temperature. The principal components of the chemical shift tensor could be distinguished up to 40°C, suggesting that the DNA was in uniformly suppressed motion in this temperature range. Thus, the temperature dependence of chemical shift anisotropy and powder pattern are good indicators reflecting the dynamic states.

Temperature dependence of the Chemical Shift Anisotropy of the Intact Nucleic Acid-Protein Complexes. In the next step, we examined the temperature dependence of ^{31}P chemical shift anisotropy of the intact systems. The results of purified ribosome pellet of *A. espejiana*, intact chicken erythrocyte chromatin in STM-buffer solution with 30 % sucrose, λ phage, $\lambda\Delta$ mutant phage in λ-buffer solution with 30 % sucrose and PM2 phage in buffer-B2 solution with 60 % sucrose are shown in Figures VII-5 A, B, C, E and D, respectively. The chemical shift anisotropy of the ribosome was -212 ppm at 0°C, and its absolute value decreased gradually with the increase of temperature. The temperature dependence of chemical shift anisotropy of the ribosome in NTCM-buffer solution with 60 % sucrose showed the similar tendency. The powder pattern of the spectrum did not changed in the range from 0 to 42°C. However, its principal components began to become unclear above 45°C, and it gave rise to the powder pattern of denatured ribosome similar to that of Figure

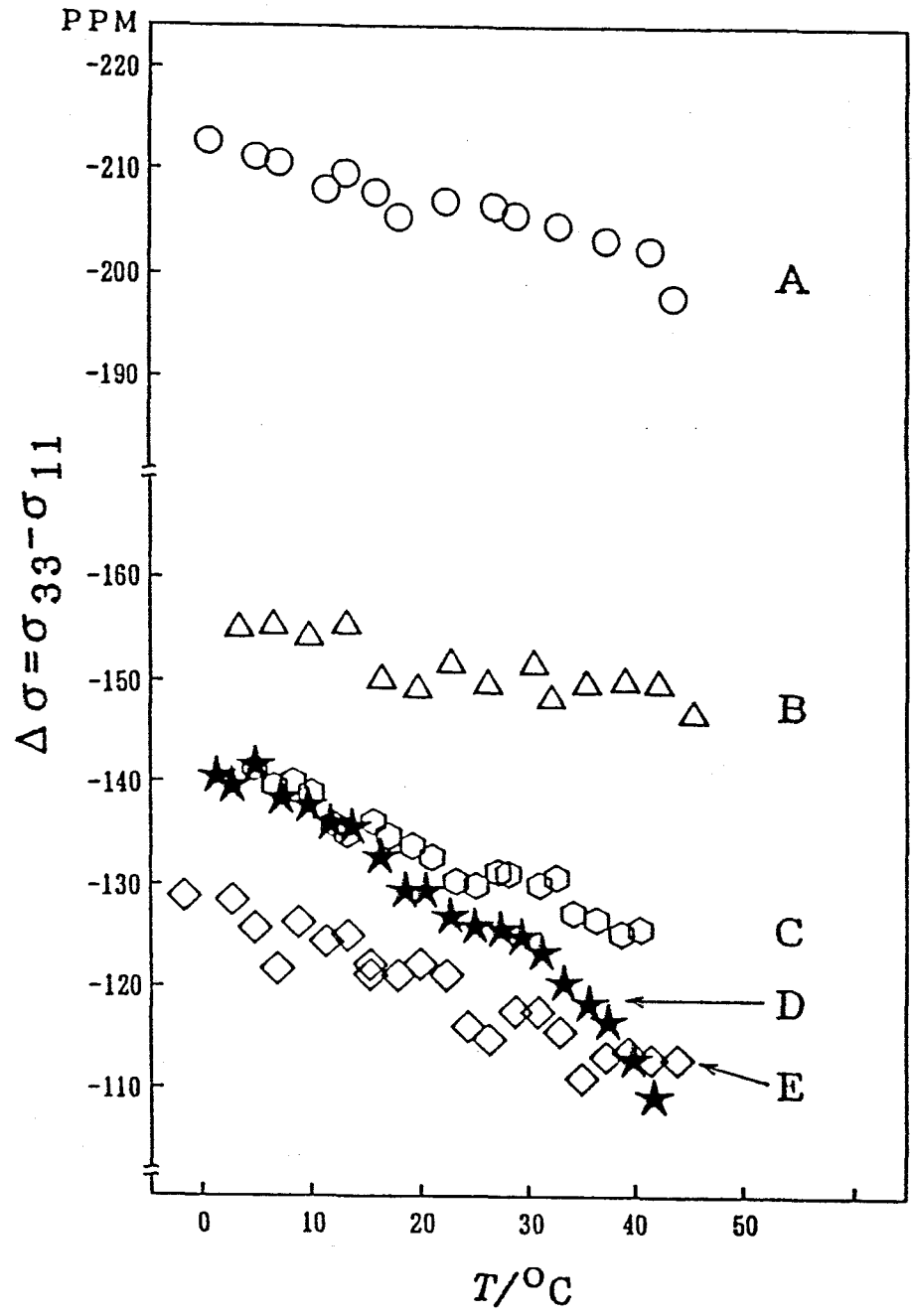

Figure VII-5. Temperature (T) dependence of ^{31}P chemical shift anisotropy ($\Delta\sigma=\sigma_{33}-\sigma_{11}$) of (A) purified ribosome pellet of *A. espejiana*, (B) intact chicken erythrocyte chromatin in STM-buffer solution with 30 % sucrose, (C) intact λ phage, (D) intact $\lambda\Delta$ mutant phage in λ-buffer solution with 30 % sucrose, and (E) intact PM2 phage in buffer-B2 solution with 60 % sucrose. The spectra were measured by the cross-polarization method at a thermal contact time of 0.7 ms. The Hartmann-Hahn condition was redetermined for every measurement.

VII-3 A at 50°C. This result suggests that the intermolecular interactions between rRNA and ribosomal proteins became weak at 50°C. The results of chicken erythrocyte chromatin, λ and λΔ mutant phages showed that the absolute values of their ^{31}P chemical shift anisotropies decreased with the increase of temperature, and that all of their spectra gave rise to asymmetric powder patterns with the clear principal components below 40°C. This suggests that the proteins in these systems are stable against the heat in the temperature range examined. The chemical shift anisotropy of PM2 phage changed more significantly than those of the other intact systems. The principal components in the spectrum of PM2 phage began unclear above 26°C. This temperature is close to the inflection point in the temperature dependence of the chemical shift anisotropy. These results agreed with that reported by Akutsu *et al* [1]. The temperature dependence of the chemical shift anisotropy was the smallest in intact chicken erythrocyte chromatin and increased in order of the ribosome, λ and λΔ phage and PM2 phage. Where the temperature dependence of λ and λΔ phages were almost equal to each other. A remarkable point in Figure VII-5 is that the slope of the plots is not exactly correlated to the order of the values of chemical shift anisotropy at the same temperature.

$T_{1\rho}$(H) of DNA and Complexes. Spin-lattice relaxation time of protons in the rotating frame ($T_{1\rho}$(H)) expected to be a good indicator of slow motions of molecules, because this parameter is closely related to the correlation time of the motion in the range around 10^{-5} s. We observed $T_{1\rho}$(H) for the intact systems and calf thymus DNA in buffer-A solution with 60 % sucrose. Cross-polarization spectra of the intact chicken erythrocyte chromatin in a STM-buffer solution with 30 % sucrose at 5°C were measured at several thermal contact times (t). The integrated intensity of the spectrum is plotted as a function of contact time in Figure VII-6 A. The cross-relaxation time between the proton and phosphorus spins (T_{HP}) and $T_{1\rho}$(H) were obtained by nonlinear least-squares fitting by the use of Equation (1) [9, 10],

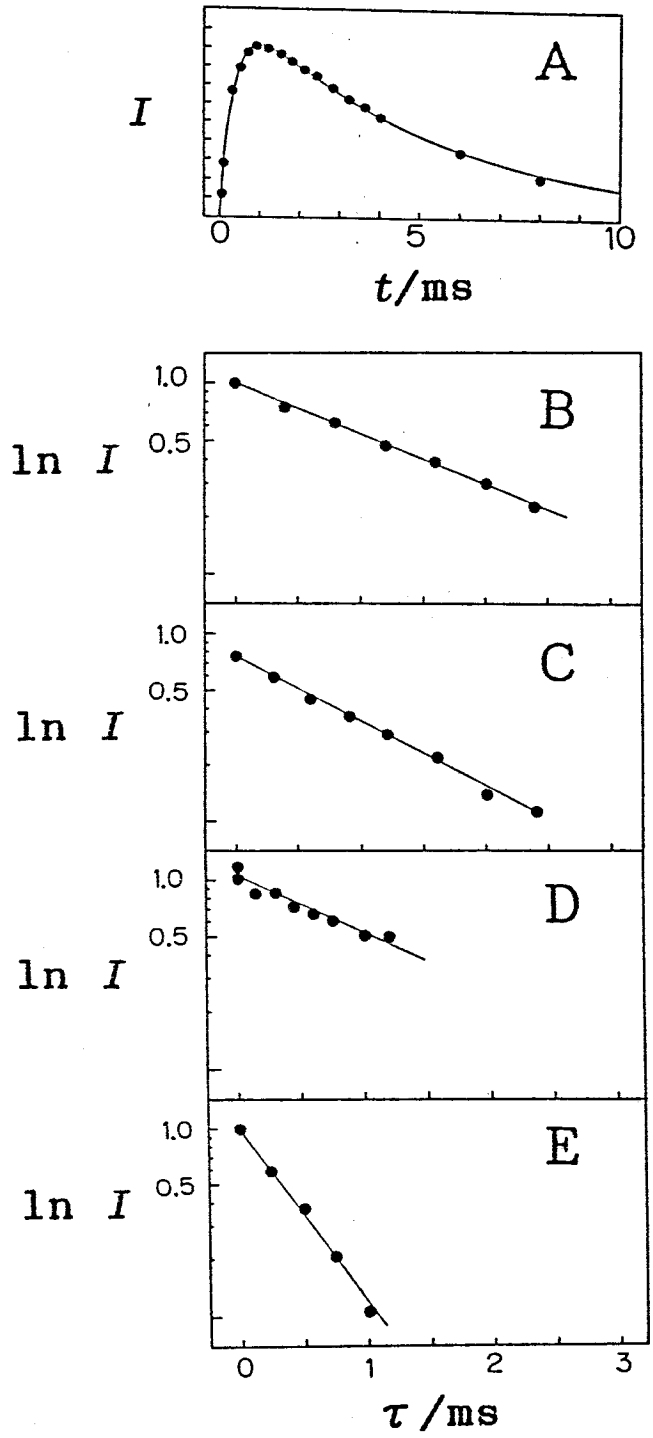

Figure VII-6. $T_{1\rho}$(H) determination by the cross-polarization method at 5°C. (A) Contact time (t) dependence of the integrated intensity (I) of the cross-polarization spectra of intact chicken erythrocyte chromatin in STM-buffer solution with 30 % sucrose. The thermal contact time and the 90° pulse were 1.0 ms and 6.7 μs, respectively. The pulse delay of 3 s was used. The interval (τ) dependence of the integrated intensity (I) of cross-polarization spectra of (B) purified ribosome pellet of *A. espejiana*, (C) intact λ phage in λ-buffer solution with 30 % sucrose, (D) intact PM2 phage in buffer-B2 solution with 60 % sucrose, and (E) calf thymus DNA in buffer-A solution with 60 % sucrose. The pulse delay was 4, 3, 4 and 4 s for B, C, D and E, respectively. The 90° pulse width was 10.8, 14.0, 12.2, 12.5 and 11.6 μs for B-1, -2, C, D and E, respectively.

$$M_P(t)=K(1+\varepsilon\alpha^2-T_{HP}/T_{1\rho}(H))^{-1} \times[\exp(-t/T_{1\rho}(H))-\exp(-t(1+\varepsilon\alpha^2)/T_{HP})], \quad (1)$$

where $M_P(t)$ means the efficiency of cross-polarization, $\alpha=\gamma_P B_{1P}/\gamma_H B_{1H}$, $\varepsilon=N_P/N_H$ and $K=\alpha(\gamma_H/\gamma_P)M_{P0}$. Here t, γ, B_1, N and M_{P0} represent the contact time, the gyromagnetic ratio, the amplitude of the rotating magnetic field, the number of spins and Zeeman magnetization of phosphorus spins, respectively. The best fit curve is shown by the solid line, which gave 0.36 and 5.5 ms for T_{HP} and $T_{1\rho}(H)$, respectively. However, this method does not work with the intact system containing two or more different phosphorus components such as PM2 phage. Therefore, we applied the cross-polarization method according to Stejskal *et al* [11]. to the intact systems. This method is promising for that case, because the starting time (τ) of ^{31}P spin locking from ^{1}H spin locking is varied under the constant thermal contact time in the pulse sequence. It is necessary to compare $T_{1\rho}(H)$ measured under the same amplitude of spin-locking magnetic field for the knowledge of the dynamic state of molecule, because $T_{1\rho}(H)$ depends on the amplitude. Therefore, we measured $T_{1\rho}(H)$ of the samples at 5^oC under 4.9×10^{-4} T of spin-locking magnetic field which corresponds to about 12 μs of 90^o pulse width. The results of purified ribosome pellet of *A. espejiana*, λ phage in λ-buffer solution with 30 % sucrose, PM2 phage in buffer-B2 solution with 60 % sucrose and calf thymus DNA in buffer-A solution with 60 % sucrose at 5^oC are shown in Figures VII-6 B, C, D and E, respectively. The logarithm of the integrated intensity of the spectrum is plotted as a function of the starting time of ^{31}P spin locking. $T_{1\rho}(H)$ of each samples were obtained by a simple least-square fitting using Equation (2) [10],

$$M_P(\tau)=C\exp(-\tau/T_{1\rho}(H)), \quad (2)$$

where $M_P(\tau)$ is the magnetization transferred by cross-polarization with a delay at τ, and C is constant. The best fit lines are shown by the solid straight lines. $T_{1\rho}(H)$ obtained by such way is summarized in Tables 1 and 2. Namely, Tables 1 and 2 respectively show spin-locking magnetic field amplitudes and temperature dependence of $T_{1\rho}(H)$ of the samples. $T_{1\rho}(H)$ of chromatin, ribosome, λ phage and calf thymus DNA became shorter

Table VII-1. The spin-lattice relaxation time ($T_{1\rho}$(H)) of proton in the rotating frame at several spin-locking fields (B_{1H}) at 5°C.

Sample	90° pulse/μs	B_{1H}	$T_{1\rho}$(H)/ms
Chromatin			
	4.9	1.20	4.53
	5.0	1.17	4.40
	5.8	1.01	4.08
	6.6	0.89	3.73
	6.7	0.88	3.79
	8.2	0.72	3.08
	8.4	0.70	3.63
	11.2	0.52	2.71
	17.0	0.35	1.98
Ribosome			
	6.5	0.90	2.56
	6.5	0.90	2.45
	8.3	0.71	1.91
	10.8	0.54	1.69
	14.0	0.42	1.26
λ Phage			
	6.5	0.90	2.15
	7.8	0.75	1.85
	9.2	0.64	1.68
	12.2	0.48	1.23
	19.0	0.31	0.85
Calf Thymus DNA			
	5.4	1.09	0.87
	6.6	0.89	0.75
	8.7	0.68	0.59
	11.6	0.51	0.45
PM2 Phage			
	12.5	0.47	1.30

Table VII-2. The spin-lattice relaxation time ($T_{1\rho}$(H)) of proton in the rotating frame at several temperatures (T).

Sample	T/°C	90° pulse/μs	$B_{1H}/10^{-3}$T	$T_{1\rho}$(H)/ms
Ribosome				
	0	12.0	0.49	1.97
	4	12.0	0.49	1.90
	8	12.5	0.47	1.88
	12	13.0	0.45	1.75
	16	12.5	0.47	1.75
	20	12.5	0.47	1.69
	24	12.5	0.47	1.69
	28	13.0	0.45	1.50
	32	13.0	0.45	1.43
	36	13.0	0.45	1.43
	40	13.0	0.45	1.34
λ Phage				
	4	6.1	0.96	2.21
	15	6.8	0.86	1.80
	25	6.3	0.93	1.93
	35	6.7	0.88	1.48

with the increase of the effective field amplitude in the rotating frame in all cases. These results mean that the motions of the nucleic acid molecules are in the slow-motional regime at 5°C. The temperature dependencies of $T_{1\rho}$(H) of the ribosome and λ phage resulted in shorter $T_{1\rho}$(H) with the increase of temperature, i.e., with the increase of their mobility. This means that the motions of RNA and DNA in the complexes are in the slow-motional regime in the temperature ranges examined. The results of the temperature dependence of $T_{1\rho}$(H) is in good agreement with its effective field dependence. The effective field dependence in the rotating frame of $T_{1\rho}$(H) has not yet been examined for the DNA of PM2 phage. However, since the chemical shift anisotropy and the powder pattern of its cross-polarization spectrum are similar to those of λ phage, the DNA of PM2 phage would be in the slow-motional regime. Since all the nucleic acids investigated in this work are in the slow-motional regime, we can determine the order of their dynamic state by the comparison of their $T_{1\rho}$(H) at the same effective field in the rotating frame. Table VII-1 showed that the DNA of the chromatin is in the most suppressed motion among the samples examined, and that the dynamic state increases in order of the ribosome, λ phage, PM2 phage and calf thymus DNA. This result is in good agreement with the order of the chemical shift anisotropy as far as the DNAs are concerned, but the RNA of the ribosome does not hold such a good correlation. This inconsistency might reflect the difference in the structure and/or the dynamics between the DNA and RNA in these complexes.

VII-3. Discussion

The protein-nucleic acid complexes used in this work are suitable systems for studying the relationship between the structure and dynamic state, because the modes of interaction are different among these complexes. ^{31}P solid-state NMR method was shown to be powerful for the investigation of such systems in this chapter.

In the first place, we examined pure DNA. It is known that the primary hydration in DNA is achieved at about 80 % of relative humidity [12] and that a transition from A to B form DNA occurs in the range of relative humidity 84 % to 92 % with the progress of the second hydration [8, 13]. The change in the spectrum from Figures VII-1 A to B corresponds to the A - B DNA transition and the increase of the mobility with it. Since the rapid overall motion would not be expected for high molecular weight of calf thymus DNA, we can conclude that the rapid segmental motion occurs in the B form DNA in the presence of water. The chemical shift anisotropies of DNAs at dry and 71 % relative humidity, which take on amorphous and A form, respectively , did not change significantly up to 45^{o}C. On the other hand, the temperature dependence of the spectrum for the B form DNA was reported by Diveroi and Opella [14]. It was reported that the powder pattern and the chemical shift anisotropy changed drastically depending on the temperature. These results also support the idea that backbone of DNA in the B form is structurally mobile. Since the second hydration waters, which play a key role in the A to B transition, are not firmly adhere to the primary hydration water molecules, it is expected that rapid segmental motion is effectively induced by the Brownian motions of the second hydration waters.

The spectra of calf thymus DNA in the solution with 60 % of sucrose suggested that its motion was uniformly suppressed in spite of its enough water content. The effeciency of sucrose on the suppression of the motion of whole system depended on the system. In the case of pure DNA, it can only partially suppress the segmental motion by its high viscosity. On the other hand, the rotational motion of large complexes such as chromatins and T4 phages was completely suppressed, judged from the spectra at different concentration of sucrose. In the case of small complexes such as PM2 and ribosomes, the extent of the suppression depended on the concentration of the complex itself. At the concentration used in this work, most of overall motions were suppressed at a low temperature, judged from the chemical shift anisotropy.

The solvent fractions in the cores of λ, λΔ mutant and PM2 phages are 60, 67 and 73 %, respectively. The chemical shift anisotropy of phages increases in order of λΔ mutant, PM2 and λ phage. It is reasonable that λ phage shows a larger anisotropy than λΔ mutant phage, because the latter is different from the former only in the content of the DNA. However, the $-\Delta\sigma$ of PM2 phage is larger than that of λΔ phage by 11.4 ppm at 5°C, in spite of more water content of the former. It suggests that PM2 contains something to interact with its DNA in the nucleocapsid. This was also supported by the heating experiment. Moreover, although judged from the water content in the core, their DNAs should take on B form, their spectra showed asymmetric powder patterns characteristic of the presence of rigid components. This result suggests that the DNAs are rigidly packaged in the very small virions so that their segmental motions are suppressed.

The temperature dependence of the chemical shift anisotropy of PM2 was larger than those of λ and λΔ phages, and was rather similar to that of calf thymus DNA in the presence of sucrose. This result was contrary to what was expected from their chemical shift anisotropy at 5°C, and means that either the folding of PM2 DNA or/and the interactions among the DNA, protein IV and nucleocapsid membrane is sensitive to the change of temperature. The small temperature dependence of the chemical shift of λ and λΔ phages can be ascribed to the stable head structure. The curve of the temperature dependence of PM2 was separated into three parts in the slope, namely, 0 - 22, 22 - 30 and above 30°C. The result is coincident with the result of single-pulse NMR spectrum reported by Akutsu *et al* [1]. The phenomenon was confirmed. They ascribed the change in the slope between 0-22 and 22 - 30°C to the increase of the membrane fluidity with the phase transition. The explanation is reasonable, because the chemical shift anisotropy, its temperature dependence and the heating experiment supported a model of PM2 that the phage particle has DNA-binding proteins (protein IV) anchoring themselves in the inner leaflet of its bilayer membrane and interacting with the DNA in the virion [1, 4, 5, 6].

The chemical shift anisotropy of the DNA of PM2 phage changed more dramatically than that of the change of the lipid-bilayer shown in Chapter V. This is ascribed to the difference in the dynamic mode of the DNA and lipid molecules. In the previous paper [1], the early event of the infection of PM2 phage to the host cell was examined as a function of temperature. An enhancement of the infectivity was observed in the temperature region from 15 to 23°C. The process of the infection contains two stages, namely, the absorption of the phage particle to the surface of the host cell and the release of the DNA into the host cell. Taking into account the result that the interaction became weak with an increase of temperature, there is a possibility that a change in the structure of the phage particle induced by the phase transition of the membrane may be necessary for the infection process. Anyhow, it became clear that the dynamic state of the DNA and/or the lipid bilayer was related to the infectivity.

Although the fine structures of RNAs and proteins in ribosome particles are not yet known, it is evident that the RNA contains double- and single stranded parts [15]. The double-stranded RNA is known only to take on A form [12]. The heating experiment showed that there is direct interaction between the RNA and the proteins in ribosome particles. On the other hand, the double-stranded DNA in chromatin [2, 3], which is thought to be in the B form [12], is bound to histone proteins with many positively charged amino acid residues through electrostatic interaction. The spectrum of the ribosome particles showed a larger chemical shift anisotropy than that of the chromatin. However, the $T_{1\rho}$(H) suggested that the DNA in chromatin is more rigid than the RNA in ribosome. Thus, the results from the chemical shift anisotropy and $T_{1\rho}$(H) are apparently inconsistent. Although it is difficult to give a clear answer to this question at this stage, it is possible that the single stranded part of the RNA is more mobile than the helix region so that $T_{1\rho}$(H) is dominated by the motion of this part.

Through the characterization of $T_{1\rho}$(H), it turned out that all of the nucleic acids used in this work were in the slow-motional regime. This result is reasonable, because the nucleic

acids are in high molecular weight in any case, and the segmental motions of the nucleic acids in the intact complexes are significantly restricted by the direct or indirect interaction with proteins.

References

[1] Akutsu, H., Satake, H. and Franklin, R. M. (1980) *Biochemistry*, 19, 5264.

[2] Kornberg, R. D. and Klug, A. (1981) *Sci. Amer.*, 244, 48.

[3] Klug, A., Rhodes, D., Smith, J., Finch, J. T. and Thomas, J. O. (1980) *Nature*, 287, 509.

[4] Hinnen, R., Chassin, R., Schäfer, R., Franklin, R. M., Hitz, H. and Schafer, D. (1975) *Eur. J. Biochem.*, 68, 139.

[5] Schneider, D., Zulauf, M., Schäfer, R. and Franklin, R. M. (1978) *J. Mol. Biol.*, 124, 97.

[6] Satake, H., Kanua, M. and Franklin, R. M. (1981) *Eur. J. Biochem.*, 114, 623.

[7] Lake, J. A. (1985) *Ann. Rev. Biochem.*, 54, 507.

[8] Cooper, P. J. and Hamilton, L. D. (1966) *J. Mol. Biol.*, 16, 562.

[9] Mehring, M. (1983) "*Principles of High Resolution NMR in Solid*" 2nd ed., Springer-Verlag, Berlin.

[10] Akutsu, H. (1986) *J. Magn. Reson.*, 66, 250.

[11] Stejskal, E. O., Sefcik, M. D. and McKay, R. A. (1981) *Macromolecules*, 14, 275.

[12] Saenger, W., (1983) "*Principles of Nucleic Acid Structure*", Springer Verlag, New York.

[13] Shindo, H., Fujiwara, T., Akutsu, H., Matsumoto, V. and Shimidzu, M. (1984) *J. Mol. Biol.*, 17, 221.

[14] Diverdi, J. A. and Opella, S. J. (1981) *J. Mol. Biol.*, 149, 307.

[15] Gutell, R. R., Weiser, B., Woese, C. R. and Noller, H. F. (1985) *Prog. Nucleic Acid Res. Mol. Biol.*, 32, 155.

Chapter VIII

Application of the Method to Cells under the Physiological Conditions

Summary

By applying the ^{1}H-^{31}P cross-polarization NMR technique to intact marine bacterial cells, an asymmetric powder pattern spectrum of nucleic acids in a cell was revealed. The major contributor to the spectrum was ribosomes. The powder pattern changed dramatically with the physiological conditions of the cells.

VIII-1. Introduction

Nuclear magnetic resonance (NMR) is now widely used for investigations on biological systems *in vivo* [1, 2]. In most cases, the behavior of small and soluble molecules is monitored because only such molecules can give rise to high resolution signals in cell or organs. However, a biological system contains many macromolecules and supramolecular structures, as well as small metabolites. The latter play important roles in organizing biochemical reactions in a biological system. Therefore, it would be very useful if information on a particular macromolecular or supramolecular system could be obtained selectively. Since the motion of such systems is highly restricted, the solid state NMR method is most promising. ^{2}H-NMR was used to obtain information on selectively deuterated membranes of *E. coli* [3] and fibroblasts [4]. We used ^{1}H-^{31}P cross-polarization NMR to investigate the dynamic structures of chromatins in intact chicken erythrocytes [5], This method is powerful for the investigation of phosphorus-containing supramolecular systems. In this study, this technique was applied to intact bacterial cells and was shown to be very useful for monitoring the physiological dynamic structures of nucleic acid macromolecules.

VIII-2. Results and Discussion

The ^{31}P NMR spectrum of intact cells of a marine bacterium, *A. espejiana*, harvested in the logarithmic phase, was measured with a conventional single pulse at 4°C and is shown in Figure VIII-1 B1. This spectrum comprises the superposed signals of all the phosphorus-containing molecules in a bacterial cell. The components of the spectrum can be classified into two major groups on the basis of the linewidth, namely, the sharp and symmetrical peak at the center and broad components. The former would come from the soluble molecules which exhibit fast motion. The latter would be due to macromolecules and supramolecular systems, which exhibit restricted motion. The former is now well characterized [6]. Although the latter have been neglected so far, they should provide important information as well. With the ^{1}H-^{31}P cross-polarization method there may be no contribution by the soluble molecules, because the polarization transfer from proton to phosphorus spin systems is mediated by heteronuclear dipolar interactions, which are averaged out by fast motion [5, 6].

The ^{31}P NMR spectrum of intact *A. espejiana* cells observed with a ^{1}H-^{31}P cross-polarization pulse sequence with a contact time of 0.7 ms is shown in Figure VIII-1 B2. As expected, the sharp peak had completely disappeared. Only the broadest component of the single pulse spectrum was observed in this spectrum. This is a partially-averaged asymmetric powder pattern. A similar powder pattern spectrum was obtained with a contact time of 1.0 ms. This powder pattern got weaker and was gradually replaced by an axial symmetric powder pattern with an increase in the contact time. The cross-polarization efficiency was maximum with a thermal contact time of 0.7 ms. The chemical shielding anisotropy ($\Delta\sigma=\sigma_{33}-\sigma_{11}$) of this asymmetric powder pattern was about -170 ppm.

In order to determine the pattern's origin, *E. coli* cells in the logarithmic phase were examined, since their chemical composition is well known. The ^{31}P NMR spectra obtained with the single-pulse and cross-polarization methods are shown in Figures

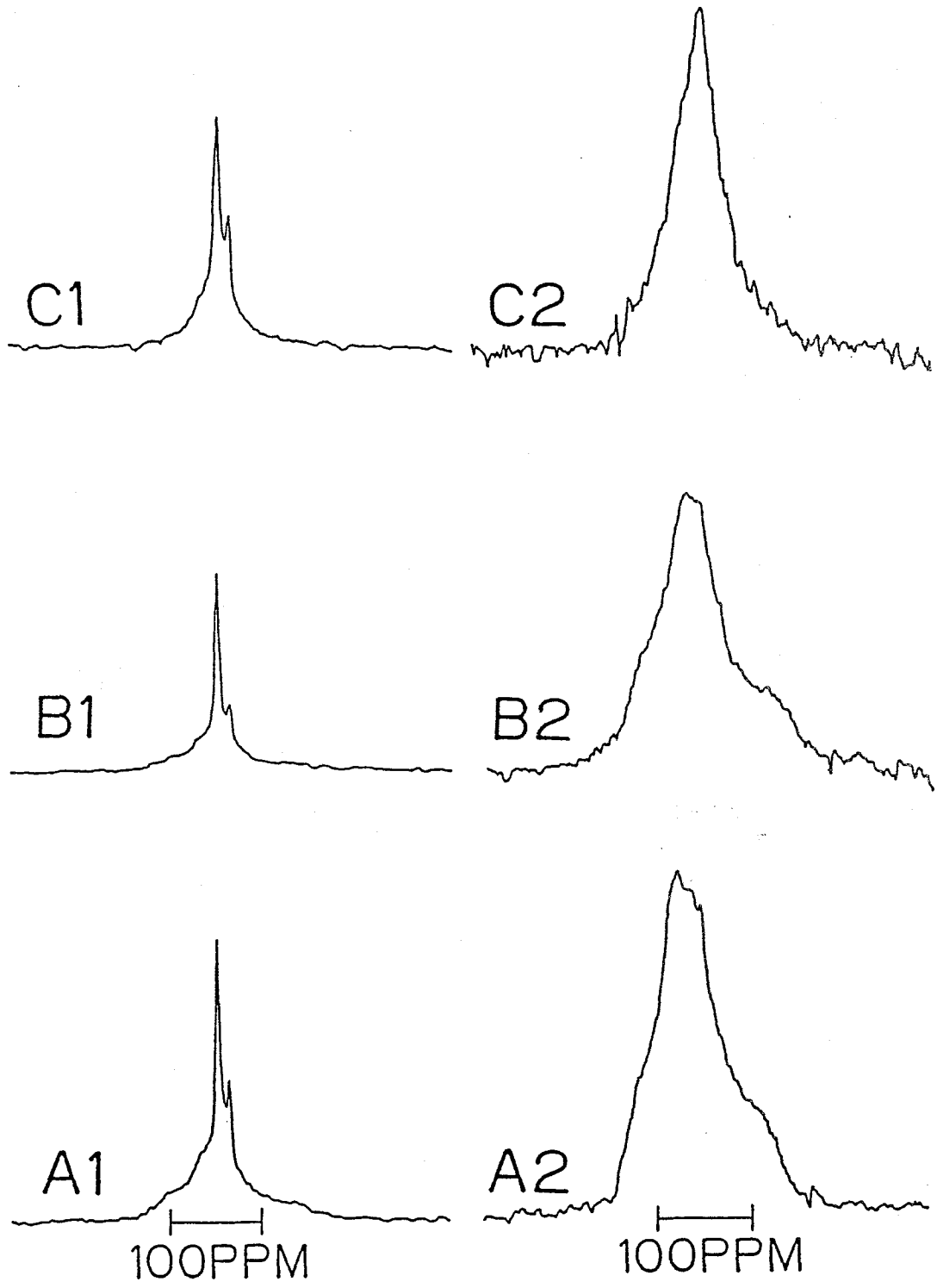

Figure VIII-1. ^{31}P NMR spectra of intact *A. espejiana* and *E. coli* cells at 4°C. Series 1 and 2 were obtained with the single-pulse and cross-polarization methods, respectively. The contact time for the latter was 0.7 ms. A: *E. coli* cells harvested in the logarithmic phase. B: *A. espejiana* cells harvested in the logarithmic phase. C: *A. espejiana* cells harvested at the beginning of the saturation phase. 1,600 and 4,000 transients were accumulated for the single-pulse and cross-polarization pulse spectra, respectively. The 90° pulse width was 10 μs and 10.3 μs for the single-pulse and cross-polarization pulse modes, respectively. A 45° pulse width was used for the measurement of the single-pulse spectra. A relaxation delay time of 3.6 s was used. An exponential window function with a 100 Hz broadening factor was used.

VIII-1 A1 and A2, respectively. The spectra of *A. espejiana* and *E. coli* are very similar to each other with both methods. This suggests that the spectra in Figures VIII-1 A2 and B2 originate from a similar molecular species. The major phosphorus-containing substances in a cell are phospholipids and nucleic acids. Since the efficiency of the cross-polarization was maximum with a thermal contact time of about 1 ms for DNA but with one of about 10 ms for the phospholipid bilayer [5, 7], the powder patterns in Figures VIII-1 A2 and B2 should be due to nucleic acids. DNA and RNA in a *E. coli* cell in the logarithmic phase account for 1 and 6 % of the total cell weight, respectively [8]. The major component of RNA is ribosomal RNA (70 %) [8]. Thus, the contact time dependence of the spectral intensity was examined for ribosomes purified from *A. espejiana* cells in NTCM-buffer with 60 % sucrose (w/w). The cross-polarization efficiency was maximum with a thermal contact time of 0.7 ms and the spectrum had a typical asymmetric powder pattern with -210 ppm chemical shift anisotropy. The agreement as to the optimal thermal contact time between the intact cells and purified ribosomes strongly supports that the major contribution to the powder patterns in Figures VIII-1 A2 and B2 is due to the ribosomes. Of course, the contribution by DNA should be included in them as well. We also examined the contact time dependence of calf thymus DNA with 50 % (w/w) NTCM-buffer as well as purified ribosomes. It was found that the optimal contact time was 0.7 ms. But the spectra showed a powder pattern lacking the principal values of a chemical shift tensor, which differs from Figure VIII-1 B2.

The effect of the water content on the spectral pattern of the purified ribosomes was examined. Figure VIII-2 A is the spectrum for the pellet obtained in the cross-polarization pulse mode with a contact time of 0.7 ms at $4^{o}C$. It showed a typical asymmetric powder pattern of rigid phosphorus with chemical shift anisotropy of -210 ppm. This is similar to the spectrum of the purified ribosomes in NTCM-buffer containing 60 % sucrose, suggesting that 60 % sucrose was enough to suppress the rotational motion of ribosomal particles at a high concentration. Figures VIII-2 B, C and D are the spectra of the ribosomes suspended in

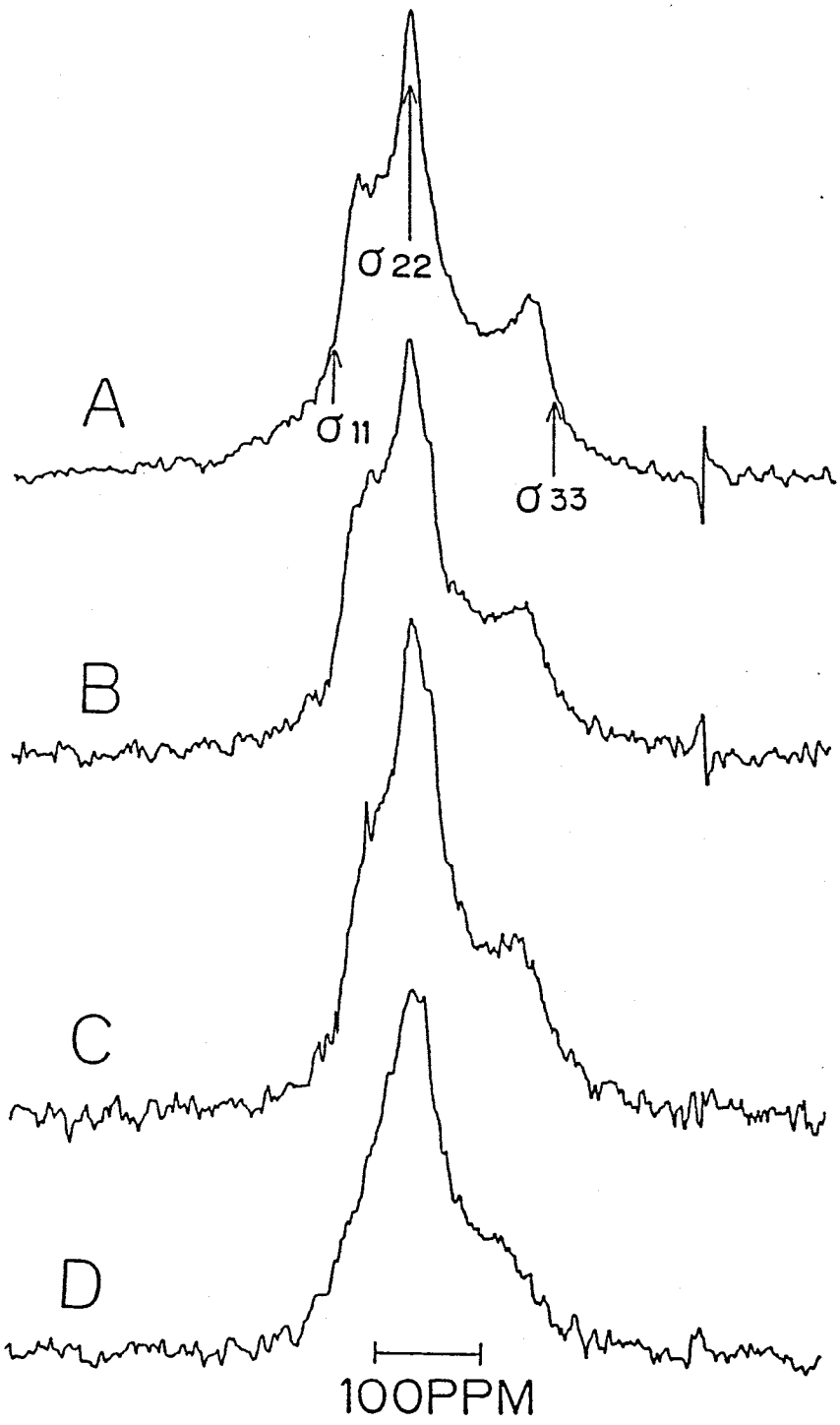

Figure VIII-2. ^{31}P NMR spectra of purified ribosome of *A. espejiana* at 4°C. The spectra were obtained with a cross-polarization pulse sequence with a thermal contact time of 0.7 ms. (A) Pellet; (B), (C) and (D) pellets were suspended in one, three and four volumes of NTCM-buffer, respectively. The aggregated ribosomes were removed by low speed centrifugation. 1,200, 3,000, 6,000 and 8,000 transients were accumulated for (A), (B), (C) and (D), respectively. 0.35 g of a pellet was used for each measurement. The conditions for measurements were the same as in Figure VIII-1.

one volume, three volumes and four volumes of the NTCM-buffer solution, respectively. The absolute value of the chemical shift anisotropy decreased with an increase in the water content. The chemical shift anisotropy was -200, -185 and -175 ppm for Figures VIII-2 B,C and D, respectively. The last value is quite close to those in Figures VIII-1 A2 and B2. This suggests that the dynamic state of ribosomes in an intact cell is similar to that in a solution with four volumes of NTCM-buffer.

The phosphorus chemical shift anisotropy of DNA of the chromatin in intact chicken erythrocytes was reported to be -156 ppm [5]. The anisotropy was ascribed to histon-DNA interactions. The large anisotropy of the ribosomal RNA shows that the interactions between ribosomal proteins and RNA are much stronger than the histon-DNA interactions.

Next, whether or not the growth phase of *A. espejiana* affects the ^{31}P NMR spectrum was examined. Figures VIII-1 C1 and C2 show the ^{31}P NMR spectra of intact *A. espejiana* cells in the saturation phase obtained at $4^{o}C$ in the single-pulse and cross-polarization modes, respectively. Although it is not so easy to detect a difference between the single-pulse spectra, Figures VIII-1 B1 and C1, a distinct difference was observed between the cross-polarization spectra, Figures VIII-1 B2 and C2. In the spectrum for the saturation phase, the characteristics of the asymmetric powder pattern disappeared and the linewidth became narrower, suggesting that nucleic acid components of intact cells in the full growth phase are more mobile than those in the logarithmic growth phase. The spectra with thermal contact times of 0.7 and 1.0 ms were very alike each other as to the powder pattern. The spectral intensity with a thermal contact time of 0.7 ms was larger than with one of 1.0 ms. This also suggests that the cross-polarization spectrum with a thermal contact time of 0.7 ms is mainly due to ribosomes in intact cells. Furthermore, the fact that no broad component is left in the spectrum provides direct evidence for that DNA in a *A. espejiana* cell in the full-growth phase does not take on such a rigid structure as the chromatin in a eucaryotic cell [5]. Since there is much more transcription and translation activity in the logarithmic phase

than in the saturation phase, the spectral difference between Figures VIII-1 B2 and C2 should be elucidated in terms of these activities. It is well known that DNA, mRNA and ribosomes form a transcriptional-translational complex in a bacterial cell, which can form a huge supramolecular structure and restrict the motion of ribosomes and DNA. The other possibility is a reduction in the viscosity of the cytoplasm in the stationary state, which could be the result of reductions in the amounts of ribosomes, mRNA, tRNA and metabolic molecules [9]. Both factors would contribute to the change of the spectrum. But we cannot determine at this stage which one is the major contributor. In any case, we can conclude that the cross-polarization method can provide information on the dynamic state of the supramolecular system of nucleic acids in a cell, which reflects the physiological conditions of the growth phase.

References

[1] Brindle, K. M., Rajagopalan, B., Bolas, N. M. and Radda, G. K. (1987) *J. Magn. Reson.*, **74**, 356

[2] Muller, S., Aue, W. P. and Seelig, J. (1985) *J. Magn. Reson.*, **63**, 530

[3] Borle, F. and Seelig, J., (1983) *Biochemistry*, **22**, 5536

[4] Scherer, F. and Seelig, J. (1987) *EMBO J.*, **6**, 2945

[5] Nishimoto, S., Akutsu, H. and Kyogoku, Y. (1987) *FEBS Letters*, **231**, 293

[6] Seelig, J. (1986) "*Physics of NMR Spectroscopy in Biology and Medicine*" ed. by Maraviglia, N., 389-411, North-Holland Physics Publishing, 1000 AC Amsterdam.

[7] Akutsu, H. (1986) *J. Magn. Reson.*, **66**, 250

[8] Watson, J. D. (1975) "*Molecular Biology of the Gene*" 3rd ed., p69, W. A. Benjamin Inc, Melon Park, California.

[9] Ishihama, A. and Fukuda, R. (1980) *Mol. Cell. Biochem.*, 31, 177

Chapter IX

Conclusion

The author was successful in selective observation of ^{31}P NMR spectrum of nucleic acids and biomembranes in intact biological systems by the use of the ^{1}H-^{31}P cross-polarization technique. The results on PM2 phage gave a firm basis for the selective observation, and the results of *A. espejiana* showed that this method was powerful for the study of an intact system as complicated as procaryotic cells. Selective observation of ^{31}P NMR spectra of nucleic acids and biomembranes are based on the fact that the mode of motion of these components are essentially different from each other in the intact biological systems. The difference in the dynamics is reflected on T_{HP} and $T_{1\rho}(H)$, which dominate the ^{1}H-^{31}P cross-polarization efficiency. In all nucleoprotein complexes examined, the motion of the nucleic acids was the suppressed segmental one that falls in the slow motional regime near the minimum (τ_c:1.7x10^{-6}s) of $T_{1\rho}(H)$. On the other hand, phospholipids in biomembranes undergo rapid axially symmetric motions which fall in the fast motional regime far from the minimum. Therefore, both of T_{HP} and $T_{1\rho}(H)$ of nucleic acids are shorter than those of phospholipid bilayers. Furthermore, T_{HP} and $T_{1\rho}(H)$ of other smaller molecules are much more longer. These differences become the physicochemical basis of the selective observation of ^{31}P NMR spectrum of nucleic acids or biomembranes in intact biological systems. Furthermore, $T_{1\rho}(H)$ is closely connected with the effective magnetic field in the rotating frame and the dynamic state of molecules which depend on temperature. Thus, contact time, effective magnetic field in the rotating frame (90^{o} pulse width) and temperature are the important parameters for the selective observation.

Usually, the sensitivity of a rare spin is enhanced by the cross-polarization method. It is also the case with the selectively observed spectrum of nucleic acids. The sensitivity of biomembrane spectrum is, however, much lower because of its longer T_{HP} and $T_{1\rho}(H)$. This is the disadvantage of the biomem-

brane. On the other hand, it is impossible to observe DNA and RNA separately in intact systems, because their dynamic states are similar to each other. In contrast, the selectivity of the biomembrane from other components was very high, because procaryotic cells do not have any component that is in the dynamic state similar to the cell membranes. This is the advantage of the biomembrane. However, the situation would be different with eucaryotic cells, because they have more complicated intracellular membrane systems.

The selective observation of each component enabled us to measure $T_{1\rho}(H)$ of each component even for intact systems. This is very important for the study of dynamic state of biological substances, because it provides us with quantitative information on the dynamic state of each component.

In order to make this method more feasible, it is necessary to improve several points. In the first place, signal to noise ratio should be improved for the short measurement time of intact biological systems. This is expected to be achieved by increasing the static magnetic field, namely, by the use of a superconducting magnet NMR machine. However, since high power is needed for irradiation at a higher field, it becomes more difficult to control the temperature of the sample. This problem should be solved. Secondly, the cross-polarization method can be applied to other nuclei than ^{31}P. This would open possibility to get information from different sources of supramolecular systems. For example, combination of this technique with specific labeling by ^{15}N would provide information on specific proteins in supramolecular systems such as membrane proteins, ribosome proteins etc. In the last, it is also necessary to develop this method to such a level that it can be applied to eucaryotic cells. In the application to higher organisms, it would be interesting to examine the characteristics of each organ and to investigate the contributions from a variety of the intracellular membranes in the cells.

List of Publications

The contents of this thesis have been published or will be published in the following papers.

Chapter IV and V

Direct Observation of Phase Behavior of Lipid Bilayers of Phage PM2 and Intact Host Cells by ^{1}H-^{31}P Cross-Polarization NMR

Odahara, T., Akutsu, H. and Kyogoku, Y.

Biochemistry, in press.

Chapter VI

Dynamics of Phospholipid Membranes of PM2 and *A. espejiana* as Monitored by $T_{1\rho}(H)$

Odahara, T., Akutsu, H. and Kyogoku, Y.

in preparation.

Chapter VII

Dynamic Structures of Nucleic Acids and Their Protein Complexes Studied by ^{1}H-^{31}P Cross-Polarization NMR

Odahara, T., Nishimoto, S., Akutsu, H. and Kyogoku, Y.

in preparation.

Chapter VIII

Physiological Dynamic Structures of Nucleic Acids in *A. espejiana* Cells Detected on ^{1}H-^{31}P Cross-Polarization NMR

Odahara, T., Akutsu, H. and Kyogoku, Y.

J. Biochem., to be submitted.

Acknowledgment

The present work has been performed under the direction of Professor Y. Kyogoku, Institute for Protein Research, Osaka University. The author would like to express his sincere gratitude to Professor Y. Kyogoku for letting him work in good environment and free atmosphere. The author also wishes his sincere thanks to Dr. H. Akutsu, Department of Physical Chemistry, Faculty of Engineering, Yokohama National University, for his continuing discussion and encouragements. The author also thanks to Dr. H. Sugeta, Institute for Protein Research, Osaka University, for his help in the calculations. The author is grateful to Sinku Riko Inc. for letting him use their facilities in thermal analysis.

The author wishes to thank deeply Professor H. Chihara and Professor H. Suga, Faculty of Science, Osaka University, for their examination of the thesis and valuable suggestion.

Finally, the author thanks sincerely to his families for their unfailing understanding and affectionate encouragements.

Takayuki Odahara

February, 1990